

D.L. Ferretti

Extension of the Use of a Single Degree of Freedom Model for Non-Uniform Load Distributions

Extension of the Use of a Single Degree of Freedom Model for Non-Uniform Load Distributions

By

David L. Ferretti

in partial fulfilment of the requirements for the degree of

Master of Science
in Civil Engineering

at the Delft University of Technology,
to be defended publicly on August 25, 2016.

Supervisor:	Ir. A. van Doormaal		TNO
Thesis committee:	Prof. dr. ir. L.J. Sluys	(Chair)	TU Delft
	Dr. ir. K.N. van Dalen		TU Delft
	Dr. ir. J. Weerheijm		TU Delft
	Ir. L.J.M. Houben		TU Delft

An electronic version of this thesis is available at <http://repository.tudelft.nl/>.

Abstract

To model the response of a structural element subjected to explosions, single degree of freedom (SDOF) systems can be used. It only takes seconds to perform an SDOF calculation. This is a lot faster than finite element analyses. The SDOF method is therefore a powerful method to perform vulnerability analyses in which dozens of scenarios need to be analysed.

To perform an SDOF calculation a representative load as function of time is needed. Usually inconsistent methods are used to determine a representative load. For non-uniform or asymmetric load distributions this might result in inaccurate estimations.

In this report an approach has been presented to translate an arbitrary non-uniformly distributed load acting on an elastic-plastic simply supported beam to an equivalent uniform load. For this translation factors have analytically been determined. The factors are dependent on the geometry and boundary conditions of the structural element. To determine the model capabilities and the accuracy of the estimations, the obtained response of a 6 meter long beam using the SDOF model has been compared with the obtained response using finite element software.

For the investigated 6 meter long simply supported beam it holds that the determined factors can be used for explosions at 1 meter or higher. If the scenarios are scaled (beam dimensions, distance explosions, etc.) it is likely that errors of the same order will be obtained, since the relative load distribution on the beam remains similar. Using the factors accurate estimations of the deflection have been obtained with the SDOF model. In case of linear-elastic deformation errors have been obtained in the range of -23% to +7% and in case of elastic-plastic deformation in the range of -29% to +33%. The order of the obtained errors are consistent with the basic errors of the SDOF method itself.

Preface

This report presents the results of the research that has been carried out during my MSc. thesis at the University of Technology Delft. This thesis has been done in collaboration with research institute TNO. In this research the translation of non-uniform load distributions to equivalent uniform load distributions has been investigated. The equivalent uniform load can be used as input for a single degree of freedom model to compute vulnerability analyses in which hundreds of scenarios need to be analysed.

First of all I would like to thank all my committee members for their guidance during this research. I would like to thank TNO who gave me the opportunity to perform the research at their firm. Thanks to all my colleagues at TNO for the great work environment and the pleasant coffee breaks.

*David L. Ferretti
Delft, August 2016*

Table of contents

ABSTRACT	V
PREFACE	VII
TABLE OF CONTENTS	IX
LIST OF FIGURES	XIII
LIST OF TABLES	XVII
LIST OF SYMBOLS	XIX
CHAPTER 1 INTRODUCTION	1
1.1 PROBLEM DEFINITION	1
1.2 RESEARCH OBJECTIVE	1
1.3 RESEARCH SCOPE	2
1.4 METHOD OF APPROACH.....	2
<i>Part I - Literature/background study</i>	2
<i>Part II - Determination of the weightfactors and their applicability</i>	2
<i>Part III - Accuracy of the LS-DYNA estimations</i>	3
<i>Part IV - Accuracy of the SDOF estimations</i>	3
<i>Part V – Conclusions and recommendations</i>	4
PART I LITERATURE/BACKGROUND STUDY	5
CHAPTER 2 BLAST LOADING	7
2.1 EXPLOSION	7
2.2 IDEAL BLAST WAVES	7
2.3 REFLECTION AND DIFFRACTION.....	9
2.4 SCALING	10
CHAPTER 3 THE SDOF MODEL	11
3.1 MASS-SPRING-SYSTEM	12
3.1.1 <i>Equivalent mass</i>	12
3.1.2 <i>Equivalent load</i>	13
3.1.3 <i>Equivalent resistance</i>	13
3.1.4 <i>Load-mass factor</i>	13
PART II DETERMINATION OF THE WEIGHTFACTORS AND THEIR APPLICABILITY	17
CHAPTER 4 ANALYTICAL CALCULATION OF THE WEIGHTFACTORS OF A BEAM	19
4.1 CURRENT APPROACH (BEAMBLAST + SDOF).....	20
4.1.1 <i>Beamblast model</i>	20
4.1.2 <i>Single-degree-of-freedom model</i>	20
4.2 EQUIVALENT UNIFORM LOAD	20
4.3 WEIGHTFACTORS	21

4.4	BENDING STRESSES	22
4.4.1	<i>Partially distributed uniform load at the centre of the beam</i>	23
4.4.2	<i>Partially distributed uniform load at the end of the beam</i>	24
4.4.3	<i>Partially distributed uniform load at different positions along the beam</i>	25
4.5	DISCREPANCY OF SDOF PARAMETERS	27
4.6	CONCLUSION	28
CHAPTER 5 VALIDITY WEIGHTFACTORS – PLASTICITY		31
5.1	SUPERPOSITION	32
5.2	WEIGHTFACTORS	32
5.2.1	<i>Case 1: Stiffness 10% of the initial stiffness</i>	34
5.2.2	<i>Case 2: Stiffness 0.01% of the initial stiffness</i>	34
5.2.3	<i>Case 3: 90% of the beam decreased stiffness</i>	35
5.2.4	<i>Case 4: Two sections with decreased stiffness</i>	35
5.2.5	<i>Conclusion</i>	37
5.3	EQUIVALENT UNIFORM LOAD	37
5.3.1	<i>Conclusion</i>	39
5.4	FINITE ELEMENT ANALYSIS	40
5.5	SUMMARY	41
PART III ACCURACY OF THE LS-DYNA ESTIMATIONS.....		43
CHAPTER 6 ACCURACY OF THE STATIC DEFLECTION OF A LINEAR-ELASTIC BEAM		45
6.1	EXAMPLE CALCULATION	46
6.2	BOUNDARY CONDITIONS	47
6.2.1	<i>Conclusion</i>	49
6.3	ACCURACY OF THE DEFLECTION OF DIFFERENT LOAD TYPES	49
6.3.1	<i>Conclusion</i>	51
6.4	SUMMARY	51
CHAPTER 7 ACCURACY OF THE DYNAMIC RESPONSE OF A BEAM		55
7.1	DETERMINE PRESSURE DUE TO BLAST LOAD.....	56
7.2	DETERMINE EQUIVALENT UNIFORM LOAD	58
7.2.1	<i>Impulse</i>	59
7.3	ACCURACY OF THE LINEAR-ELASTIC RESPONSE	60
7.3.1	<i>Deflection at midspan</i>	61
7.3.2	<i>Stresses</i>	63
7.4	ACCURACY OF THE ELASTIC – PLASTIC RESPONSE	64
7.4.1	<i>Deflection</i>	65
	<i>Accuracy of the estimations</i>	66
	<i>Influence of the ratio between the load duration and the fundamental period</i>	73
7.4.2	<i>Stresses</i>	76
7.5	CONCLUSION	76
	<i>Load distribution</i>	76
	<i>Equivalent uniform load</i>	77
	<i>Accuracy of the Linear-Elastic Response</i>	77
	<i>Accuracy of the Elastic – Plastic Response</i>	77
PART IV ACCURACY OF THE SDOF ESTIMATIONS.....		79

CHAPTER 8 SDOF CALCULATIONS.....	81
8.1 BEAM PROPERTIES.....	82
8.2 INPUT	82
8.2.1 Load-mass factor	82
8.2.2 Resistance-deflection function.....	83
8.2.3 Load	84
8.3 ERRORS OF THE OBTAINED DEFLECTIONS	84
8.3.1 SDOF response versus LS-DYNA response using the equivalent uniform load	84
8.3.2 SDOF response versus LS-DYNA response using the non-uniform blast load.....	86
8.4 CONCLUSION.....	89
Errors of the obtained deflections.....	89
PART V CONCLUSIONS AND RECOMMENDATIONS	91
CHAPTER 9 CONCLUSIONS AND RECOMMENDATIONS	93
9.1 CONCLUSIONS	93
Cause of the error of the estimations	93
Order of the error of the estimations.....	93
Load regime in which the translation factors are recommended to be used.....	93
9.2 RECOMMENDATIONS	94
CHAPTER 10 REFERENCES	95
PART VI APPENDICES	97

List of figures

FIGURE 1.1: IDEALIZATION OF A NON-UNIFORM LOADED PLATE AS A MASS-SPRING-SYSTEM	1
FIGURE 1.2: RESEARCH APPROACH	4
FIGURE 2.1: BLAST WAVE PROPAGATION	7
FIGURE 2.2: IDEAL BLAST WAVE PROFILE	8
FIGURE 2.3: A) BLAST PARALLEL TO THE SURFACE B) BLAST WAVE PERPENDICULAR TO THE SURFACE C) BLAST WAVE AT AN ANGLE BETWEEN 0 AND 40° D) BLAST WAVE AT AN ANGLE BETWEEN 40 AND 90°	9
FIGURE 2.4: SCALING OF A BLAST WAVE.....	10
FIGURE 3.1: EQUIVALENT MASS-SPRING-SYSTEM	12
FIGURE 3.2: ASSUMED PLASTIC DEFORMATION SHAPE WITH A HINGE AT MIDSPAN	15
FIGURE 4.1: FLOWCHART CHAPTER 4	19
FIGURE 4.2: DETERMINING AN EQUIVALENT UNIFORM LOAD.....	21
FIGURE 4.3: MOMENT DIAGRAM FOR UNIFORMLY DISTRIBUTED LOAD. LEFT PARTIALLY LOADED AND RIGHT ENTIRELY LOADED	22
FIGURE 4.4: LOAD SCENARIO	23
FIGURE 4.5: LOAD SCENARIO	23
FIGURE 4.6: STRESSFACTORS FOR A LOAD WITH DIFFERENT WIDTHS (h) AT THE CENTRE	24
FIGURE 4.7: RATIO OF THE MAXIMUM OCCURRING STRESS OF A LOCALLY LOADED BEAM AND THE MAXIMUM OCCURRING STRESS OF A BEAM LOADED BY THE EQUIVALENT UNIFORM LOAD FOR A LOAD AT THE CENTRE	24
FIGURE 4.8: STRESSFACTORS FOR A LOAD STARTING AT THE BOUNDARY (a=0)	25
FIGURE 4.9: RATIO OF THE MAXIMUM OCCURRING STRESS OF A LOCALLY LOADED BEAM AND THE MAXIMUM OCCURRING STRESS OF A BEAM LOADED BY THE EQUIVALENT UNIFORM LOAD FOR A LOAD STARTING AT THE BOUNDARY (a=0).....	25
FIGURE 4.10: STRESSFACTORS FOR A PARTIALLY UNIFORMLY DISTRIBUTED LOAD (h=L/20) AT DIFFERENT LOCATIONS ALONG THE LENGTH OF THE BEAM.	26
FIGURE 4.11: RATIO OF THE MAXIMUM OCCURRING STRESS OF A LOCALLY LOADED BEAM AND THE MAXIMUM OCCURRING STRESS OF A BEAM LOADED BY THE EQUIVALENT UNIFORM LOAD FOR A LOAD AT DIFFERENT LOCATIONS ALONG THE LENGTH OF A BEAM (h=L/20)	26
FIGURE 4.12: RATIO OF THE MAXIMUM OCCURRING STRESS OF A LOCALLY LOADED BEAM AND THE MAXIMUM OCCURRING STRESS OF A BEAM LOADED BY THE EQUIVALENT UNIFORM LOAD FOR A LOAD STARTING AT THE BOUNDARY (a=0)	28
FIGURE 5.1: FLOWCHART CHAPTER 5	31
FIGURE 5.2: SUPERPOSITION PRINCIPLE FOR LINEAR SYSTEMS.....	32
FIGURE 5.3: SITUATION HOW THE DISTRIBUTION OF THE BENDING STIFFNESS MIGHT BE IN REALITY	32
FIGURE 5.4: SIMPLIFICATION OF THE YIELDED AREA WITH DECREASED BENDING STIFFNESS	33
FIGURE 5.5: STRESS-STRAIN CURVE OF STEEL.	33
FIGURE 5.6: WEIGHTFACTORS FOR A BEAM WITH A DECREASED BENDING STIFFNESS OF 10% OF THE INITIAL STIFFNESS. THE SECTION WITH DECREASED BENDING STIFFNESS IS AT $x=0.25*L$ AND HAS WIDTH J	34
FIGURE 5.7: WEIGHTFACTORS FOR A BEAM WITH A DECREASED BENDING STIFFNESS OF 0.01% OF THE INITIAL STIFFNESS. THE SECTION WITH DECREASED BENDING STIFFNESS IS AT $x=0.25*L$ AND HAS WIDTH J	35
FIGURE 5.8: WEIGHTFACTORS FOR A BEAM WITH A REDUCED STIFFNESS OF 90% OF THE LENGTH OF THE BEAM (WITH MIDDLE POINT $x=0.50*L$).	35
FIGURE 5.9: BEAM WITH TWO PREDEFINED "PLASTIC" SECTIONS.....	36
FIGURE 5.10: WEIGHTFACTORS FOR A DECREASED BENDING STIFFNESS OF 10% OF THE INITIAL STIFFNESS AT $x=0.25*L$ AND $x=0.75*L$	36

FIGURE 5.11: WEIGHTFACTORS FOR A DECREASED BENDING STIFFNESS OF 0.01% OF THE INITIAL STIFFNESS AT $x=0.25*L$ AND $x=0.75*L$	36
FIGURE 5.12: UNIFORM LOAD DISTRIBUTION	37
FIGURE 5.13: EQUIVALENT LOAD FOR A BEAM WITH DECREASED BENDING STIFFNESS AT $x=0.25*L$	38
FIGURE 5.14: EQUIVALENT LOAD FOR A BEAM WITH DECREASED BENDING STIFFNESS AT $x=0.40*L$	38
FIGURE 5.15: EQUIVALENT LOAD FOR A BEAM WITH DECREASED BENDING STIFFNESS AT $x=0.50*L$	38
FIGURE 5.16: EQUIVALENT LOAD FOR A BEAM WITH DECREASED BENDING STIFFNESS AT $x=0.25*L$ AND $x=0.75*L$	39
FIGURE 5.17: EQUIVALENT LOAD FOR A BEAM WITH DECREASED BENDING STIFFNESS AT $x=0.40*L$ AND $x=0.60*L$	39
FIGURE 5.18: LOAD SCENARIO	40
FIGURE 5.19: MAXIMUM DEFLECTION AT EACH POINT OF THE BEAM (AT DIFFERENT POINTS IN TIME)	41
FIGURE 5.20: MAXIMUM VON MISES STRESS AT EACH POINT OF THE BEAM (AT DIFFERENT POINTS IN TIME)	41
FIGURE 5.21: SIMPLIFICATION OF THE DECREASED BENDING STIFFNESS DUE TO YIELDING	42
FIGURE 5.22: COMPARISON BETWEEN THE DURATION OF A BLAST LOAD OF 1KG TNT EQUIVALENT WITH A STAND-OFF OF 2M AND THE FUNDAMENTAL PERIOD OF A 6M LONG BEAM.	42
FIGURE 6.1: FLOWCHART CHAPTER 6	45
FIGURE 6.2: SIMPLIFICATION OF A NON-UNIFORMLY DISTRIBUTED LOAD.....	46
FIGURE 6.3: TRANSLATION TO EQUIVALENT UNIFORM LOAD.....	46
FIGURE 6.4: SIMPLY SUPPORTED BEAM LOADED BY A LOAD IN THE FORM OF A HALF OF A SINE PERIOD PLUS 1.....	47
FIGURE 6.5: FIXED BEAM, PARTLY LOADED BY A LOAD IN THE FORM OF A HALF OF A SINE PERIOD.....	48
FIGURE 6.6: ACCURACY OF A $T/2$ SINE LOAD SPREAD OVER $H = L/10$. LOAD DIVISION INTO 1 TO 30 PARTS	48
FIGURE 6.7: ACCURACY OF A $T/2$ SINE LOAD SPREAD OVER $H = L/5$. LOAD DIVISION INTO 1 TO 30 PARTS	49
FIGURE 6.8: DIFFERENT LOAD TYPES.....	49
FIGURE 7.1: FLOWCHART CHAPTER 7	55
FIGURE 7.2: PRESSURE DISTRIBUTION OVER THE LENGTH OF A 6M LONG BEAM SUBJECTED TO AN EXPLOSION OF 1KG TNT EQUIVALENT AT 3M ABOVE THE CENTRE	56
FIGURE 7.3: PRESSURE PROPAGATION AT DIFFERENT LOCATIONS ON A 6M LONG BEAM FOR AN EXPLOSION OF 1KG TNT EQUIVALENT AT 3M ABOVE THE CENTRE	57
FIGURE 7.4: MAXIMUM PRESSURE OVER THE LENGTH OF A 6M LONG BEAM SUBJECTED TO AN EXPLOSION OF 1 KG TNT EQUIVALENT AT 3M HEIGHT AT DIFFERENT LOCATIONS (x) ALONG THE LENGTH OF THE BEAM	57
FIGURE 7.5: RELATIVE PRESSURE DISTRIBUTION OVER THE LENGTH OF A 6M LONG BEAM SUBJECTED TO AN EXPLOSION OF 1KG TNT EQUIVALENT AT DIFFERENT DISTANCES (z) ABOVE THE CENTRE OF A BEAM WITH LENGTH 6M.....	57
FIGURE 7.6: ABSOLUTE PRESSURE DISTRIBUTION OVER THE LENGTH OF A BEAM SUBJECTED TO AN EXPLOSION OF DIFFERENT MASSES AT 3M ABOVE THE CENTRE OF A 6M LONG BEAM.	58
FIGURE 7.7: RELATIVE PRESSURE DISTRIBUTION OVER THE LENGTH OF A BEAM SUBJECTED TO EXPLOSIONS OF DIFFERENT TNT EQUIVALENT MASSES (M) AT 3M ABOVE THE CENTRE OF A 6M LONG BEAM.....	58
FIGURE 7.8: EQUIVALENT UNIFORM LOAD FOR AN EXPLOSION OF 1KG TNT EQUIVALENT AT 3M ABOVE THE CENTRE OF THE BOTTOM SURFACE OF A 6 METERS LONG BEAM	59
FIGURE 7.9: WEIGHTFACTORS FOR A SIMPLY SUPPORTED BEAM SPLIT INTO 10 PARTS	60
FIGURE 7.10: DEFLECTION AT MIDSPAN OF A BEAM WITH YIELD STRENGTH 2.85E6Pa DUE TO AN EXPLOSION AT 2 METERS ABOVE $x=0.50*L$. LINES FOR 15 AND 240 PARTS OVERLAP EACH OTHER.....	60
FIGURE 7.11: COORDINATE SYSTEM OF THE BEAM	61
FIGURE 7.12: DEFLECTION AT MIDSPAN OF A BEAM FOR AN EXPLOSION 3 METERS ABOVE $x=0.5*L$. THE CURVE OF 10 AND 240 PARTS OVERLAP EACH OTHER.....	61
FIGURE 7.13: DEFLECTION AT MIDSPAN OF A BEAM FOR AN EXPLOSION AT 3 METERS ABOVE $x=0.25*L$. THE CURVE OF 10 AND 240 PARTS OVERLAP EACH OTHER	62
FIGURE 7.14: DEFLECTION AT MIDSPAN OF A BEAM FOR AN EXPLOSION AT 3 METERS ABOVE $x=0.00*L$. THE CURVE OF 10 AND 240 PARTS OVERLAP EACH OTHER	62

FIGURE 7.15: DEFLECTION OF A 6M LONG BEAM SUBJECTED TO AN EXPLOSION OF 1KG TNT AT 2 METERS ABOVE $x=0$ AT DIFFERENT TIME STEPS	62
FIGURE 7.16: MAXIMUM OCCURRING VON MISES STRESSES OVER THE LENGTH OF THE BEAM FOR AN EXPLOSION 3 METERS ABOVE $x=0.50*L$. THE RATIO BETWEEN THE MAXIMUM OCCURRING STRESSES IS 0.73. (USING 240 PARTS).....	63
FIGURE 7.17: MAXIMUM OCCURRING VON MISES STRESSES OVER THE LENGTH OF THE BEAM. FOR AN EXPLOSION 3 METERS ABOVE $x=0.25*L$. THE RATIO BETWEEN THE MAXIMUM OCCURRING STRESSES IS 0.71. (USING 240 PARTS).....	63
FIGURE 7.18: MAXIMUM OCCURRING VON MISES STRESSES OVER THE LENGTH OF THE BEAM FOR AN EXPLOSION 3 METERS ABOVE $x=0$. THE RATIO BETWEEN THE MAXIMUM OCCURRING STRESSES IS 0.38. (USING 240 PARTS).....	64
FIGURE 7.19: DEFLECTION AT MIDSPAN OF A BEAM DUE TO AN EXPLOSION 2 METERS ABOVE $x=1/4*L$. YIELD STRENGTH = 3.35E6 PA. THE CURVE OF 10 AND 240 PARTS OVERLAP EACH OTHER	65
FIGURE 7.20: DEFLECTION AT MIDSPAN OF A BEAM DUE TO AN EXPLOSION 2 METERS ABOVE $x=1/8*L$. YIELD STRENGTH = 3.35E6 PA. THE CURVE OF 10 AND 240 PARTS OVERLAP EACH OTHER	65
FIGURE 7.21: RELATIVE ERROR FOR EXPLOSIONS AT DIFFERENT LOCATIONS ($x;y;z$) AND OF DIFFERENT MASSES	67
FIGURE 7.22: OBTAINED RELATIVE ERROR OF THE ESTIMATED DEFLECTION AT MIDSPAN FOR EXPLOSIONS AT 2M AND 3M HEIGHT ABOVE $x=1/4*L$, $x=3/8*L$ AND $x=1/2*L$	68
FIGURE 7.23: ELASTIC DEFLECTION SHAPES OF A 6M LONG BEAM DUE TO AN EXPLOSION OF 1KG TNT AT 2 METERS ABOVE $x=0$, AT DIFFERENT POINTS IN TIME	68
FIGURE 7.24: ELASTIC DEFLECTION SHAPES OF A 6M LONG BEAM DUE TO THE EQUIVALENT UNIFORM LOAD FOR AN EXPLOSION OF 1KG TNT AT 2 METERS ABOVE $x=0$, AT DIFFERENT POINTS IN TIME.....	69
FIGURE 7.25: ELASTIC-PLASTIC DEFLECTION SHAPE OF A 6M LONG BEAM SUBJECTED TO AN EXPLOSION 2M ABOVE THE CENTRE, AT DIFFERENT POINTS IN TIME.	70
FIGURE 7.26: ELASTIC-PLASTIC DEFLECTION SHAPE OF A 6M LONG BEAM SUBJECTED TO THE EQUIVALENT LOAD FOR AN EXPLOSION 2M ABOVE THE CENTRE, AT DIFFERENT POINTS IN TIME.	70
FIGURE 7.27: OBTAINED RELATIVE ERROR OF THE ESTIMATED DEFLECTION AT MIDSPAN FOR EXPLOSIONS AT 1M HEIGHT ABOVE $x=1/4*L$, $x=3/8*L$ AND $x=1/2*L$	71
FIGURE 7.28: ELASTIC DEFLECTION SHAPES OF A 6M LONG BEAM DUE TO THE EQUIVALENT UNIFORM LOAD FOR AN EXPLOSION OF 1KG TNT AT 1 METER ABOVE $x=3M$, AT DIFFERENT POINTS IN TIME.....	71
FIGURE 7.29: OBTAINED RELATIVE ERROR OF THE ESTIMATED DEFLECTION AT MIDSPAN FOR EXPLOSIONS AT 2M AND 3M HEIGHT ABOVE $x=0$ AND $x=1/8*L$	72
FIGURE 7.30: ELASTIC DEFLECTION SHAPES OF A 6M LONG BEAM DUE TO AN EXPLOSION OF 1KG TNT AT 2 METERS ABOVE $x=0$, AT DIFFERENT POINTS IN TIME	72
FIGURE 7.31: ELASTIC-PLASTIC DEFLECTION SHAPES OF A 6M LONG BEAM DUE TO AN EXPLOSION OF 1KG TNT AT 2 METERS ABOVE $x=0$, AT DIFFERENT POINTS IN TIME. $F_y = 2.35E6PA$	73
FIGURE 7.32: OBTAINED RELATIVE ERROR OF THE ESTIMATED DEFLECTION AT MIDSPAN FOR EXPLOSIONS AT 1M HEIGHT ABOVE $x=0$ AND $x=1/8*L$	73
FIGURE 7.33: ACCURACY OF THE ESTIMATED DEFLECTION WITH THE EQUIVALENT UNIFORM LOAD FOR A RATIO $T_D/T_N \leq 1.0$	74
FIGURE 7.34: ACCURACY OF THE ESTIMATED DEFLECTION WITH THE EQUIVALENT UNIFORM LOAD FOR A RATIO $T_D/T_N = 3.0$	74
FIGURE 7.35: ACCURACY OF THE ESTIMATED DEFLECTION WITH THE EQUIVALENT UNIFORM LOAD FOR A RATIO $T_D/T_N = 10.0$	75
FIGURE 7.36: DEFLECTION AT MIDSPAN OF A BEAM SUBJECTED TO AN EXPLOSION 2 METERS ABOVE $x=0$. $F_{yD} = 1E8PA$. $T_D/T_N = 10.0$	75
FIGURE 7.37: MAXIMUM OCCURRING VON MISES STRESSES OVER THE LENGTH OF A BEAM WITH A YIELDING STRENGTH OF 2.35E6 PA DUE TO AN EXPLOSION OF 1KG TNT EQUIVALENT AT $x=0M$ AT TWO METER HEIGHT	76
FIGURE 7.38: VON MISES STRESSES OF A BEAM WITH A YIELDING STRENGTH OF 2.35E6 PA DUE TO AN EXPLOSION OF 1KG TNT EQUIVALENT AT $x=0M$ AT TWO METERS HEIGHT	76
FIGURE 8.1: FLOWCHART CHAPTER 8.....	81
FIGURE 8.2: EQUIVALENT MASS SPRING SYSTEM.....	82
FIGURE 8.3: LOAD-MASS FACTOR IN THE ELASTIC AND PLASTIC REGIME	83
FIGURE 8.4: RESISTANCE-DISPLACEMENT CURVE FOR A SIMPLY SUPPORTED HOMOGENOUS BEAM	83

FIGURE 8.5: RELATIVE ERROR OF THE ESTIMATED DEFLECTION OBTAINED WITH THE SDOF MODEL COMPARED TO THE DEFLECTIONS OBTAINED WITH THE UNIFORM LOAD IN LS-DYNA FOR EXPLOSIONS AT DIFFERENT LOCATIONS (x;y;z).....	85
FIGURE 8.6: DEFLECTION AT MIDSPAN OF A BEAM WITH YIELD STRENGTH 2.85E6Pa DUE TO AN EXPLOSION AT 2 METERS ABOVE $x=0.50*L$	85
FIGURE 8.7: DEFLECTION AT MIDSPAN OF A BEAM WITH YIELD STRENGTH 2.85E6Pa DUE TO AN EXPLOSION AT 2 METERS ABOVE $x=0.25*L$	86
FIGURE 8.8: DEFLECTION AT MIDSPAN OF A BEAM WITH YIELD STRENGTH 2.85E6Pa DUE TO AN EXPLOSION AT 2 METERS ABOVE $x=0.125*L$	86
FIGURE 8.9: DEFLECTION AT MIDSPAN OF A BEAM WITH YIELD STRENGTH 7.35E5Pa DUE TO AN EXPLOSION AT 1 METERS ABOVE $x=0.5*L$	86
FIGURE 8.10: RELATIVE ERROR OF THE ESTIMATED DEFLECTION OBTAINED WITH THE SDOF MODEL COMPARED TO THE DEFLECTIONS OBTAINED WITH THE BLAST LOAD IN LS-DYNA FOR EXPLOSIONS AT DIFFERENT LOCATIONS (x;y;z).....	87
FIGURE 8.11: RELATIVE ERROR OF THE ESTIMATED DEFLECTION OBTAINED WITH THE SDOF MODEL COMPARED TO THE DEFLECTIONS OBTAINED WITH THE BLAST LOAD IN LS-DYNA FOR EXPLOSIONS AT 2M AND 3M HEIGHT ABOVE $x=1/4*L$, $3/8*L$ AND $1/2*L$	88
FIGURE 8.12: RELATIVE ERROR OF THE ESTIMATED DEFLECTION OBTAINED WITH THE SDOF MODEL COMPARED TO THE DEFLECTIONS OBTAINED WITH THE BLAST LOAD IN LS-DYNA FOR EXPLOSIONS AT 1M HEIGHT ABOVE $x=1/4*L$, $3/8*L$ AND $1/2*L$	88
FIGURE 8.13: RELATIVE ERROR OF THE ESTIMATED DEFLECTION OBTAINED WITH THE SDOF MODEL COMPARED TO THE DEFLECTIONS OBTAINED WITH THE BLAST LOAD IN LS-DYNA FOR EXPLOSIONS AT 2M AND 3M HEIGHT ABOVE $x=0$ AND $x=1/8*L$	88
FIGURE 8.14: RELATIVE ERROR OF THE ESTIMATED DEFLECTION OBTAINED WITH THE SDOF MODEL COMPARED TO THE DEFLECTIONS OBTAINED WITH THE BLAST LOAD IN LS-DYNA FOR EXPLOSIONS AT 1M HEIGHT ABOVE $x=0$ AND $1/8*L$	89

List of tables

TABLE 4.1: WEIGHTFACTORS FOR A BEAM WHICH HAS BEEN SPLIT INTO THREE PARTS	21
TABLE 4.2: WEIGHTFACTORS FOR A BEAM WHICH HAS BEEN SPLIT INTO SIX PARTS.....	22
TABLE 4.3: STIFFNESS, RESISTANCE AND LOAD-MASS FACTOR FOR A BEAM SUBJECTED TO A UNIFORM LOAD AND FOR A BEAM SUBJECTED TO A POINT LOAD	27
TABLE 4.4: RATIO BETWEEN THE DEFLECTION OF AN SDOF MODEL FOR A POINT LOAD AND A UNIFORM LOAD	28
TABLE 4.5: RATIO BETWEEN THE DEFLECTION OF AN SDOF MODEL FOR A LOCALLY LOADED AND A UNIFORMLY LOADED BEAM.....	28
TABLE 4.6: LOAD SCENARIOS WHICH SATISFY DIFFERENT MAXIMUM ALLOWED RATIO'S BETWEEN THE ACTUAL MAXIMUM BENDING STRESS OF AN ELASTIC SIMPLY SUPPORTED BEAM DUE TO THE EQUIVALENT UNIFORM STATIC LOAD	29
TABLE 5.1: LOAD SCENARIOS WHICH SATISFY DIFFERENT MAXIMUM ALLOWED RATIO'S BETWEEN THE EQUIVALENT UNIFORM LOAD FOR A BEAM WITH A "PLASTIC" SECTION AND A BEAM WITH A CONTINUOUS STIFFNESS.....	40
TABLE 6.1: RELATIVE ERROR WHICH HAS BEEN CAUSED DUE TO SIMPLIFICATION OF THE LOAD	47
TABLE 6.2: ACCURACY OF THE DEFLECTION AT MIDSPAN. $\Delta x = L/4$	48
TABLE 6.3: RELATIVE ERROR OBTAINED BY SPLITTING A SIMPLY SUPPORTED BEAM INTO 4 PARTS	50
TABLE 6.4: RELATIVE ERROR OBTAINED BY SPLITTING A SIMPLY SUPPORTED BEAM SUCH THAT THE LOAD IS COVERED BY 2 PARTS	50
TABLE 6.5: RELATIVE ERROR OBTAINED BY SPLITTING A SIMPLY SUPPORTED BEAM SUCH THAT THE LOAD IS COVERED BY 3 PARTS	51
TABLE 6.6: RELATIVE ERROR OBTAINED BY SPLITTING A SIMPLY SUPPORTED BEAM SUCH THAT THE LOAD IS COVERED BY 4 PARTS	51
TABLE 6.7: LOAD SCENARIOS WHICH SATISFIES DIFFERENT MAXIMUM ALLOWED ERRORS OF THE ESTIMATED DEFLECTION AT MIDSPAN	52
TABLE 7.1: RATIO BETWEEN THE IMPULSE OF THE EQUIVALENT LOAD AND THE IMPULSE OF THE BLAST OF 1KG TNT EQUIVALENT AT 1 METER HEIGHT ABOVE DIFFERENT LOCATIONS ALONG THE LENGTH OF THE BEAM.....	59
TABLE 7.2: RATIO BETWEEN THE IMPULSE OF THE EQUIVALENT LOAD AND THE IMPULSE OF THE BLAST OF 1KG TNT EQUIVALENT AT 2 METER HEIGHT ABOVE DIFFERENT LOCATIONS ALONG THE LENGTH OF THE BEAM.....	59
TABLE 7.3: PROPERTIES OF THE INVESTIGATED BEAM.....	61
TABLE 7.4: RATIO BETWEEN MAXIMUM OCCURRING VON MISES STRESSES DUE TO THE EQUIVALENT UNIFORM LOAD AND THE NON- UNIFORM BLAST LOAD. (USING 240 PARTS).....	64
TABLE 7.5: INVESTIGATED SCENARIO'S WITH DIFFERENT T_D/T_N RATIO'S	74

List of Symbols

Blast wave

t	time [s]
t_a	time arrival of blast wave [s]
p	pressure [Pa]
P_0	ambient pressure [Pa]
p_s^+	peak overpressure (resp. to ambient pressure) due to a blast wave [Pa]
p_s^-	peak under pressure (resp. to ambient pressure) due to a blast wave [Pa]
p_r	peak positive reflected overpressure [Pa]
p_s	positive incident (or side-on) overpressure [Pa]
T^+	positive phase of the blast wave [s]
T^-	negative phase of the blast wave [s]
R	distance from the explosive [m]
d	diameter of the explosive [m]
I_s^+	positive impulse of a blast wave [N.s]
I_s^-	negative impulse of a blast wave [N.s]
b	parameter which allows freedom in matching I_s^+ , I_s^- and initial decay rate [-]
α	angle of incident of the blast wave [°]
Z	scaled distance [$\text{m.kg}^{-1/3}$]
W	equivalent TNT charge mass [kg]
U_s	blast wave front velocity [m/s]
U_r	reflected blast wavefront speed [m/s]
U_m	Mach stem wavefront speed [m/s]

SDOF

M	mass [kg]
K	stiffness [N/m]
F	load [N]
R	resistance [N]
R_u	maximum resistance [N]
x	deformation [m]
x_{el}	elastic deformation limit [m]
M_e	equivalent mass [kg]
F_e	equivalent load [N]
K_e	equivalent stiffness [N/m]
R_e	equivalent resistance [N]
K_{el}	elastic stiffness [N/m]
K_M	mass factor [-]
K_L	load factor [-]
K_{LM}	load-mass factor [-]
$\varphi(x)$	shape function [-]
$W_{max,lsdyna(blast)}$	max. obtained deflection with the SDOF model [m]

Beam

E	Young's modulus [N/mm ²]
I	second moment of area [mm ⁴]
ρ	density [kg/m ³]
l	length [m]
A	cross-sectional area [m ²]
w	deflection [m]
w_0	max. deflection [m]
$w_{approximate}$	approximated deflection [m]
w_{exact}	exact deflection [m]
w_{el}	elastic deformation limit of a static uniformly loaded beam [m]
$w_{max,lsdyna(blast)}$	max. obtained deflection in LS-DYNA using the blast load [m]
$w_{max,lsdyna(uniform)}$	max. obtained deflection in LS-DYNA using the equivalent uniform load [m]
$w_{max,SDOF}$	maximum obtained deflection with the SDOF model [m]
q	distributed load [N/m]
t_d	load duration [ms]
M_{max}	max. occurring bending moment [Nm]
M_p	plastic moment capacity [Nm]
f	weightfactor [-]
$f_{stress,max}$	stressfactor [-]
Δx	the size of the parts for determining weightfactors [m]
j	width of the section with reduced bending stiffness [m]
h	size of the loaded part(s) [m]
a	distance between the loaded part and the left support [m]
T	period [ms]
T_n	fundamental period [ms]

Errors

$error_{lsdyna,uniform}$	error of the estimated deflection at the centre of a beam subjected to an equivalent uniform load [%]
$error_{SDOF,uniform}$	error of the estimated deflection using the SDOF model compared with the deflection at the centre of a beam subjected to an equivalent uniform load using FEM [%]
$error_{SDOF,blast}$	error of the estimated deflection using the SDOF model compared with the deflection at the centre of a beam subjected to a blast load using FEM [%]

1.1 Problem definition

To model the response of a wall subjected to explosions, single-degree-of-freedom (SDOF) systems are being used. At the moment an SDOF model is in particular suitable for simple structural components under more or less uniform loads. This is for the situation in which the explosion is at great distance. To use an SDOF model for explosions at shorter distances or in enclosed rooms, which give non-uniformly distributed loads, it is more complicated to determine an equivalent load input for the SDOF model. For a calculation with the SDOF model a representative load is needed. A second simplification which results in a deviation from the exact solution is the neglect of higher order vibration modes with the SDOF model.

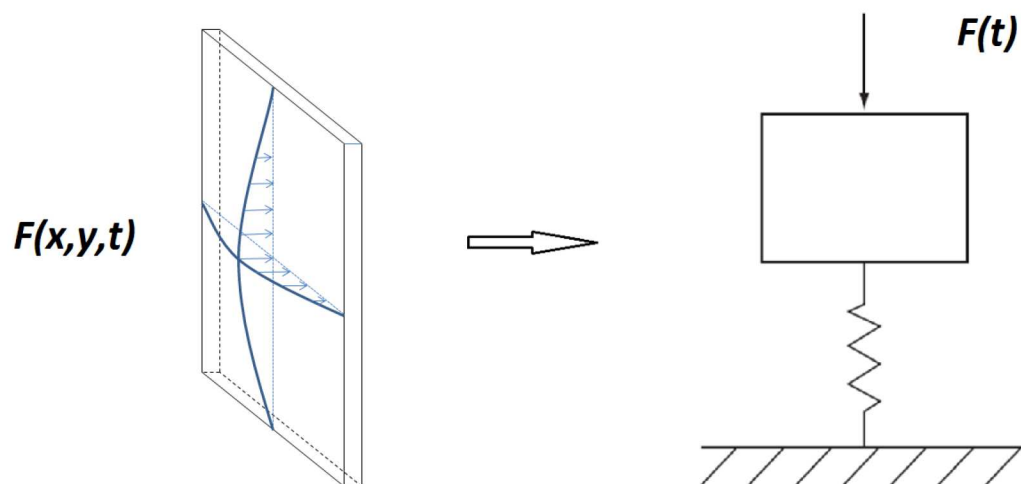


Figure 1.1: Idealization of a non-uniform loaded plate as a mass-spring-system

1.2 Research objective

A solution to determine an equivalent load for use with the SDOF model may be to calculate the value of the blast load at several locations on the wall and multiply these values with factors which translate the non-uniformly distributed load to an equivalent uniformly distributed load. With SDOF models failure of a component is usually based on a maximum deflection, therefore the factors for determining an equivalent uniform load are determined such that they give the same deflection at the centre of the component.

In this research the translation of a blast load acting on an elastic-plastic beam to an equivalent uniform load has been investigated.

1.3 Research scope

The research's main focus will lie on the determination of factors which translate a non-uniform load to an equivalent uniform load and the accuracy of the estimated deflections and stresses. The factors are determined based on the criterion that they give the same deflection at the centre of a linear elastic beam subjected to static loading, since with an SDOF model dynamic load factors are applied afterwards.

In this research the following questions have been investigated:

- In which load regime is it possible to apply the translation factors? In other words how much may the load deviate from uniform?
- Of what order are the errors of the made estimations?
- What are the influences of the material deformation properties (linear elastic vs plastic)?
- In how many elements needs the beam to be divided?

1.4 Method of approach

In Figure 1.2 the approach of the research is given in a flowchart. The research can be divided into 5 parts:

- I. Literature/Background study (chapters 2 – 3)
- II. Determination of the weightfactors and their applicability (chapters 4 – 5)
- III. Accuracy of the LS-DYNA estimations (chapters 6 – 7)
- IV. Accuracy of the SDOF estimations (chapter 8)
- V. Conclusion and recommendations (chapter 9)

Part I - Literature/background study

In the first part a brief introduction of blast loading (Chapter 2) and the SDOF model (Chapter 3) is given. In Chapter 3 available theoretical studies on how an equivalent load for the SDOF model can be determined are reviewed.

Part II - Determination of the weightfactors and their applicability

Part II consists of analytical calculations for static loading. These calculations are done to determine:

- a) The weightfactors for a simply supported beam
- b) Usability of the weightfactors

Step 1: Weightfactors

The first step is to determine the weightfactors for a simply supported beam. Weightfactors can translate a non-uniform load to a uniform load and are determined such that the uniform load will result in the same deflection at the centre of a statically loaded linear elastic beam. The process is described in Chapter 4.

Step 2: Stresses

An equivalent load obtained with the weightfactors results in different bending stresses. In Chapter 4 it has been investigated for several load cases how large the differences between the maximum

bending stresses of a simply supported beam are and what this means for the usability of the weightfactors.

Step 3: Plasticity

Since it is not known in advance where and how much yield will occur due to a blast load, a simplification of the yielded section has been made. In Chapter 5 for a beam with a fictive yielded section, the weightfactors have been determined analytically. This way it can be determined how the weightfactors could change if plasticity occurs. This investigation has been done to see if the elastic weightfactors can be used in case of plastic deformation.

Part III - Accuracy of the LS-DYNA estimations

The objective of part III is to determine:

- a) The accuracy of the estimated deflections and stresses obtained with the equivalent uniform load including higher order vibration modes
- b) The amount of parts in which the beam needs to be divided to determine an equivalent uniform load which results in accurate estimations.
- c) The influence of the material deformation properties (elastic versus elastic-plastic)

Part III consists of static (analytical) and dynamic (FE) calculations. The following steps are done in part III:

Step 1: Accuracy static response

When a non-uniform load is translated to a uniform load an approximation is made. The accuracy depends on the amount of parts in which the non-uniform load has been split to determine the equivalent uniform load. In Chapter 6 it has been investigated how accurate the weightfactors can estimate the deflection at the centre of a beam for different fictive non-uniform load distributions and into how many parts the beam needs to be split to obtain accurate estimations.

Step 2: Accuracy dynamic response

In Chapter 7 it has been Investigated how accurate the equivalent load, which is obtained with the weightfactors, can estimate the deflections and the stresses of a (elastic + plastic) beam subjected to blast loading.

Part IV - Accuracy of the SDOF estimations

The objective of part IV is to determine the accuracy of the estimations which are obtained with the SDOF model

In Chapter 8 the SDOF model is used to simulate the response of a beam subjected to equivalent uniform loads determined in part III. Using the SDOF model several simplifications, like neglecting higher order vibration modes, are made. To determine the effect of this approach, the estimations obtained with the SDOF model are compared with the response of a beam subjected to the equivalent uniform load in LS-DYNA and with the response of a beam subjected to the non-uniform blast load in LS-DYNA.

Part V – Conclusions and recommendations

In the final part of this report, Chapter 9, the research questions are answered and the conclusions and recommendations are presented.

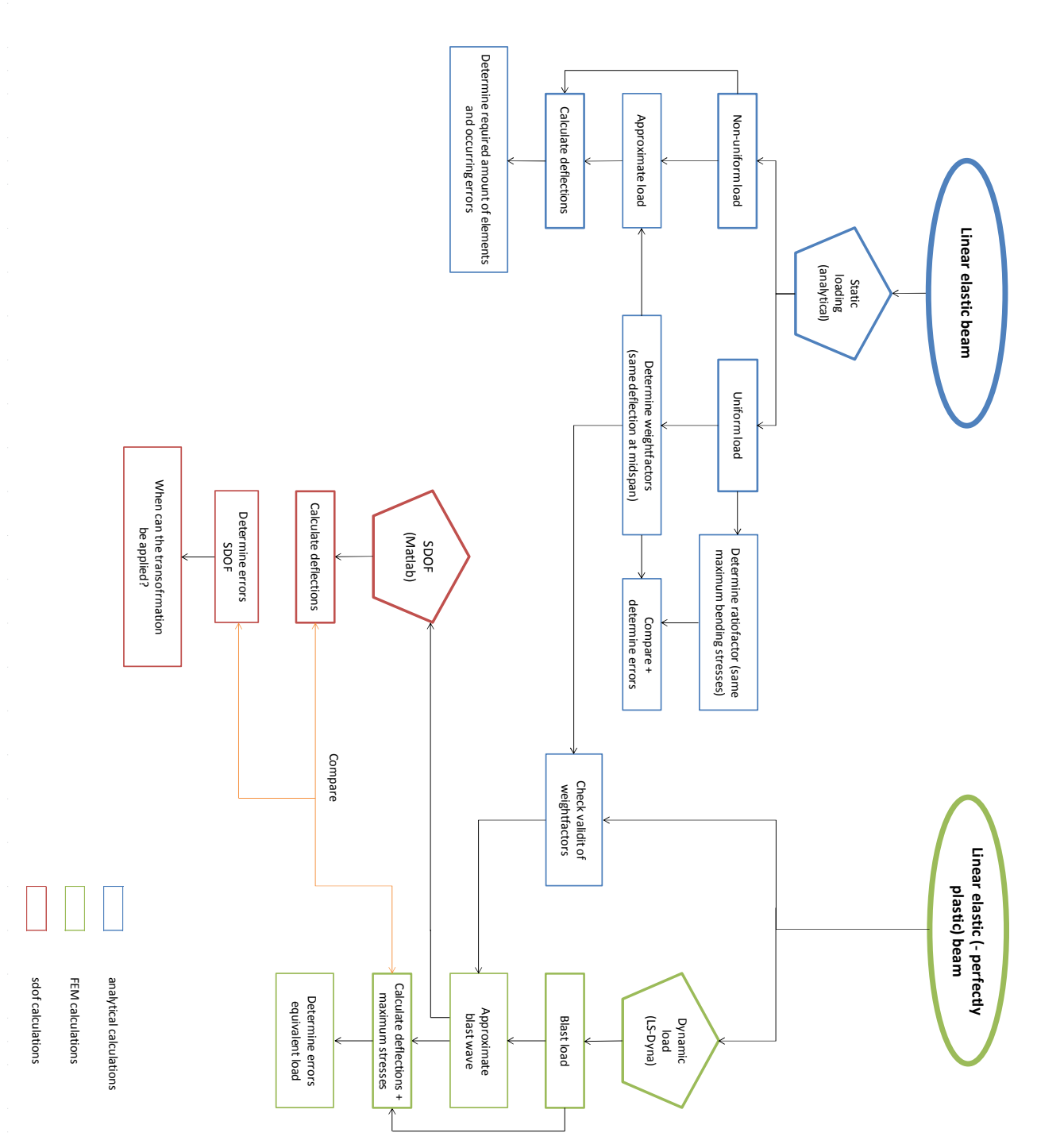


Figure 1.2: Research approach

Part I
Literature/background study

In this research the SDOF model will only be used for blast loading (i.e. the load caused by a blast wave). In this chapter a general introduction is given to Blast loading.

2.1 Explosion

An explosion is defined as the release of energy over a sufficiently small time and in a sufficiently small volume so as to generate a pressure wave [1]. A blast wave is the pressure which results after an explosion with a high energy density and power. The shock front propagates supersonically, faster than sound, in the air.

2.2 Ideal blast waves

It is assumed that the explosion occurs in a still homogeneous atmosphere and that the source is spherically symmetric. From these assumptions it follows that the blast wave is a function of time and distance from source only. In Figure 2.1 it is illustrated how the peak overpressure decreases over the distance. At a fixed distance from the source, R , the graph of the idealized pressure profile will look like the graph in Figure 2.2. At the arrival time t_0 of the pressure wave, the pressure rises instantaneously to the peak value $P_0 + P_s^+$, where P_0 is the ambient pressure and P_s^+ the peak overpressure. The pressure then decays to ambient in time T^+ , the positive phase. After the positive phase the pressure drops to a partial vacuum of $p_0 - p_s^-$ and then returns to ambient in time T^- , the negative phase [2].

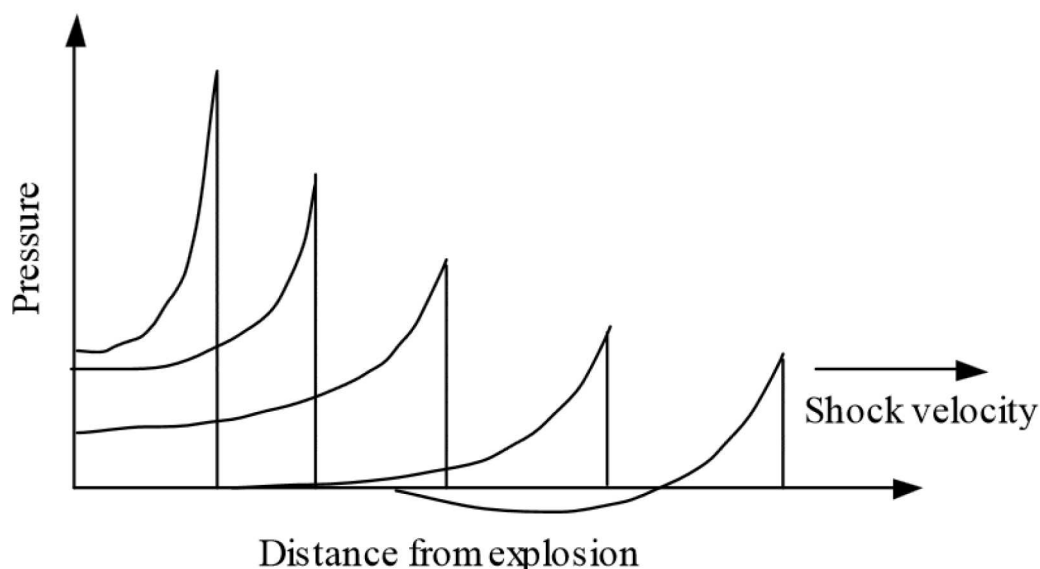


Figure 2.1: Blast wave propagation

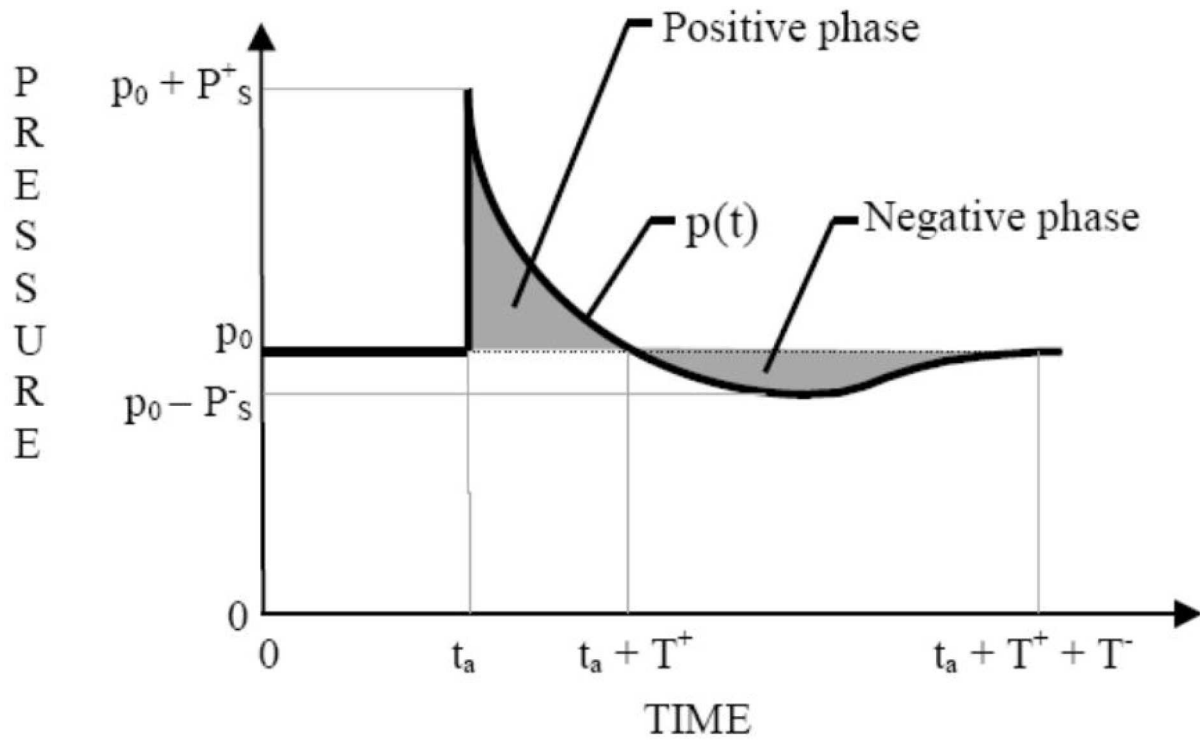


Figure 2.2: Ideal blast wave profile

The positive and negative impulses (I_s^+ and I_s^-) are defined by the area under the positive and negative phase of the pressure time curve:

$$I_s^+ = \int_{t_a}^{t_a + T^+} (p(t) - p_0) dx \quad (2.1)$$

$$I_s^- = \int_{t_a + T^+}^{t_a + T^+ + T^-} (-p(t) + p_0) dx \quad (2.2)$$

In this research LS-DYNA has been used to compute simulations with non-uniform blast loading. LS-DYNA is a finite element program for general-purposes and can be used for simulating the response of a component subjected to blast loading. In LS-DYNA the modified Friedlander equation has been used to describe the decay of blast waves [3]:

$$p(t) = p_0 + P_s \cdot \left(1 - \frac{t}{T^+}\right) \cdot e^{-\frac{bt}{T^+}} \quad (2.3)$$

Where

t measured from time of arrival t_a

b parameter which allows freedom in matching I_s^+ , I_s^- and initial decay rate [-]

The modified Friedlander equation is a commonly used equation to describe the decay of blast waves. It is a simple equation which allows accurate matching with observed parameters.

2.3 Reflection and diffraction

Blast waves will be affected when they encounter any solid or dense objects. Reflections from and diffraction around this object happen. Depending on the angle of incidence, α , the wave will be differently reflected. When α is 90° (parallel to the surface) there is no reflection and the surface is only loaded by the incident overpressure. When $0 < \alpha < 40^\circ$ normal reflection happens. When α exceeds 40° , Mach reflection occurs. Mach reflection is a complex process. It can be described as an effect where the incident wave skims of the reflecting surface. The reflected wave catches up with and fuses with the incident wave causing a third wave front, the Mach stem [4].

To calculate the peak pressure and impulse of a blast wave the used module in LS-DYNA takes into account the angle of incidence of the wave, but neglects the effect of diffraction around objects.

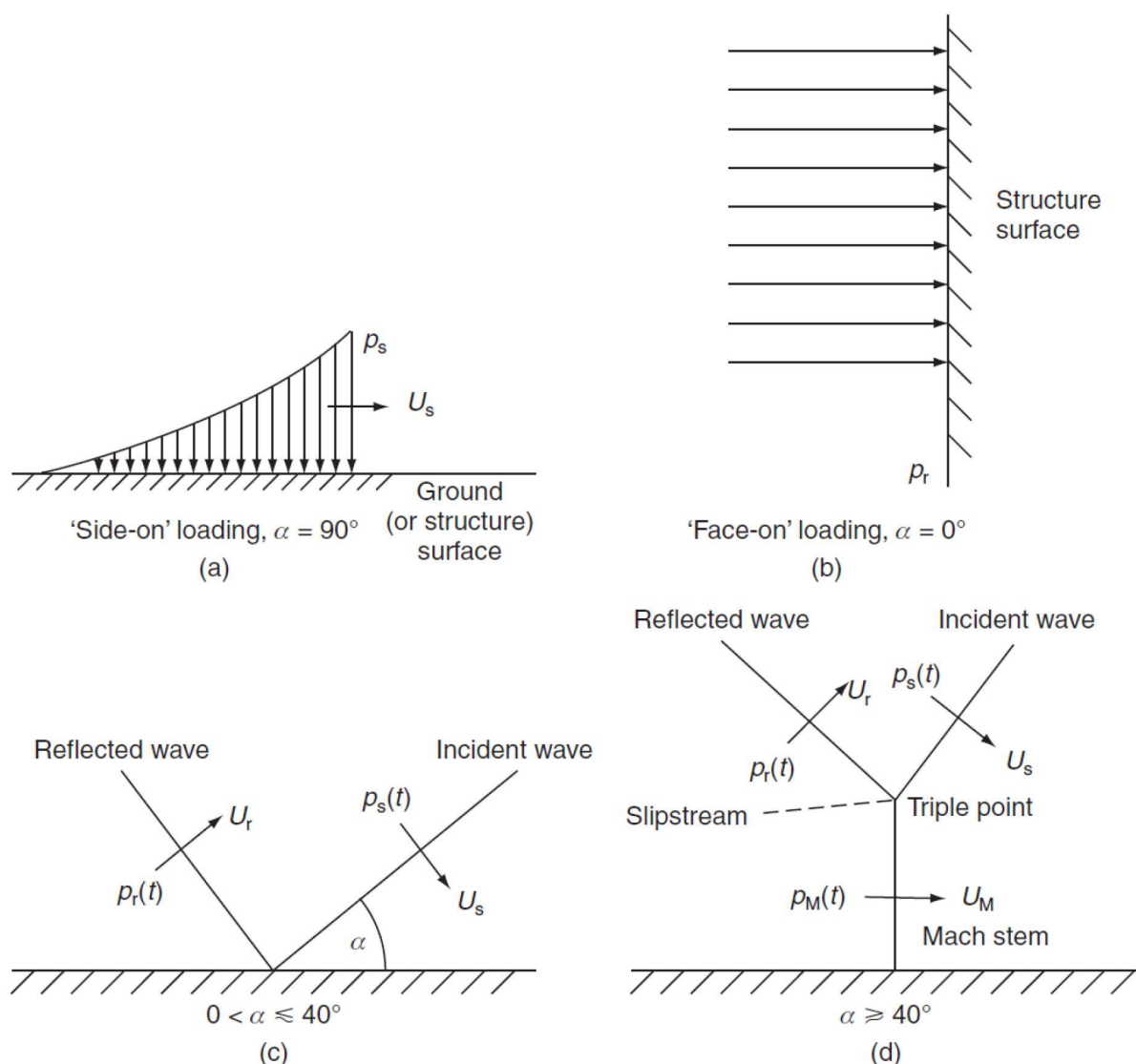


Figure 2.3: a) Blast parallel to the surface b) Blast wave perpendicular to the surface c) Blast wave at an angle between 0 and 40° d) Blast wave at an angle between 40 and 90° .

2.4 Scaling

To predict the properties of blast waves of different sizes, scaling laws are commonly used. The Hopkinson-Cranz scaling is the most widely used approach to blast wave scaling [2]. It is a cube root scaling, which states that if both the distance and mass of an explosion are multiplied by a factor lambda, the impulse and the duration are increased with lambda as well, but the peak overpressure remains be the same.

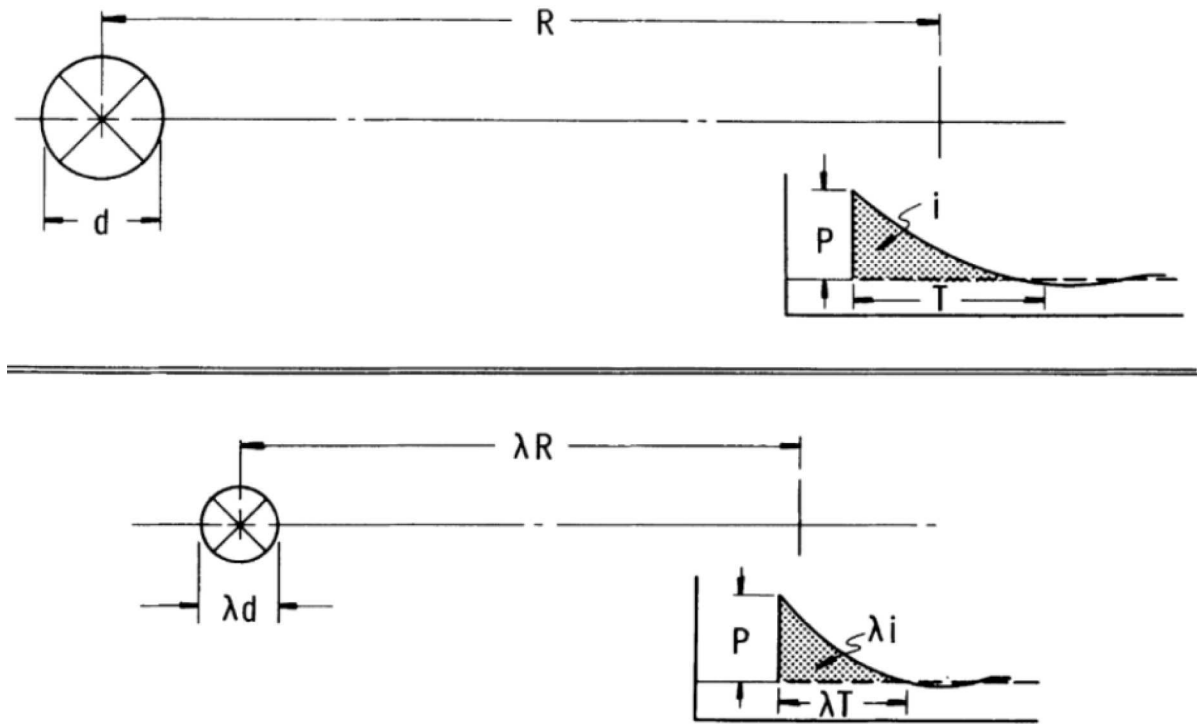


Figure 2.4: Scaling of a blast wave

The Hopkinson-Cranz approach can be used to calculate a scaled distance:

$$Z = R \cdot W^{-\frac{1}{3}} \quad (2.4)$$

Where:

R = distance from the centre of a spherical [m]
 W = equivalent TNT charge mass [kg]

Brode's formula can then be used to determine the resulting peak overpressure [4]:

$$P_s^+ = \frac{6.7}{Z^3} + 1 \quad \text{for } P_s^+ > 10 \text{ [bar]} \quad (2.5)$$

$$P_s^+ = \frac{0.975}{Z} + \frac{1.455}{Z^2} + \frac{5.85}{Z^3} - 0.019 \quad \text{for } 0.1 < P_s^+ < 10 \text{ [bar]} \quad (2.6)$$

Chapter 3

The SDOF model

In order to predict if constructions are able to withstand a blast load (which is the load of an explosion) analyses are carried out. In general, the following analysis methods are used:

- FEA: Numerical methods can be used to simulate the behaviour of a construction subjected to a blast load. These analyses give accurate and extensive results. To perform a finite element analysis a lot of time and expertise is required.
- SDOF model: The simplest way to model the response to a blast load is by making use of a single-degree-of-freedom model. This model schematizes the structure as a mass-spring-system. Reasonably accurate results are obtained this way. To run an analysis with the SDOF model little time is required. For the input only a few parameters are needed.
- MDOF-model: This technique has several advantages over SDOF analyses. It can give more accurate and more reliable results in several cases. MDOF- analyses can be used to determine the interaction between individual responses of several components in a system. Compared to a combination of individual SDOF analyses, an MDOF-model gives a better global behaviour of the system. However, MDOF-analyses require more time to execute, partly because it is more complex and partly due to the more parameters needed to run the model.

Executing an SDOF model requires less time, is easier to set up compared to an MDOF-model and gives reasonably accurate results. Therefore, TNO has chosen to set up an SDOF model to analyse the effect of blast loading on walls. This model is still in development. The weightfactors that are determined in this research will give directions how to use the SDOF model in order to get reliable results. In this chapter a brief introduction to the SDOF model is presented. It is explained what an SDOF model is, how it works and what input is required to compute simulations.

3.1 Mass-spring-system

The midpoint deflection of a structural component can be represented by the response of an equivalent mass-spring system. A mass-spring-system has one single degree of freedom. To define a mass-spring system a mass, stiffness and load input is needed. A blast wave is a non-oscillatory load with a very high peak and a duration in the order of milliseconds. To determine failure of the component, for this kind of loading, only the maximum response is needed. Therefore, structural damping can be ignored [3]. The mass, stiffness and load of the mass-spring-system are not the same as the mass, stiffness and load of the actual component. In order to make the SDOF model respond in the same way as the actual system translation factors need to be determined. Assumptions of the deflected shape need to be made in order to determine these factors [5].

In the following subparagraphs the derivation procedure of the translation factors is described [5].

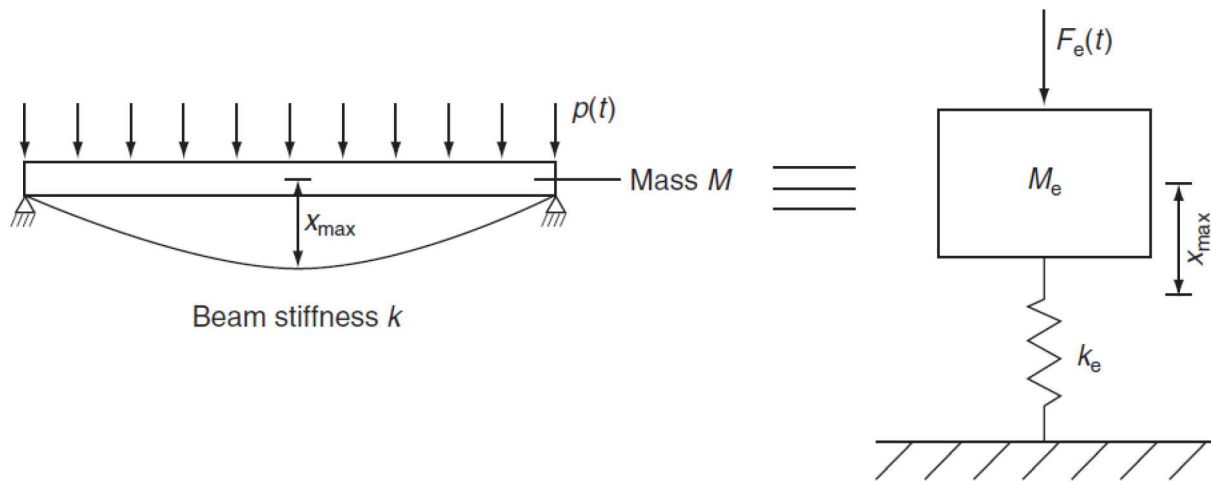


Figure 3.1: Equivalent mass-spring-system

Equation of motion of the equivalent mass-spring-system:

$$M_e \left(\frac{d^2}{dt^2} x(t) \right) + K_e x(t) = F_e(t) \quad (3.1)$$

3.1.1 Equivalent mass

By equating kinematic energies of the systems it follows that the equivalent mass can be calculated as:

$$M_e = \int_0^l m \phi(x)^2 dx \quad (3.2)$$

Where m is the mass per length and $\phi(x)$ the (unit) shape function of the structural component and l the length of the beam. The mass factor is defined as the ratio between equivalent mass and the actual mass of the structural component. The mass factor can be calculated as:

$$K_M = \frac{M_e}{M} = \frac{\int_0^l m \cdot \phi(x)^2 dx}{m \cdot l} \quad (3.3)$$

3.1.2 Equivalent load

By equating work by external forces it follows that the equivalent load can be calculated as:

$$F_e = \int_0^l q \cdot \phi(x) \, dx \quad (3.4)$$

Where q is the load per length on the structural component. The load factor is defined as the ratio between equivalent load and the actual load of the structural component. The load factor can be calculated as:

$$K_L = \frac{F_e}{F} = \frac{\int_0^l q \cdot \phi(x) \, dx}{q \cdot l} \quad (3.5)$$

3.1.3 Equivalent resistance

By equating strain energies of the systems it follows for the equivalent stiffness that:

$$k_e = \int_0^l k(x) \phi(x)^2 \, dx \quad (3.6)$$

Where:

$k(x)$ = stiffness at location x

The resistance of the structural component is the internal forces trying to restore the component to its unloaded static position. In case of static loading it holds that:

$$M \left(\frac{d^2}{dt^2} x(t) \right) = 0 \quad (3.7)$$

And the equation of motion becomes:

$$F = k \cdot x \quad (3.8)$$

It follows that the resistance-factor, defined as the ratio between equivalent resistance and the actual resistance of the structural component, is always the same as the load factor. The dynamic equation of motion of the equivalent SDOF system is given by:

$$K_M M \left(\frac{d^2}{dt^2} x(t) \right) + K_L K x(t) = K_L F(t) \quad (3.9)$$

3.1.4 Load-mass factor

To create an equivalent mass-spring-system it is sufficient to determine a load-mass factor, since the equivalent load and equivalent stiffness are obtained by multiplying the actual load and actual stiffness by the same factor. The load-mass factor is defined as:

$$K_{LM} = \frac{K_M}{K_L} \quad (3.10)$$

The equation of motion for the equivalent mass-spring-system can be written as:

$$K_{LM}M \left(\frac{d^2}{dt^2} x(t) \right) + Kx(t) = F(t) \quad (3.11)$$

Elastic deformation

The fact that the Eigen frequency of the equivalent system must be the same as that of the actual structural component leads to a second way of determining the load-mass factor. Neglecting shear deformation, in the elastic regime the natural frequencies of the first mode of a simple supported beam and a fixed beam are given by [7]:

Simply supported beam:
$$\omega = \pi^2 \cdot \sqrt{\frac{EI}{\rho A l^4}} \quad (3.12)$$

Beam fixed at both ends:
$$\omega = 4.73004^2 \cdot \sqrt{\frac{EI}{\rho A l^4}} \quad (3.13)$$

Where EI is the bending stiffness [N/mm^2], ρ the density [kg/m^3] and A the cross-sectional area [m^2]. The natural frequency of the mass-spring-system is calculated by:

$$\omega = \sqrt{\frac{K_e}{M_e}} = \sqrt{\frac{K}{K_{LM}M}} \quad (3.14)$$

By equating the natural frequency of the structural component and of the mass spring system the load-mass factor for a simple supported beam and a fixed beam can be determined. For vibration in the first mode it follows that:

Simply supported beam:
$$K_{LM} = \frac{384}{5\pi^4} \quad (3.15)$$

Beam fixed at both ends:
$$K_{LM} \approx 0.7671 \quad (3.16)$$

In the past in many textbooks, manuals and computer programs tables with mass-, load- and load-mass factors for beams and plates with different boundaries from EM 1110-345-416 have been copied. However the mass- and load factor in these tables were rounded to two decimal places and the rounded values have been used to calculate the load-mass factor [8]. This led to slightly different values than the values presented above.

Plastic deformation

Since modal analysis is a linear analysis, the formulas for the natural frequencies don't hold when plasticity occurs. In this case to determine the load-mass factor the equivalent mass and equivalent load need to be calculated first. For a simply supported beam an example calculation is given below.

To determine the equivalent mass and load an assumption has been made of the deformation shape:

$$w = \frac{2 \cdot w_0 \cdot x}{l} \quad \text{for } 0 \leq x \leq l/2 \quad (3.17)$$

$$w = 2 \cdot w_0 \cdot \left(1 - \frac{x}{l}\right) \quad \text{for } l/2 \leq x \leq l \quad (3.18)$$

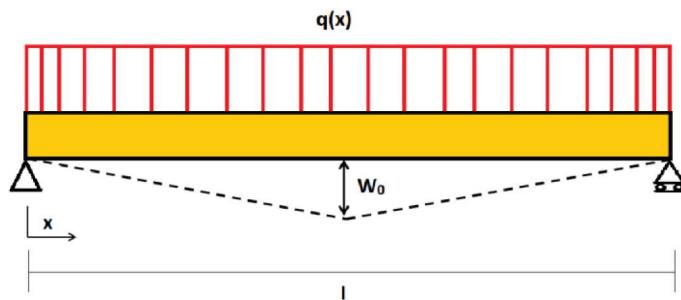


Figure 3.2: Assumed plastic deformation shape with a hinge at midspan

The equivalent mass and load can be calculated as:

$$M_e = \int_0^l \rho A \phi(x)^2 dx = \frac{1}{3} \rho A l = \frac{1}{3} M \quad (3.19)$$

$$F_e = \int_0^l q(x) \phi(x) dx = \frac{1}{2} q l = \frac{1}{2} F \quad (3.20)$$

From which follows:

$$K_{LM} = \frac{2}{3} \quad (3.21)$$

Part II
**Determination of the weightfactors and their
applicability**

Chapter 4

Analytical calculation of the weightfactors of a beam

To compute simulations with the SDOF model, non-uniform load distributions have been translated to equivalent uniform loads using weightfactors. In this chapter it is explained how the weightfactors have been determined for a beam.

The weightfactors are determined based on the criterion that they should introduce the same deflection at midspan. The occurring bending stresses however are not equal to the bending stresses of the actual situation. It has been investigated how large the differences between the maximum bending stresses are and what this means for the usability of the weightfactors.

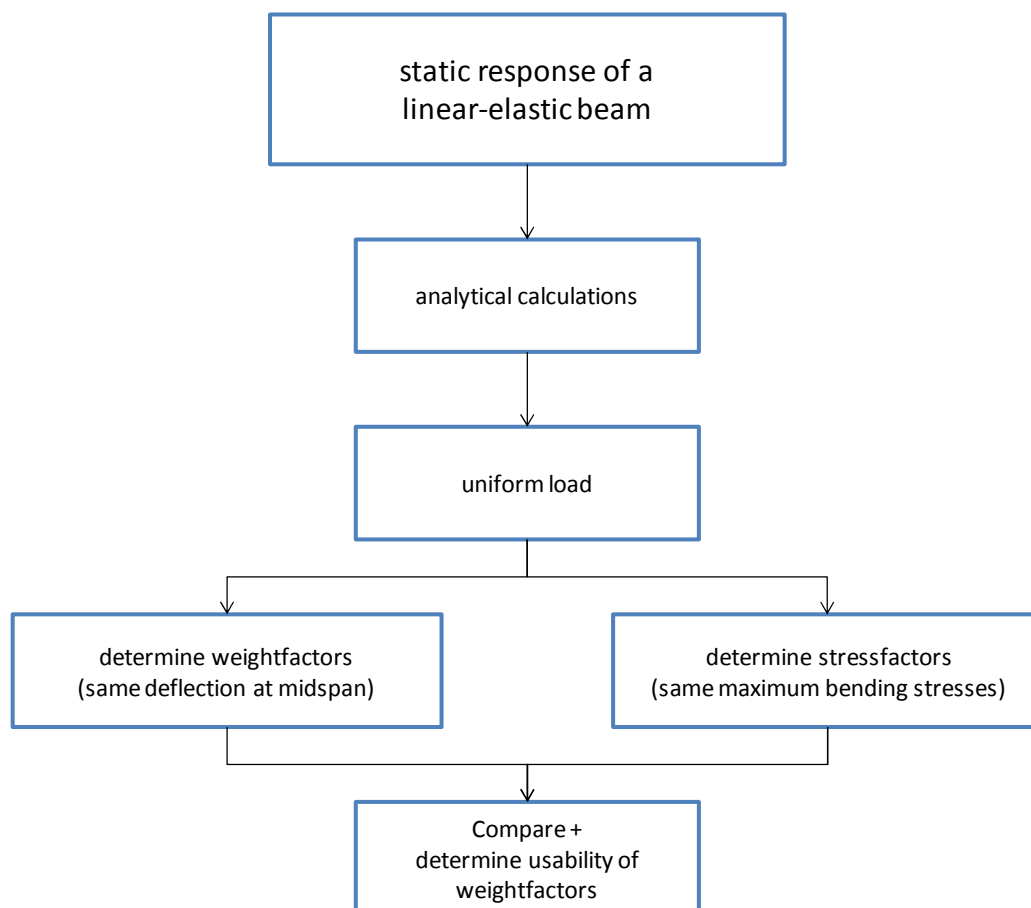


Figure 4.1: Flowchart Chapter 4

4.1 Current approach (beamblast + SDOF)

To give an idea what the actual use is of the weightfactors it is explained how the simulation of walls subjected to blast loading is currently being approached and how this could be improved.

4.1.1 Beamblast model

The Beamblast model is used to determine the load input for the SDOF model. To determine the load the user needs to define a wall in a room and the location of the sensor. The Beamblast model determines the load on the wall at the location of the sensor. In the Beamblast model various parameters can be changed, e.g.:

- The dimensions and shape of the room;
- The dimensions of the wall;
- The location of the sensor(s);
- The number of reflections inside the room that should be taken into account;
- Openings in the room.

4.1.2 Single-degree-of-freedom model

The load determined with the Beamblast model is then used as input for the SDOF model. To determine the total displacement at the middle of the component, the SDOF model assumes the load to be uniformly distributed over the entire wall.

The value of the actual non-uniform blast load at a single point of the wall is being used as a representative value for the size of the equivalent uniform load. Usually this point is chosen at the location where the user thinks the load is the highest. For close explosions, asymmetric explosions and explosions in enclosed rooms this might not be an accurate approximation. In this research it is investigated how accurate an equivalent load, based on the value of the blast load at several locations on the wall, can estimate the response of a wall subjected to blast loading.

4.2 Equivalent uniform load

A blast wave often results in a non-uniform in time varying load on the component. This non-uniform load needs to be translated to an equivalent uniform load. There are different ways to determine an equivalent uniform load. A simple approach is to calculate the blast load at midspan on the component and use this as an equivalent uniform load over the entire component. This method can be used when the blast load doesn't vary too much over the middle two thirds of the components span length (which usually is the case if the scaled standoff to midspan is greater than approximately 1.2 to $2.0 \text{ m/kg}^{1/3}$) [9]. Loading near the midspan region has a greater effect on the dynamic response than loading applied near the supports, similar to static loading. However, at very small scaled standoff in the range of 0.4 to $0.8 \text{ m/kg}^{1/3}$ localized shearing and breaching effects can occur [9]. Other simple ways to determine an equivalent load are by using a weighted average over a specified area or by choosing the largest pressure or impulse on the component.

J. C. Gannon, K. A. Marchand & E. B. Williamson [10] researched a method which replaces the blast load by both a work equivalent uniform load and three uniformly distributed loads of variable size. They used this method to determine the maximum displacement of a girder subjected to an

explosion with a distance of 12 and 20 feet ($\approx 3.7\text{m}$ and 6.1 meters) on span girders of 80, 120 and 160 feet (≈ 24.3 , 36.6 and 48.8 meters). Errors up to 40% were obtained.

The objective researched in this project is somewhat similar to that of Gannon et al, but a different approach is investigated.

4.3 Weightfactors

To make the translation from a non-uniform load to an equivalent uniform load, weightfactors have been determined. The weightfactors are based on static loading and linear-elastic deformation is assumed. The weightfactors are determined as follows:

1. The uniform load is divided into several equal parts
2. For each load part the deflection of the beam at midspan is calculated
3. For each load part it is determined what uniform load results in the same deflection at midspan
4. A weightfactor is the ratio between the uniform load and the actual load of the corresponding part

In Appendix B1 an example is presented of a calculation for the weightfactors for a simply supported beam which is divided into 10 parts.

In Figure 4.2 an illustration is shown how the weightfactors are determined. The total equivalent uniform load is the sum of the product of the load and the corresponding weightfactor.

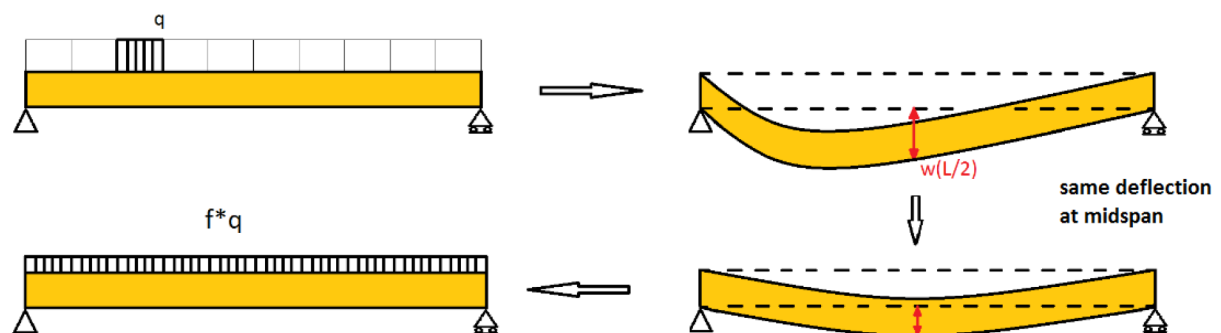


Figure 4.2: Determining an equivalent uniform load

For a division into 3 and 6 parts the weightfactors are shown in Table 4.1 and Table 4.2. It can be seen that the weightfactors and thus the equivalent load depends on the boundary conditions.

Part	Weightfactor (pinned ends)	Weightfactor (fixed ends)
1 of 3	$20/81$	$16/81$
2 of 3	$41/81$	$49/81$
3 of 3	$20/81$	$16/81$

Table 4.1: Weightfactors for a beam which has been split into three parts

Part	Weightfactor (pinned ends)	Weightfactor (fixed ends)
1 of 6	53/810	5/162
2 of 6	49/270	1/6
3 of 6	41/162	49/162
4 of 6	41/162	49/162
5 of 6	49/270	1/6
6 of 6	53/810	5/162

Table 4.2: weightfactors for a beam which has been split into six parts

4.4 Bending stresses

By using the weightfactors, the same deflection of a beam at midspan is obtained for a uniform load and for a partially uniformly distributed load. However, the occurring maximum stresses are not the same if the weightfactors have been used. It has been investigated what the ratio between the maximum occurring stresses is for a partially (uniform) loaded beam and an entirely (uniform) loaded beam (which is linearly related to the maximum moments). This ratio is called the stressfactor.

The location of the maximum occurring bending stress is dependent on the location and size of the partially distributed load. Therefore, the sum of the stressfactors for individual loads is not the same as the stressfactor for the sum of the loads.

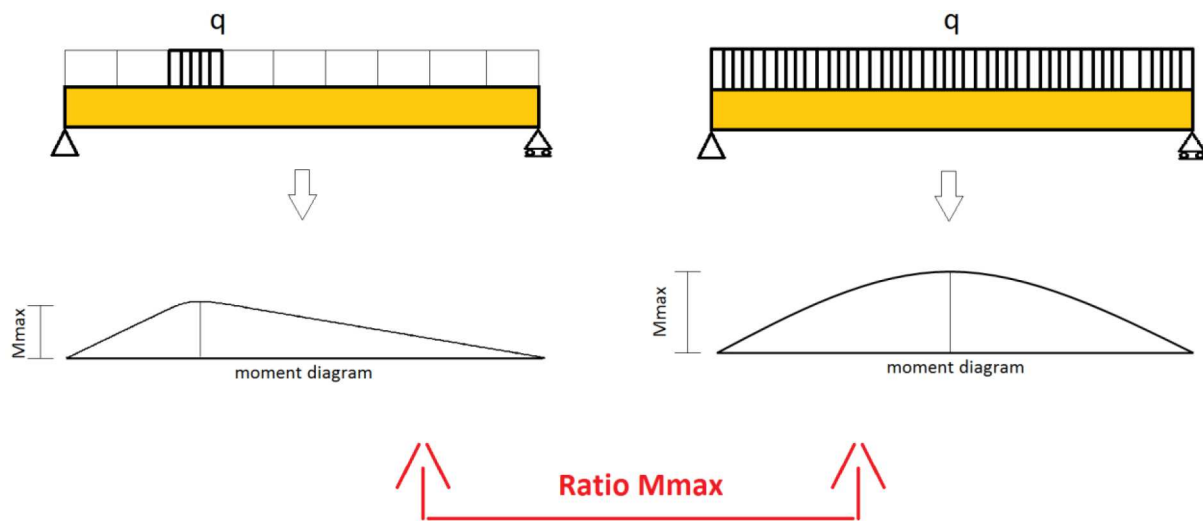


Figure 4.3: Moment diagram for uniformly distributed load. Left partially loaded and right entirely loaded

Where:

M_{max} = Maximum occurring bending moment

With the following formula the ratio between the maximum bending stresses can be calculated. For both situations a load of 1 N/m has been applied. See appendix C for its derivation.

$$f_{stress,max} = \frac{q^2}{(h - 2l)(h + 2a)(-2l + 2a + h)h} \quad (4.1)$$

Where:

$f_{stress,max}$ = stressfactor: ratio between the maximum bending stresses due to a partially distributed uniform load (q) and an entirely distributed uniform load (q)
 l = length of the beam [m]
 h = size of the part over which the uniform load is distributed [m]
 a = distance between the loaded part and the left support [m]

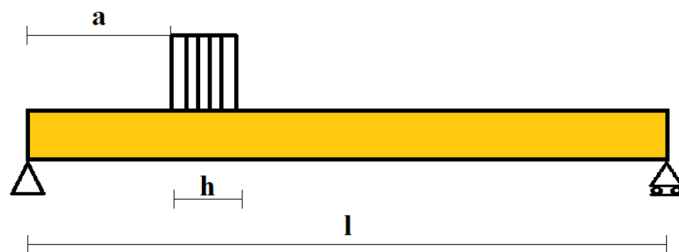


Figure 4.4: Load scenario

For the following three load scenarios the stressfactors have been investigated:

1. Partially distributed uniform load at the centre of the beam: the loaded part (h) will be increased till the boundaries are reached. The deformation shape changes, but remains symmetric. See 4.4.1
2. Partially distributed uniform load at the left end of the beam: the loaded part (h) will be increased till the right boundary is reached. The deformation shape, amount of asymmetry and the location of maximum occurring bending stresses in the actual situation are influenced. See 4.4.2.
3. Partially distributed uniform load at different positions along the beam: the location of the load (a) is changed for a constant width of the loaded part (h). The deformation shape, amount of asymmetry and the location of maximum occurring bending stresses in the actual situation are influenced. See 4.4.3.

4.4.1 Partially distributed uniform load at the centre of the beam

The loaded part is increased starting in the middle with $h = 1/10 * l$ until the boundaries are reached. See Figure 4.5.

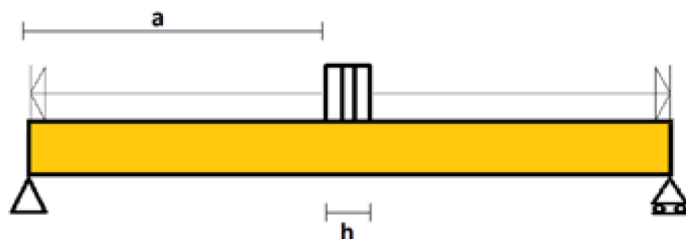


Figure 4.5: load scenario

With $a = 1/2 * (l - h)$ equation (4.1) becomes:

$$f_{stress, max} = -\frac{l^2}{(h-2l)h} \quad \text{for } a = 1/2 * (l-h) \quad (4.2)$$

In Figure 4.6 the ratio between the loads to give the same maximum bending stress is given for different widths (h) of the load.

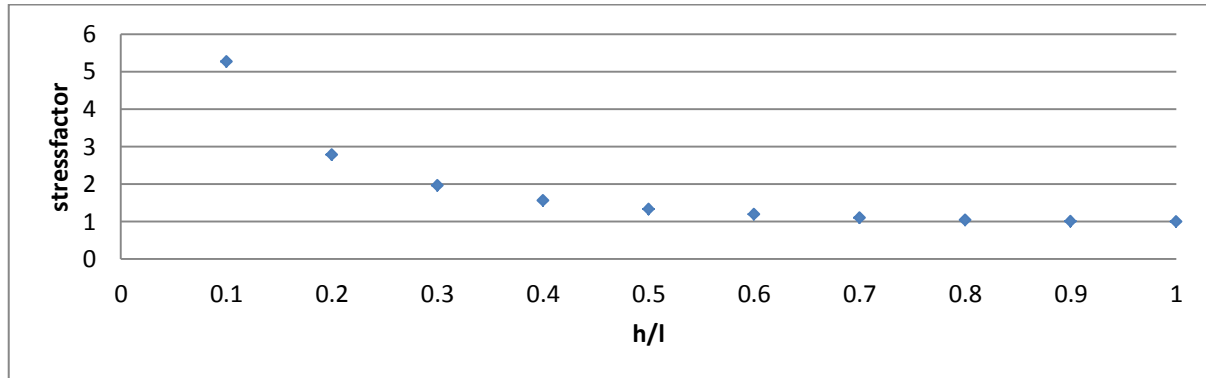


Figure 4.6: Stressfactors for a load with different widths (h) at the centre

By dividing 1 by the multiplication of the stressfactors (which translates a partially distributed load to a uniform load that causes the same maximum bending stress) and the weightfactors (which translates a partially distributed load to a uniform load that causes the same deflection at midspan) the ratio of the maximum occurring stress of a locally loaded beam and the maximum occurring stress of a beam loaded by the equivalent uniform load can be obtained.

$$\frac{1}{\text{stressfactor} \cdot \text{weightfactor}} = \frac{\text{maximum occurring stress of a locally loaded beam}}{\text{maximum occurring stress of a beam loaded by the equivalent uniform}}$$

It can be seen that the equivalent load obtained with the weightfactors result in smaller maximum bending stresses than the actual load by a factor 1 to 1.2. See Figure 4.7.

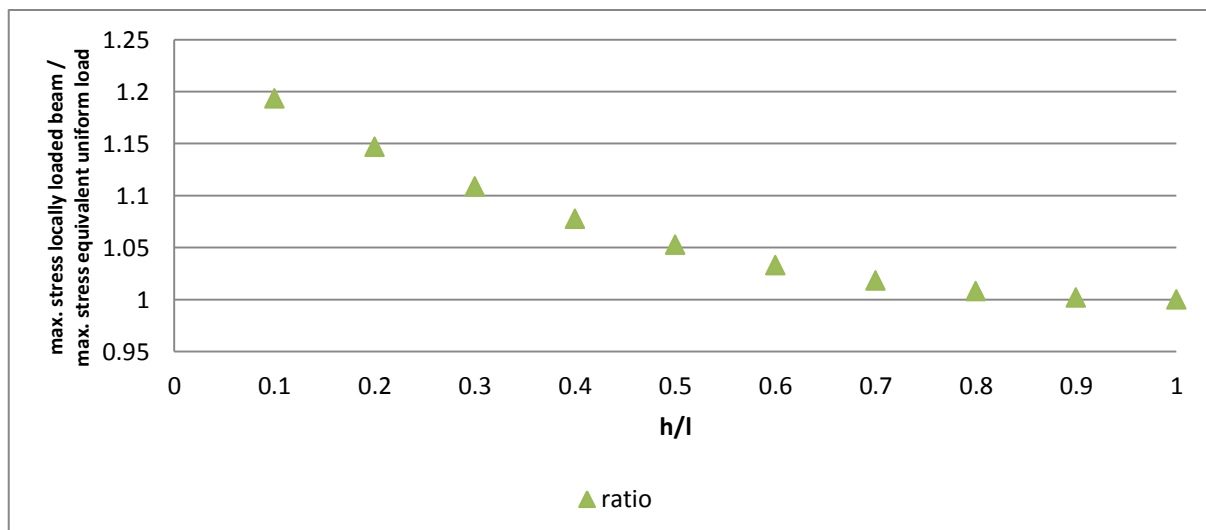


Figure 4.7: Ratio of the maximum occurring stress of a locally loaded beam and the maximum occurring stress of a beam loaded by the equivalent uniform load for a load at the centre

4.4.2 Partially distributed uniform load at the end of the beam

In the case that the load is at the left end of the beam ($a=0$) Equation (4.1) can then be written as:

$$f_{stress, max} = \frac{l^4}{(h - 2l)^2 h^2} \quad \text{for } a=0 \quad (4.3)$$

In Figure 4.8 the ratio between a partially distributed load and uniform load to cause the same bending stresses, is given for several lengths (in percentage) of the beam over which the load is spread. E.g. this means that a load spread over one-tenth at the end of the beam, the load must be 27.7 times larger than a uniformly distributed load to let the same maximum bending stresses occur.

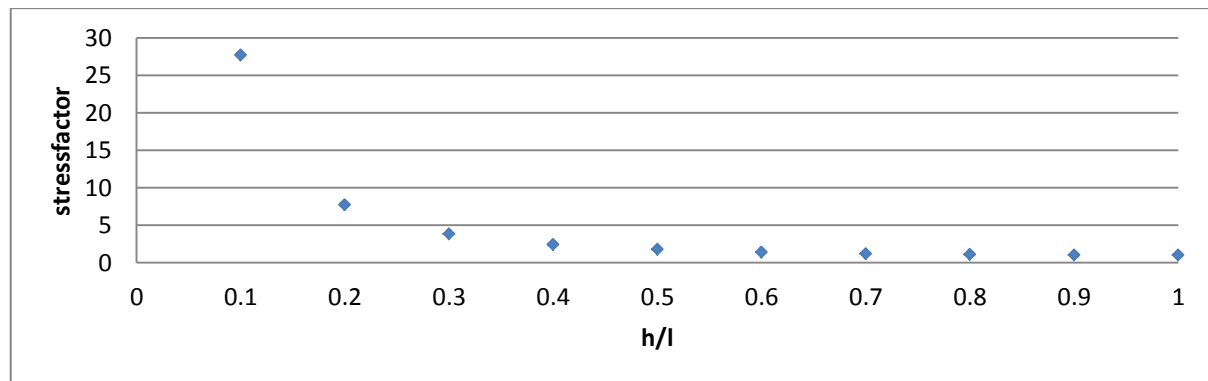


Figure 4.8: Stressfactors for a load starting at the boundary ($a=0$)

If the stressfactors are compared with the weightfactors it can be seen that the equivalent load obtained with the weightfactors result in smaller maximum bending stresses than the actual load. See Figure 4.9.

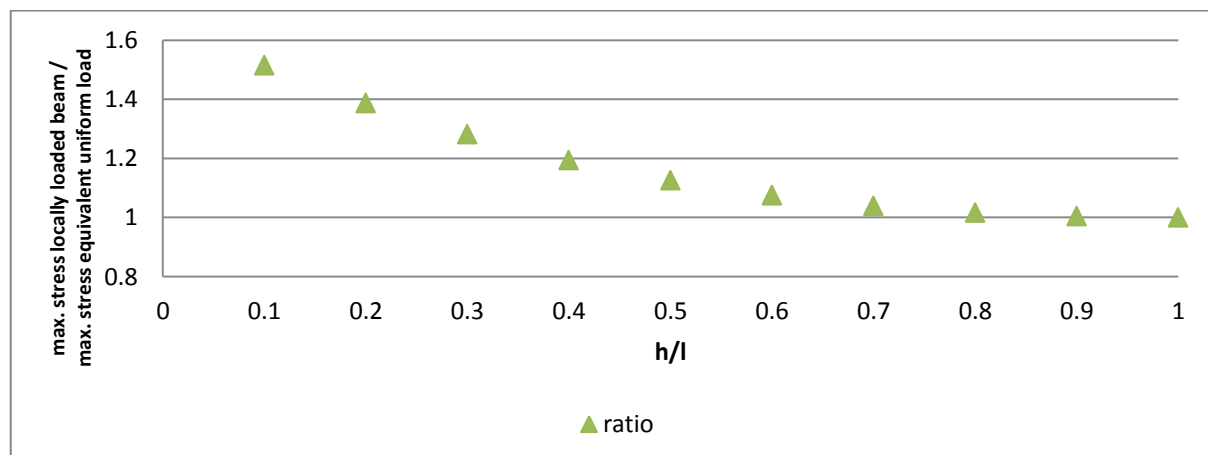


Figure 4.9: Ratio of the maximum occurring stress of a locally loaded beam and the maximum occurring stress of a beam loaded by the equivalent uniform load for a load starting at the boundary ($a=0$)

4.4.3 Partially distributed uniform load at different positions along the beam

In the case that the peak load is distributed over one-twentieth of the beam ($h=l/20$), equation (4.1.) for the ratio becomes:

$$f_{stress, max} = -\frac{160000}{39} \frac{l^2}{(40a - 39l)(40a + l)} \quad \text{for } h=l/20 \quad (4.4)$$

In Figure 4.10 the ratio between the loads to give the same maximum stress is given for different locations of the load, a . For a load spread over one-twentieth at the middle of the beam it holds that

the ratio, to obtain the same maximum bending stress, between a locally distributed uniform load and entirely loaded uniform simply supported beam is 10.26.

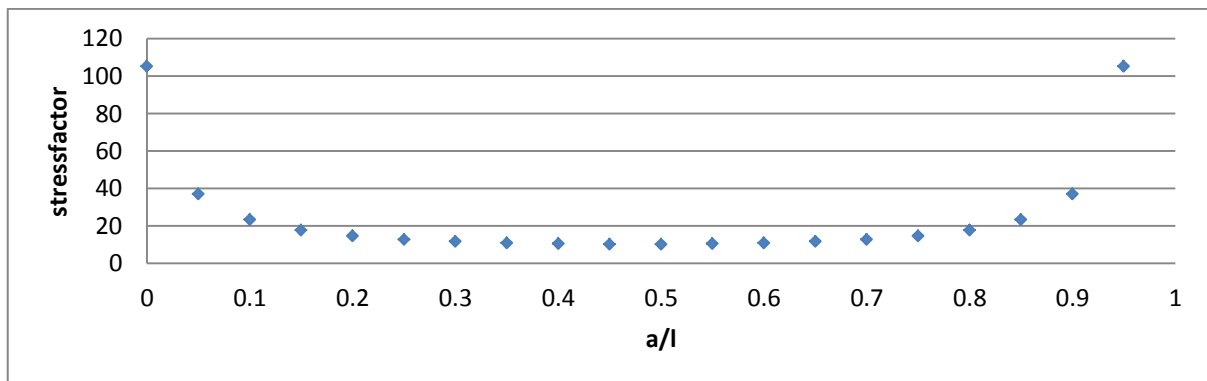


Figure 4.10: Stressfactors for a partially uniformly distributed load ($h=l/20$) at different locations along the length of the beam.

If the stressfactors are compared with the weightfactors it can be seen that the equivalent load obtained with the weightfactors results in smaller maximum bending stresses than the actual load by a factor 1.2 to 1.6. See Figure 4.11.

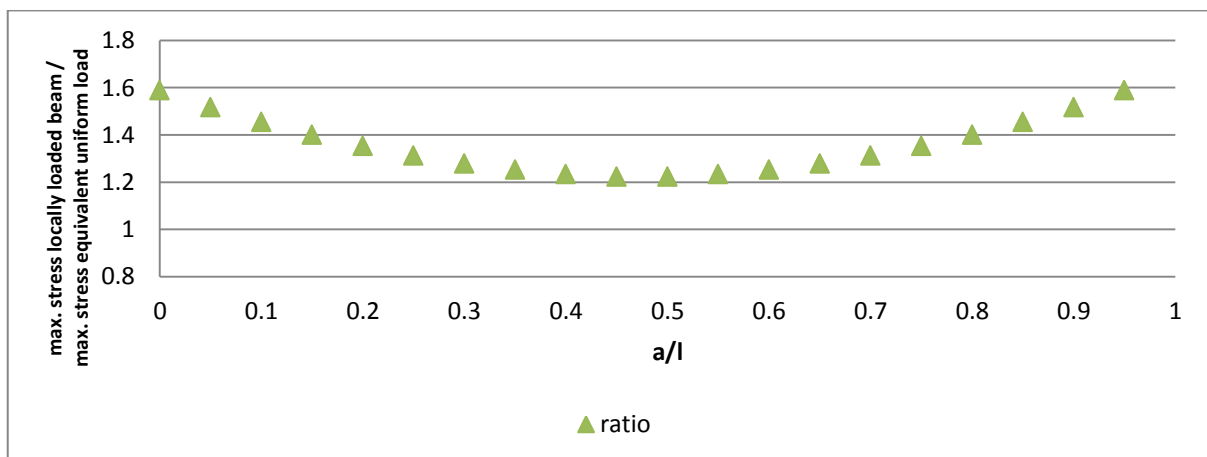


Figure 4.11: Ratio of the maximum occurring stress of a locally loaded beam and the maximum occurring stress of a beam loaded by the equivalent uniform load for a load at different locations along the length of a beam ($h=l/20$)

4.5 Discrepancy of SDOF parameters

As has been explained in Chapter 3, the parameters of an SDOF model are based on energy equivalency (kinematic energy, work by external forces and strain energy). However, if the response of an locally, asymmetrically or non-uniformly loaded beam is approached by an representative uniformly loaded beam the energy requirements may be violated. Whether and to what extent this violation occurs has been studied in this paragraph, by:

- Checking whether the two SDOF models are quantitatively equivalent, i.e. all characteristics change with the same “scaling” factor
- By quantifying the influence of discrepancies in the “scaling” factor on the predicted deflections by the SDOF model.

Due to the different SDOF parameters a different estimation of the deflection at midspan of a beam will be obtained. For several load scenarios the displacement obtained using the SDOF parameters for the actual load is compared with the displacement obtained using the SDOF parameters of a representative uniform load. For the scenario in which a point load acts at midspan of a simply supported beam it is explained how the calculations have been computed.

First, the stiffness, resistance and load-mass factor of both systems have been calculated. They are presented in Table 4.3. Since, the ratio between the elastic load-mass factor of the two systems is more or less the same as the ratio between the stiffness of the two systems, both systems act the same in the elastic range. However, this doesn't hold for all load scenarios and therefore, some minor differences between the elastic response of the two systems may occur.

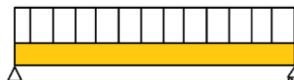
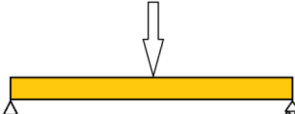
	uniform load 	point load at center 	ratio (uniform load / point load)
stiffness	$384EI/5l^3$	$EI/48l^3$	1.6
resistance (elastic)	$8M_p/l$	$4M_p/l$	2
resistance (plastic)	0	0	-
load-mass factor (elastic)	0.79	0.49	1.62
load-mass factor (plastic)	0.67	0.33	2
load-mass factor (average elastic plastic)	0.73	0.41	1.78

Table 4.3: Stiffness, resistance and load-mass factor for a beam subjected to a uniform load and for a beam subjected to a point load

By calculating the ratio between the SDOF parameters of the uniform load and the SDOF parameters of the point load, the two systems can be compared as follows:

SDOF parameters for uniform load: arbitrary values

SDOF parameters for point load: arbitrary values / ratio

First the arbitrary values have been chosen such that the response is in the elastic regime, next the load input has been increased stepwise to introduce different amounts of plasticity. In Figure 4.12 the ratio between the maximum displacement obtained with the SDOF model for the uniform load

and the maximum displacement obtained with the SDOF model for the point load are presented. It can be seen that the ratio between the deformation approached an asymptotic value.

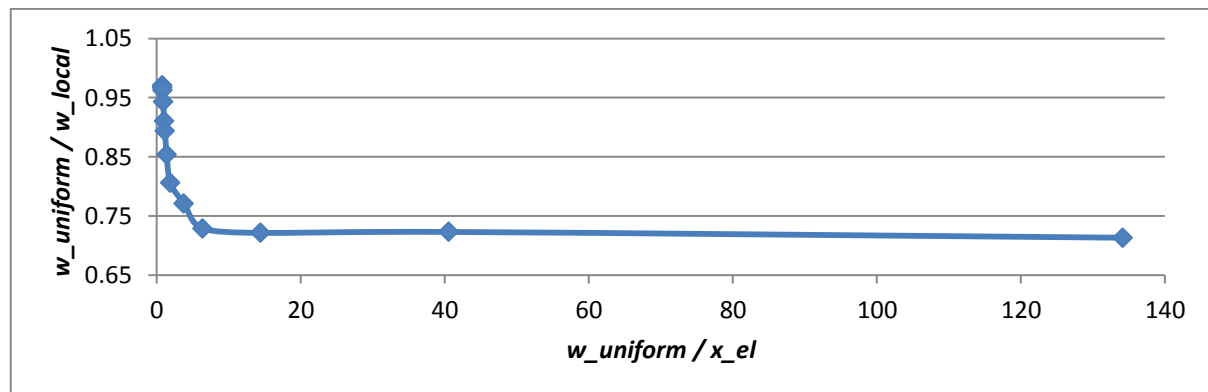


Figure 4.12: Ratio of the maximum occurring stress of a locally loaded beam and the maximum occurring stress of a beam loaded by the equivalent uniform load for a load starting at the boundary ($\alpha=0$)

Where:

$W_{uniform}$ = maximum obtained deflection with the uniform load

W_{local} = maximum deflection of a beam subjected to the equivalent uniform load

x_{el} = elastic deformation limit of the uniformly loaded beam.

In Table 4.4 and Table 4.5 for different load distributions the asymptotic value is presented. It can be observed that for point loads the deflection has been underestimated with an SDOF model using scaled parameters for uniform loading. The estimations become worse if the point load acts closer to the boundaries. For distributed loads, in Table 4.5, it can be observed that the estimations are more accurate.

location of pointload	$x=l/2$	$x=l/3$	$x=l/4$	$x=l/6$	$x=l/8$
$W_{uniform}/W_{local}$	0.71	0.76	0.69	0.58	0.50

Table 4.4: Ratio between the deflection of an SDOF model for a point load and a uniform load

width of locally distributed load ($x=l/2$)	$h=1/6*l$	$h=2/6*l$	$h=3/6*l$	$h=4/6*l$	$h=5/6*l$
$W_{uniform}/W_{local}$	0.80	0.87	0.93	0.97	0.99

Table 4.5: Ratio between the deflection of an SDOF model for a locally loaded and a uniformly loaded beam

4.6 Conclusion

Boundary conditions

The weightfactors are different for a simply supported beam and for a fixed beam. They depend on the boundary conditions. The equivalent uniform load for a simply supported beam is different than for a fixed beam.

Stresses

When a weightfactor is multiplied with a partially uniformly distributed load and then assumed to be distributed over the whole beam, it gives the same deflection at midspan as the partially uniformly

distributed static load. However, this equivalent uniform load does not result in the same bending stresses. For the, in this chapter, three investigated load scenarios the bending stresses are underestimated up to a factor 1.6 for asymmetric loading and up to a factor 1.2 for symmetric loading. In Table 4.6 the load scenarios which satisfy different ratios between the actual maximum bending stress and the maximum bending stress of an elastic simply supported beam due to the equivalent uniform static load are presented. It can be seen when a certain requirement is satisfied.

maximum allowed ratio	at the centre, varying width	starting from the boundary ($a=0$), varying width	varying locations, constant width $h=1/20$
1.05	load covers least 60% of the beam	load covers at least 70% of the beam	not possible
1.10	load covers least 40% of the beam	load covers least 60% of the beam	not possible
1.20	load covers least 10% of the beam	load covers least 40% of the beam	not possible
1.30	no restrictions	load covers least 30% of the beam	between $a=7/20$ and $a=14/20$
1.40	no restrictions	load covers least 20% of the beam	between $a=4/20$ and $a=17/20$
1.50	no restrictions	not possible	between $a=3/20$ and $a=18/20$

Table 4.6: Load scenarios which satisfy different maximum allowed ratio's between the actual maximum bending stress of an elastic simply supported beam due to the equivalent uniform static load

Discrepancy of SDOF parameters

The parameters of an SDOF model are based on energy equivalency (kinematic energy, work by external forces and strain energy). Comparing of the SDOF characteristics shows that the energy equivalency is violated if the response of a locally, asymmetrically or non-uniformly loaded beam is approached by an representative uniformly loaded beam. This introduces errors in the estimations of the SDOF model with uniform load parameters. As can be seen in Figure 4.12 the error increases if more plasticity occurs. For several load scenarios the displacement obtained using the SDOF parameters for the actual load has been compared with the displacement obtained using the SDOF parameters of a representative uniform load. In Table 4.4 and Table 4.5 the results are presented, it can be observed that for point loads the deflection has been underestimated with an SDOF model using scaled parameters for uniform loading. The estimations become worse if the point load acts closer to the boundaries. For distributed loads, in Table 4.5, it can be observed that the estimations are more accurate.

Usability

In case of ductile material the failure of a component is usually based on a maximum allowed deflection. In this case the weightfactors are usable if linear-elastic deformation occurs. The deflection shape changes if plastic deformation occurs. Since the weightfactors are based on the elastic deformation shape, they are not valid if yielding occurs. The influence of yielding on the weightfactors has been investigated in Chapter 5.

In case of brittle material the deflection at midspan might not be representative to determine the failure of a component, since this might not be the location where failure might occur. It may be better to use factors based on bending stress. These factors can be determined such that the

equivalent load will give the same bending stress at the critical location. However, for an arbitrary blast load it is hard to estimate the critical location. Especially due to the occurrence of higher order vibration modes.

Chapter 5

Validity weightfactors – plasticity

The amount and the location(s) of plasticity that will occur due to a blast wave is/are not known in advance. Therefore, to determine the influence of plasticity on the weightfactors, a yielded area has been predefined. This yielded area has a rectangular section with a decreased bending stiffness. The width and the bending stiffness of the rectangular section have been varied to represent different amounts of plasticity. For a linear-elastic beam with a locally decreased bending stiffness the weightfactors have been calculated analytically and are compared with the weightfactors for a beam with a continuous bending stiffness. These weightfactors are determined in a way to reproduce the same deflection at midspan. To obtain a clear picture of the influence of these “plastic” weightfactors, the change of the equivalent load has been investigated.

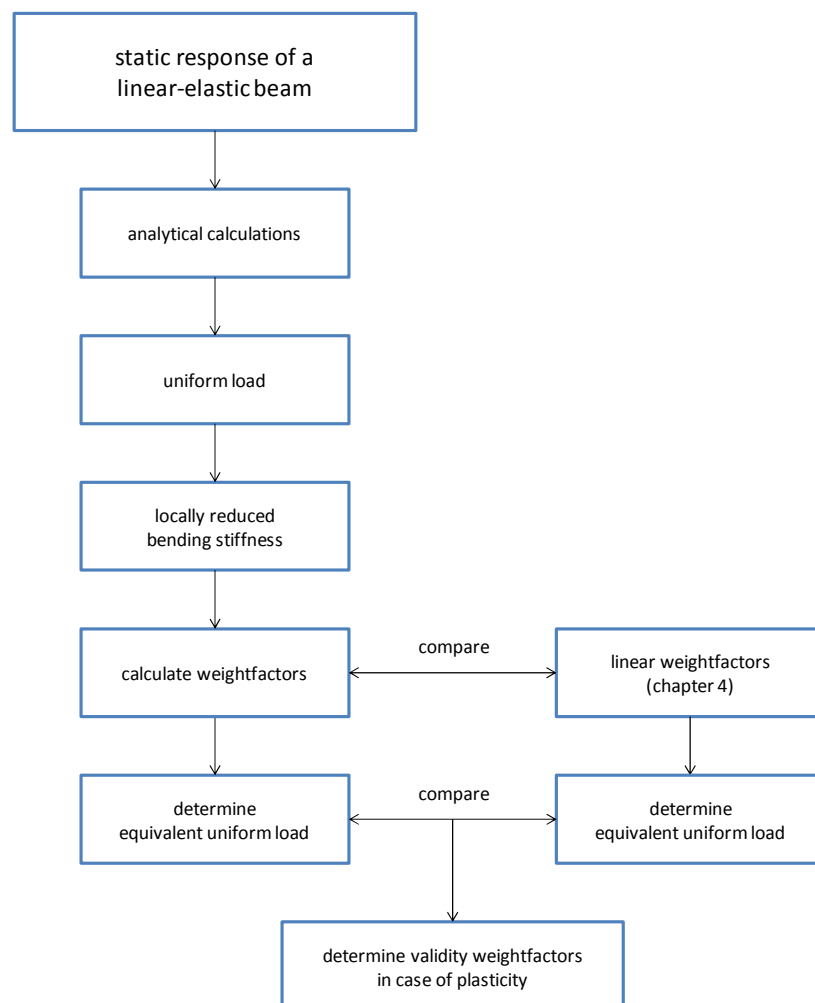


Figure 5.1: Flowchart Chapter 5

5.1 Superposition

For statically loaded linear-elastic components it holds that the sum of the response of individual loads is the same as the response of the sum of the loads. See Figure 5.2. This means that the loads multiplied with the corresponding weightfactor can be summed to obtain an equivalent uniform load. This however doesn't result in the same deflection in case of non-linear components. The individual loads might be too small to introduce plasticity, while the sum of the loads may cause plastic deformation. In case of elastic-plastic deformation superposition doesn't hold, therefore it has been investigated what the influence of plasticity on the weightfactors can be.

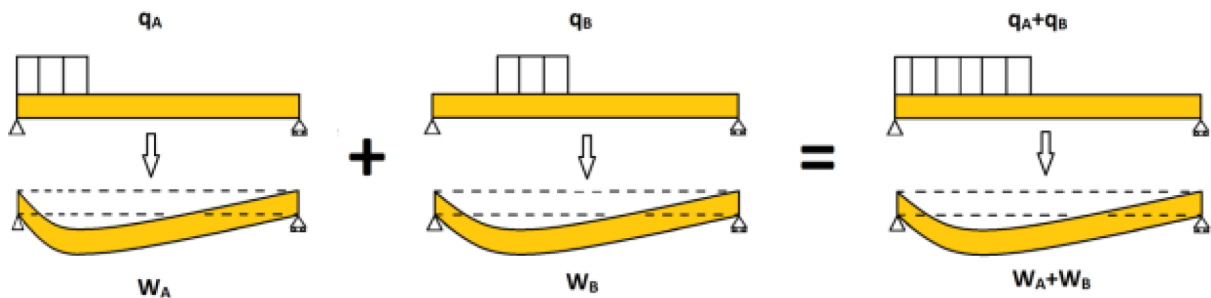


Figure 5.2: Superposition principle for linear systems

5.2 Weightfactors

Blast waves introduce a pressure on the beam which varies in time. The location of the maximum pressure on the beam might change in time (especially for asymmetric and non-uniform load distributions). This makes it hard to analytically determine how the stresses in the beam change in time. When the elastic moment capacity has been reached the material starts to yield. Initially it will only yield at the top and/or bottom. If the load further increases the plastic region will grow.

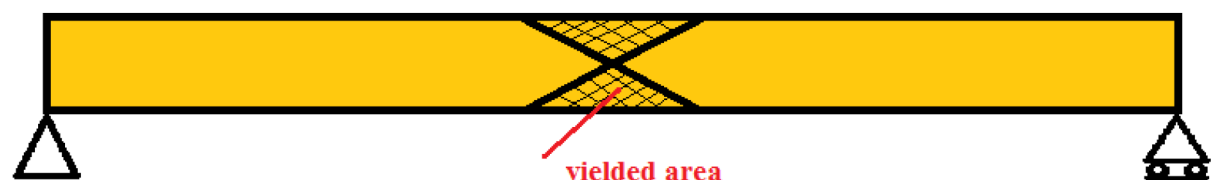


Figure 5.3: Situation how the distribution of the bending stiffness might be in reality

The stresses in a beam due to an arbitrary blast wave are not known in advance, therefore the actual size of the yielded area and the actual decreased bending stiffness are not known. The amount of yielding and the bending stiffness depend on the load scenario and the yield strength of the beam. In Figure 5.3 it can be seen that the size of the yielded cross-section may vary along the length of the beam. This means that the bending stiffness is not continuous (varies over the length of a beam).

To determine the validity of the weightfactors, despite all the unknowns in case of plasticity, the yielded area has been simplified by a rectangular section. See Figure 5.4. The width and the bending stiffness of the rectangle section have been varied to represent different amounts of plasticity. For this beam the "plastic" weightfactors have been determined.

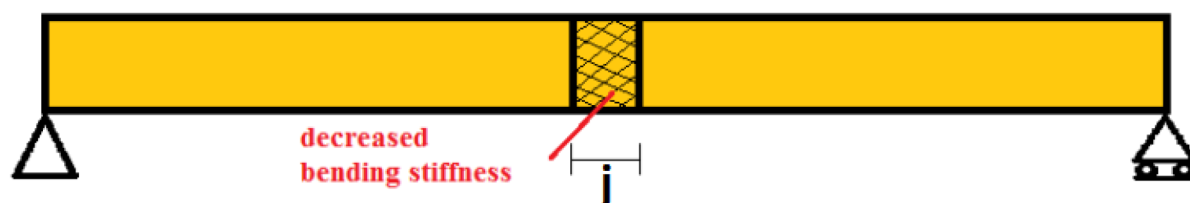


Figure 5.4: Simplification of the yielded area with decreased bending stiffness

The actual deformation behaviour of steel is given in Figure 5.5. It can be seen that once the yield strength has been reached, the bending stiffness decreases. If the bending stiffness is locally decreased, the deformation shape changes. Since the weightfactors are dependent on the deformation shape, they are dependent as well on the amount of yielding.

Therefore, the weightfactors should change during the loading process. Weightfactors which have been calculated for a beam with a locally reduced bending stiffness are momentary weightfactors. This fictive reduced bending stiffness is fixed and does not change as in the graph below. The “plastic” weightfactors are calculated to see how they could change in case of plasticity and are not to be used with the SDOF model.

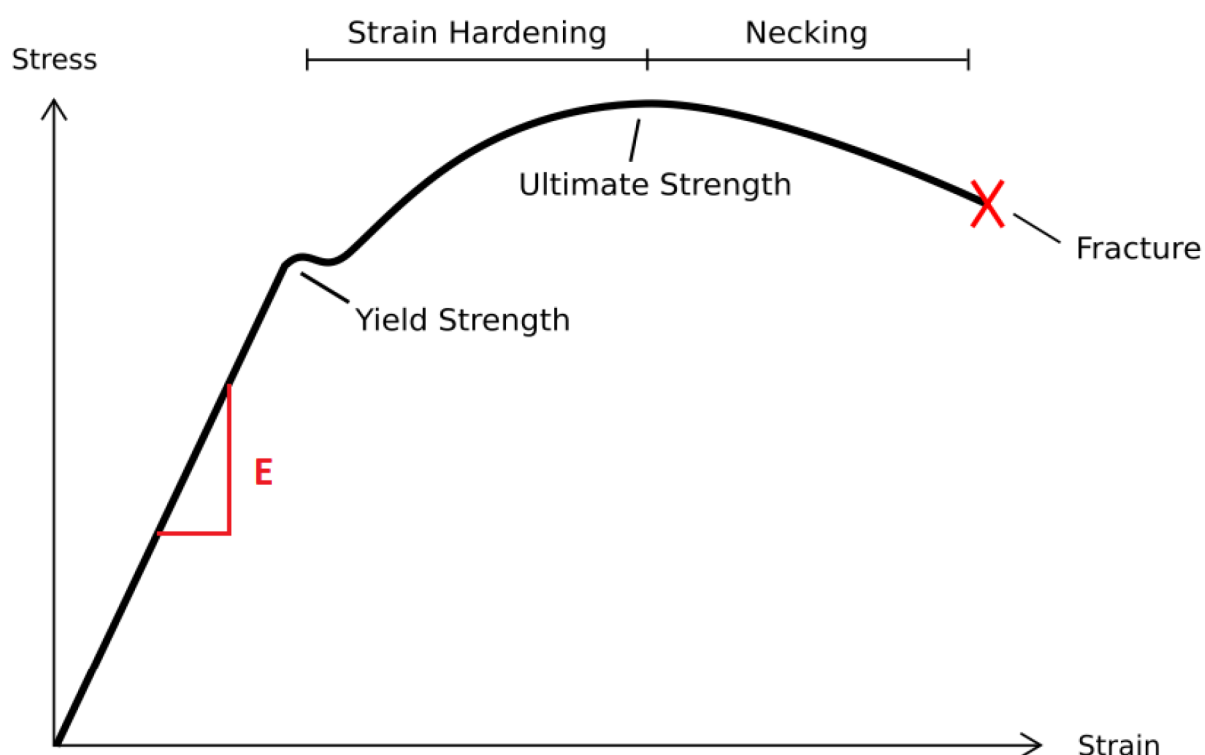


Figure 5.5: Stress-strain curve of steel.

A logical value of how much the bending stiffness will reduce in case of blast loading is hard to determine. This depends, among other things, on the size of the explosions and the yield strength of the beam. It has been investigated how the weightfactors change in the case the “plastic” section has a bending stiffness of 10% or 0.01% of the reference stiffness. 10% has been chosen to represent a large amount of plasticity and 0.01% has been chosen to represent an almost full plastic cross-section. In the actual situation, depending on the scenario, the decreased bending stiffness may deviate from these values.

The following situations have been compared with the elastic weightfactors for a simply supported beam:

- Case 1: Stiffness 10% of the initial stiffness, with different decreased section widths (j)
 - a) Decreased stiffness at $x=0.25 \cdot l$ see Figure 5.6
- Case 2: Stiffness 0.01% of the initial stiffness, with different decreased section widths
 - a) Decreased stiffness at $x=0.25 \cdot l$ see Figure 5.7
- Case 3: 90% of the beam length with a decreased stiffness
 - a) Stiffness 10% of the initial stiffness see Figure 5.8
 - b) Stiffness 0.01% of the initial stiffness see Figure 5.8
- Case 4: Two sections with decreased stiffness, with different decreased section widths
 - a) Stiffness 10% of the initial stiffness at $x=0.25 \cdot l$ and $0.75 \cdot l$ see Figure 5.9
 - b) Stiffness 0.01% of the initial stiffness at $x=0.25 \cdot l$ and $0.75 \cdot l$ see Figure 5.10

5.2.1 Case 1: Stiffness 10% of the initial stiffness

In Figure 5.6 a comparison is made between the weightfactors for a beam with a section with a stiffness of 10% of the initial stiffness at $x=0.25 \cdot l$ and the weightfactors for a beam with a continuous stiffness ($j=0$). Relatively small changes of the weightfactors are obtained if the section width is increased. It can be observed that the maximum value of the weightfactors (peak) moves to the left, first decreases and for $j > 10/120 \cdot l$ the peak starts to increase. See Figure 5.6.

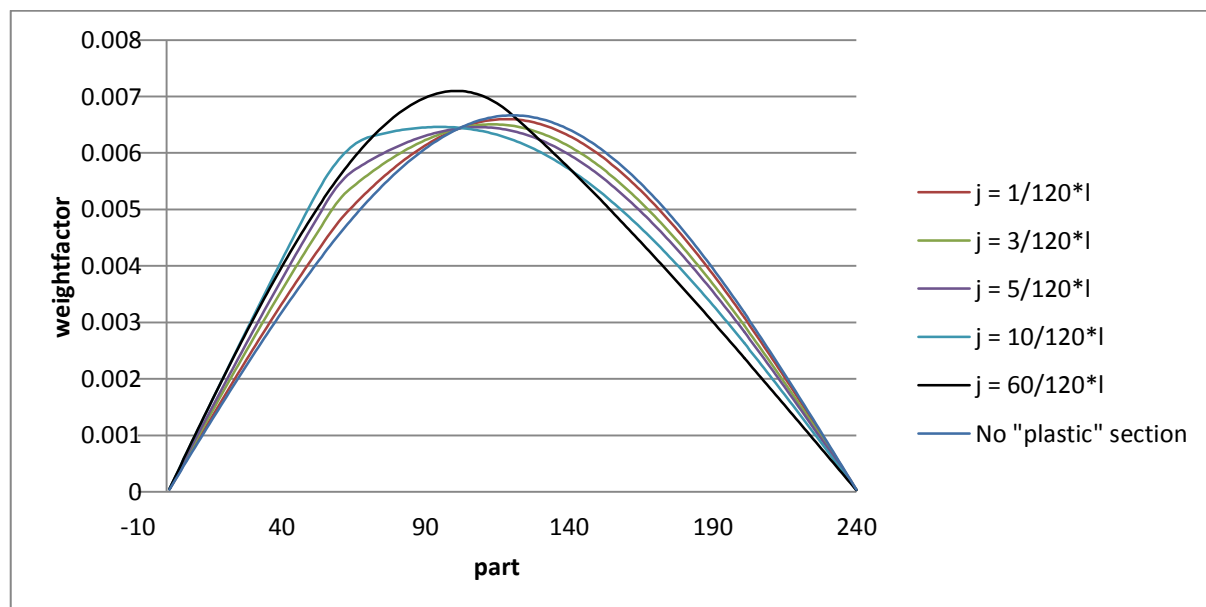


Figure 5.6: Weightfactors for a beam with a decreased bending stiffness of 10% of the initial stiffness. The section with decreased bending stiffness is at $x=0.25 \cdot l$ and has width j .

5.2.2 Case 2: Stiffness 0.01% of the initial stiffness

In Figure 5.7 a comparison is made between the weightfactors for a beam with a section with a stiffness of 0.01% of the initial stiffness at $x=0.25 \cdot l$ and the weightfactors for a beam with a continuous stiffness ($j=0$). Relatively large changes of the weightfactors are obtained. A maximum

value (peak) of the weightfactors is obtained for a very small plastic zone $j=1/120 \cdot l$ (which is as well the smallest zone investigated). If the section size with decreased stiffness is increased, the peak value of the weightfactors decreases and tends to restore to the original shape.

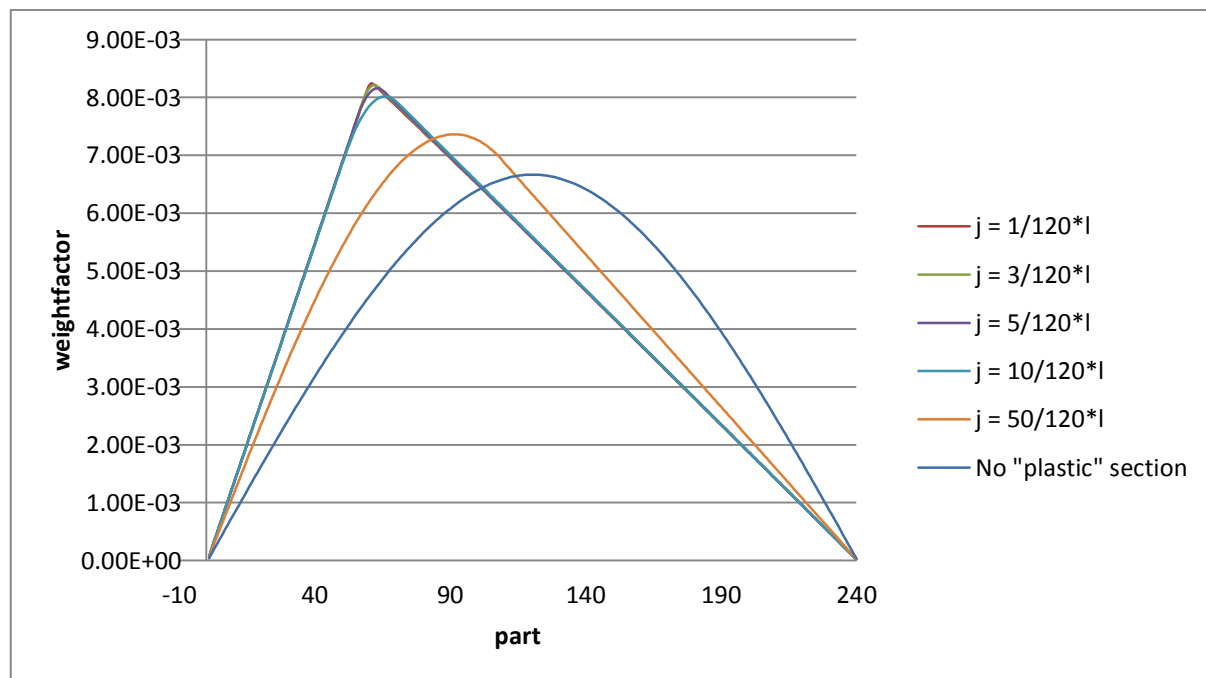


Figure 5.7: Weightfactors for a beam with a decreased bending stiffness of 0.01% of the initial stiffness. The section with decreased bending stiffness is at $x=0.25 \cdot l$ and has width j .

5.2.3 Case 3: 90% of the beam decreased stiffness

In Figure 5.8 a comparison is made between the weightfactors for a beam with a section with decreased bending stiffness which has the size of 90% of the beam length and the weightfactors for a beam with continuous stiffness. With EI the bending stiffness of the remaining part of the beam. It can be seen that the weightfactors for the two situations are almost the same as for the “elastic” weightfactors.

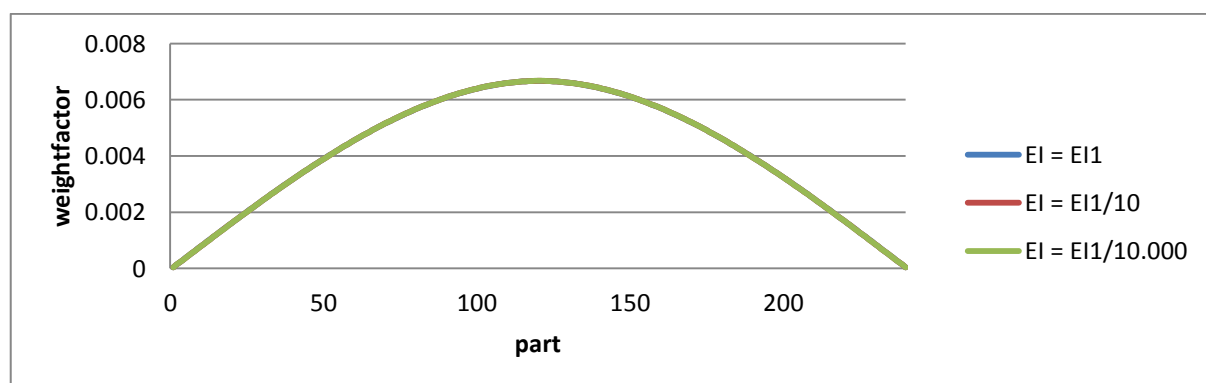


Figure 5.8: Weightfactors for a beam with a reduced stiffness of 90% of the length of the beam (with middle point $x=0.50 \cdot l$).

5.2.4 Case 4: Two sections with decreased stiffness

In the Figure 5.10 and Figure 5.11 a comparison is made between the weightfactors for a beam with two sections with a decreased bending stiffness and the weightfactors for a beam with a continuous stiffness ($j=0$). The section size, j , is the same for both sections. See Figure 5.9.



Figure 5.9: Beam with two predefined "plastic" sections

It can be observed that in the case the two sections have a bending stiffness of 10%, the change of the weightfactors is minimal. In case the two sections have a bending stiffness of 0.01% a relatively large difference in the weightfactors can be observed between $x=0.25 \cdot l$ and $x=0.75 \cdot l$ (especially at $x=0.5 \cdot l$).

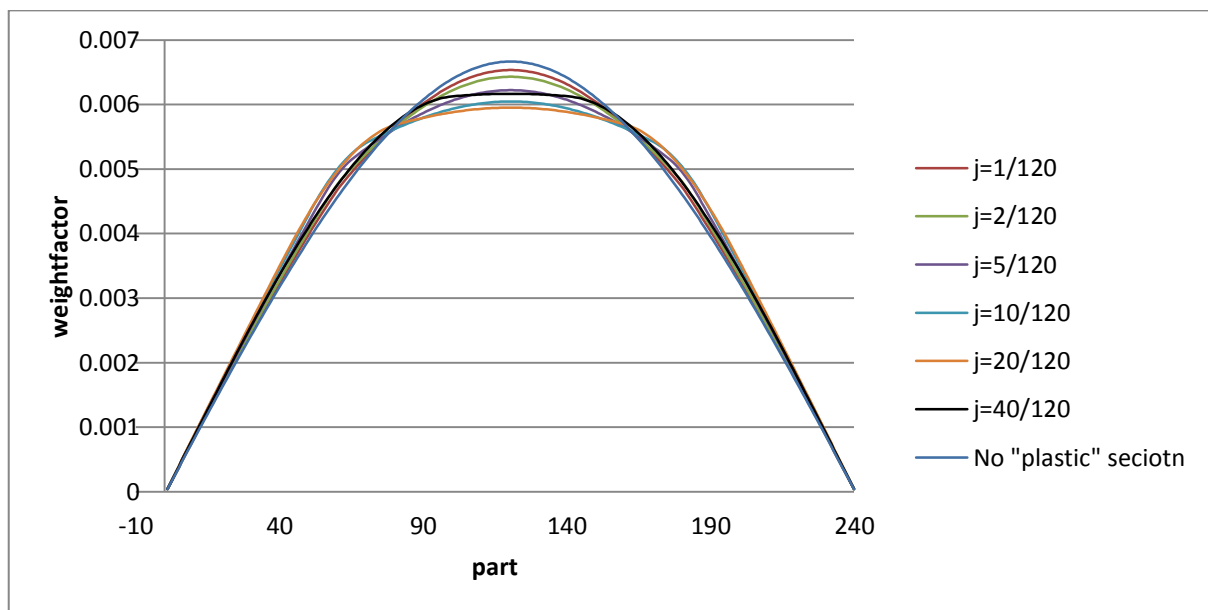


Figure 5.10: Weightfactors for a decreased bending stiffness of 10% of the initial stiffness at $x=0.25 \cdot l$ and $x=0.75 \cdot l$

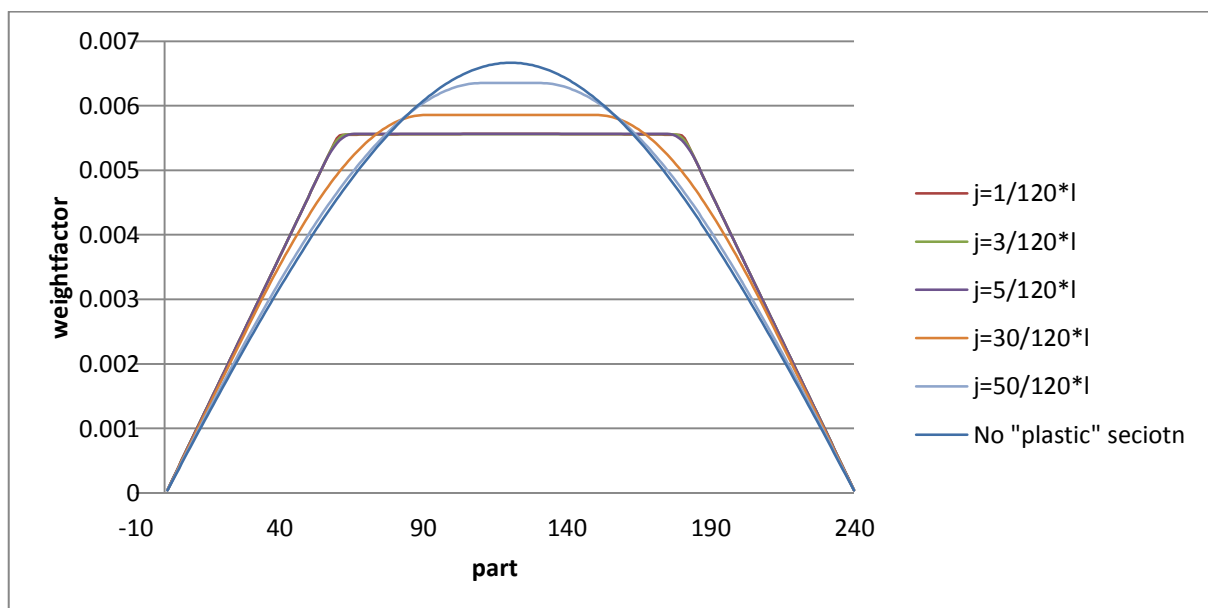


Figure 5.11: Weightfactors for a decreased bending stiffness of 0.01% of the initial stiffness at $x=0.25 \cdot l$ and $x=0.75 \cdot l$

5.2.5 Conclusion

Bending stiffness of 10% of the initial bending stiffness,

If the section with decreased bending stiffness, j , is increased, the peak (maximum value of the weightfactors) of the graph of the weightfactor increases and moves to the location of the section with the decreased bending stiffness. If the section is further increased the graph tend to restore to its initial shape, since if $j=1$ the whole beam has a reduced bending stiffness and therefore the original weightfactors are restored. This holds as well for the situation where the beam has two sections with decreased bending stiffness

For a bending stiffness of 0.01% of the initial bending stiffness,

For a small section with decreased bending stiffness ($j=1/120 \cdot I$), the peak (maximum value of the weightfactors) immediately increases to its maximum and moves to the location of the section with decreased bending stiffness. If j is increased the graph restores to its initial shape. This holds also for the situation where the beam has two sections with decreased bending stiffness. The weightfactors are continuous between the two sections.

The sum of the weightfactors always remains 1. This means that when the loading is around the section with decreased bending stiffness, large errors are obtained, but there would be compensation when the load is spread over the entire beam.

5.3 Equivalent Uniform load

Using the “plastic” weightfactors an equivalent uniform load has been determined for different uniform load distributions. The load, with its centre at the location with decreased stiffness, has been increased until one of the boundaries has been reached. See Figure 5.12.

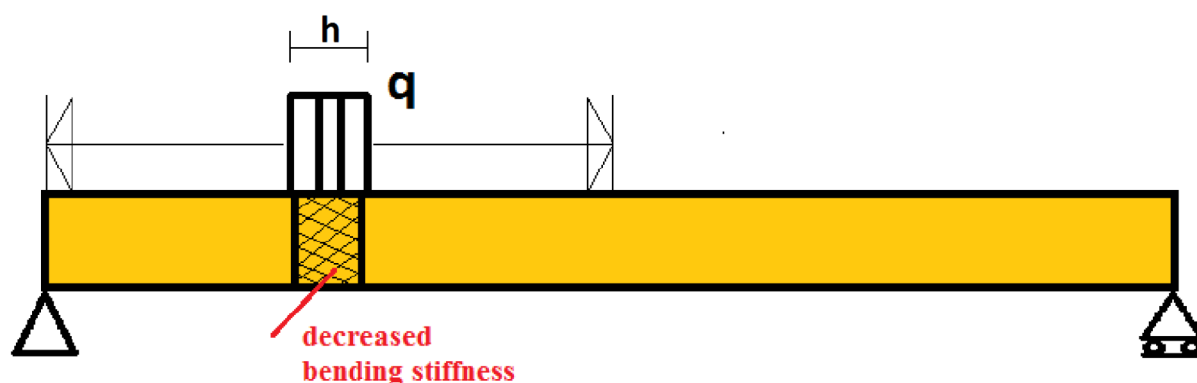


Figure 5.12: Uniform load distribution

The equivalent load using “plastic” weightfactors for a beam with a section with decreased bending stiffness have been compared with the equivalent load using the “elastic” weightfactors. The width of section with decreased bending stiffness has been chosen such that a maximum difference of the weightfactors at the location of the section is obtained (this width has been obtained in Chapter 5.2). The results are presented in Figure 5.13 to Figure 5.17. It can be seen that for load distributions over a small part of the beam the equivalent load might significantly be underestimated when the “elastic” weightfactors are used. However, if plasticity occurs at more symmetric locations, the influence of plasticity becomes minimal.

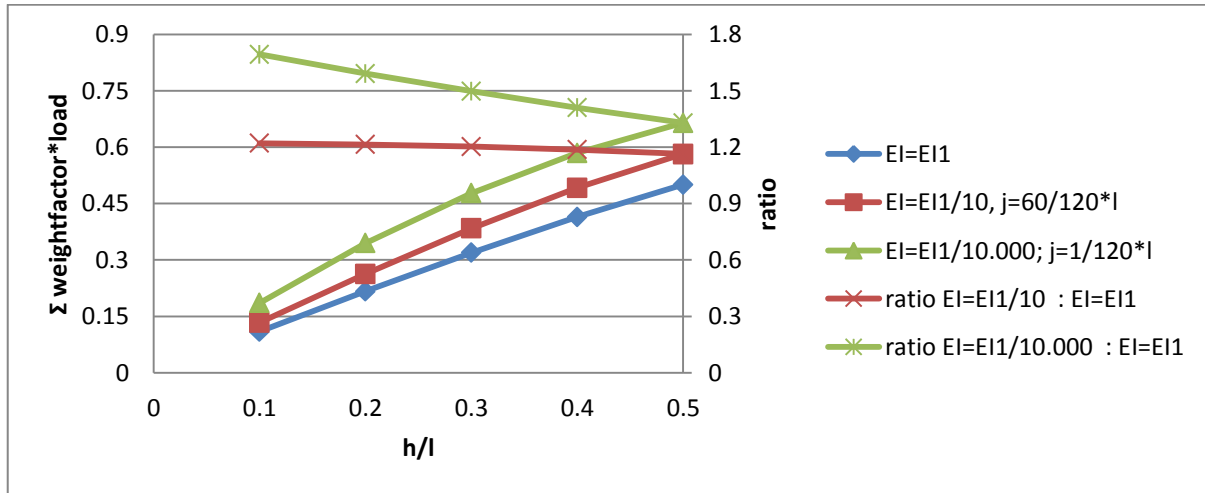


Figure 5.13: Equivalent load for a beam with decreased bending stiffness at $x=0.25 \cdot l$

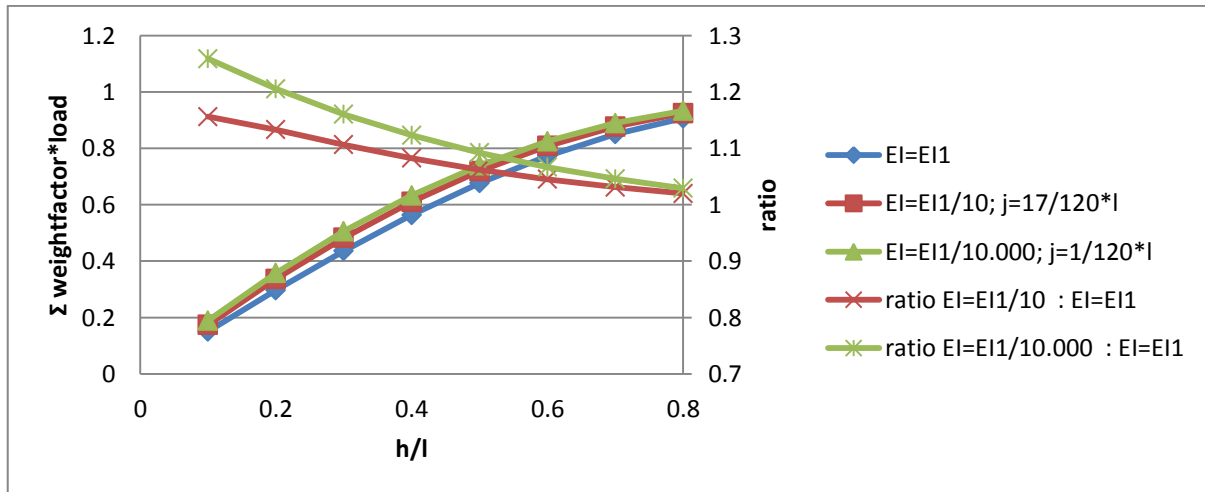


Figure 5.14: Equivalent load for a beam with decreased bending stiffness at $x=0.40 \cdot l$

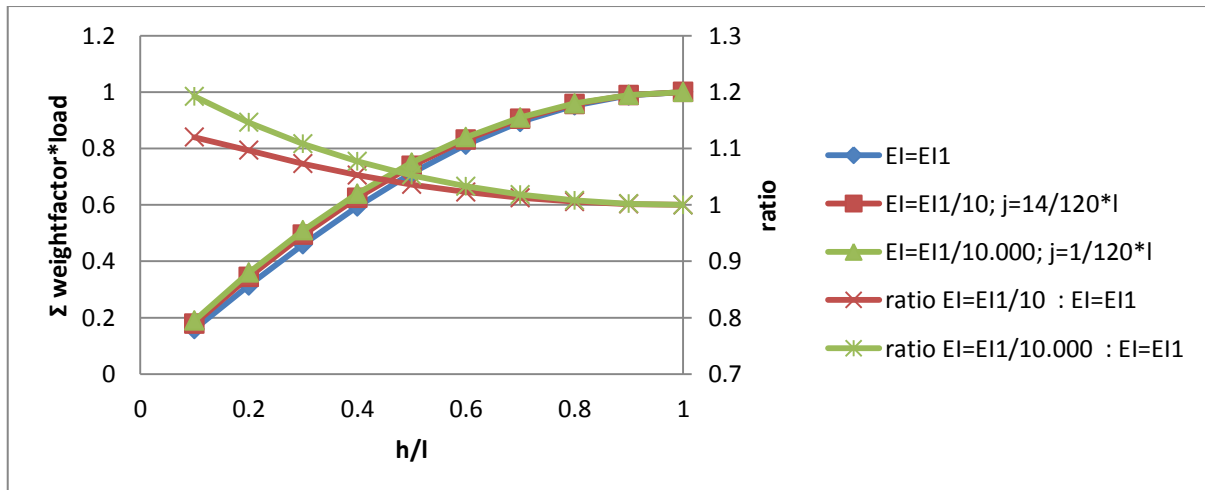


Figure 5.15: Equivalent load for a beam with decreased bending stiffness at $x=0.50 \cdot l$

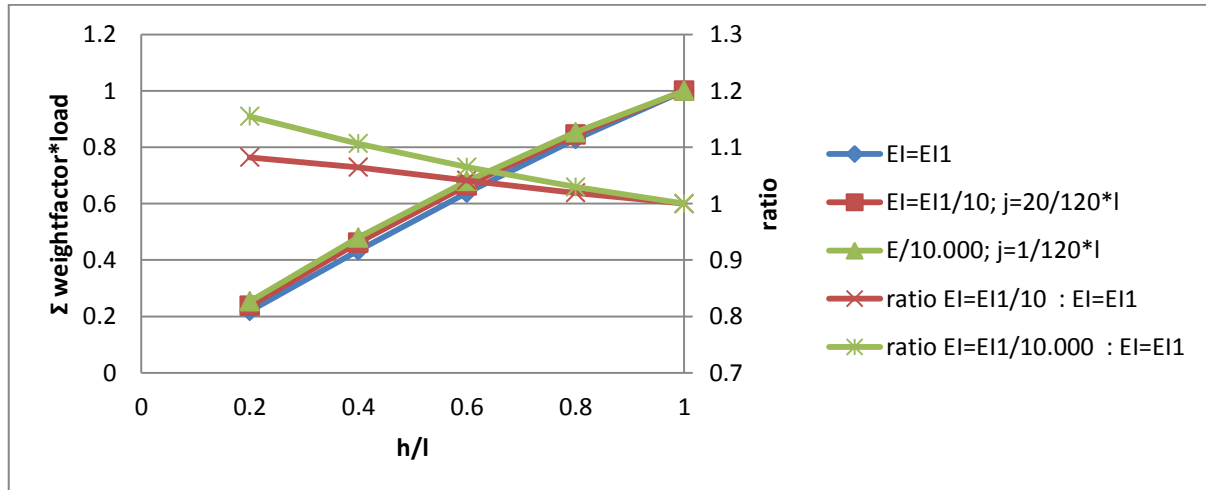


Figure 5.16: Equivalent load for a beam with decreased bending stiffness at $x=0.25*l$ and $x=0.75*l$

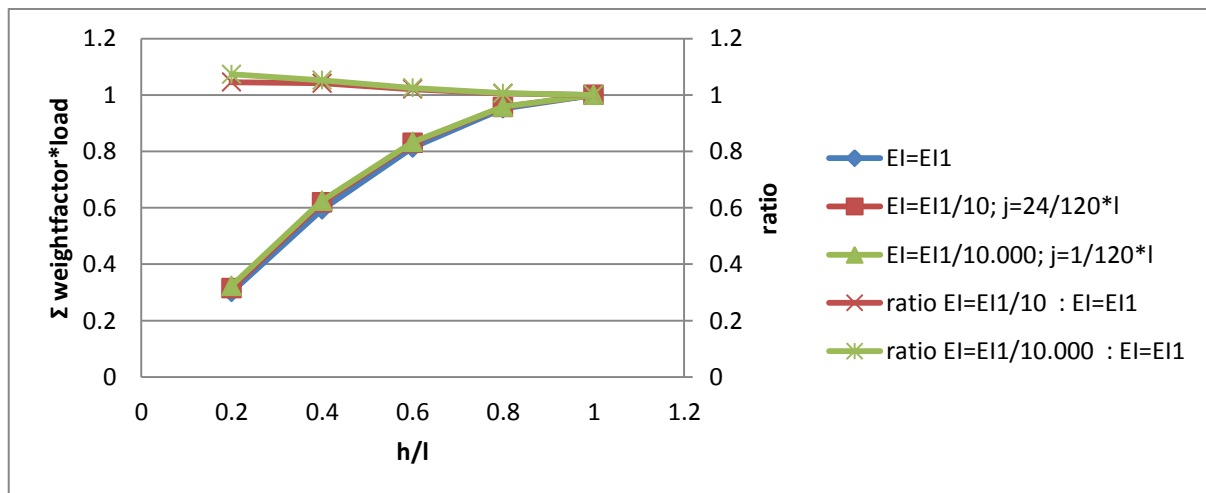


Figure 5.17: Equivalent load for a beam with decreased bending stiffness at $x=0.40*l$ and $x=0.60*l$

5.3.1 Conclusion

A summary of the obtained ratios between the equivalent loads for a beam with a “plastic” section and a beam with continuous stiffness is presented in Table 5.1. For each scenario it is shown what size the load should have to satisfy a certain ratio between the equivalent load using the “plastic” and “elastic” weightfactors.

When the section with decreased bending stiffness is close to the support (e.g. at $x=0.25*l$) the difference between the elastic and plastic equivalent uniform load becomes large (using “plastic” weightfactors a max. of 69% increase with $h=0.1*l$ and $EI=EI1/10.000$ has been obtained). However, when the section with decreased bending stiffness is at the centre of the beam or when there are two sections with decreased bending stiffness, e.g. at $x=0.25*l$ and $x=0.75*l$, the difference between the elastic and plastic equivalent uniform load remains small (using “plastic” weightfactors a max. of 19% increase for $x=0.5*l$, $h=0.1*l$ and $EI=EI1/10.000$ and a max. of 15% increase for $x=$ both $0.25*l$ and $0.75*l$, $h=0.1*l$ and $EI=EI1/10.000$ has been obtained).

x-location j	EI	ratio [-]				
		1.05	1.10	1.20	1.40	1.60
$x=0.25 \cdot l$	$EI1/10$	-	-	$h/l \geq 0.4$	satisfied	satisfied
$x=0.40 \cdot l$	$EI1/10$	$h/l \geq 0.6$	$h/l \geq 0.4$	satisfied	satisfied	satisfied
$x=0.50 \cdot l$	$EI1/10$	$h/l \geq 0.5$	$h/l \geq 0.2$	satisfied	satisfied	satisfied
$x=0.25 \cdot l + 0.75 \cdot l$	$EI1/10$	$h/l \geq 0.6$	satisfied	satisfied	satisfied	satisfied
$x=0.40 \cdot l + 0.60 \cdot l$	$EI1/10$	satisfied	satisfied	satisfied	satisfied	satisfied
$x=0.25 \cdot l$	$EI1/10.000$	-	-	-	$h/l \geq 0.5$	$h/l \geq 0.2$
$x=0.40 \cdot l$	$EI1/10.000$	$h/l \geq 0.7$	$h/l \geq 0.5$	$h/l \geq 0.3$	satisfied	satisfied
$x=0.50 \cdot l$	$EI1/10.000$	$h/l \geq 0.6$	$h/l \geq 0.4$	satisfied	satisfied	satisfied
$x=0.25 \cdot l + 0.75 \cdot l$	$EI1/10.000$	$h/l \geq 0.8$	$h/l \geq 0.6$	$h/l \geq 0.4$	satisfied	satisfied
$x=0.40 \cdot l + 0.60 \cdot l$	$EI1/10.000$	$h/l \geq 0.6$	satisfied	satisfied	satisfied	satisfied

Table 5.1: Load scenarios which satisfy different maximum allowed ratio's between the equivalent uniform load for a beam with a "plastic" section and a beam with a continuous stiffness.

5.4 Finite Element Analysis

A FEA has been carried out to see the influence of a section with decreased bending stiffness on the response of a beam subjected to an explosion above the left end support. Linear-elastic deformation is assumed. This has been done to see how the deformation shape and stresses are affected. The following 2 scenarios of a simply supported beam, with properties as described in table 7.3, have been investigated:

1. Explosion at the left boundary; section with a bending stiffness of 10% of reference stiffness; section with a width of $10/120 \cdot l$; section at $x=0.25 \cdot l$
2. Explosion at the left boundary; section with a bending stiffness of 0.01% of the reference stiffness; section with a width of $1/120 \cdot l$; section at $x=0.25 \cdot l$

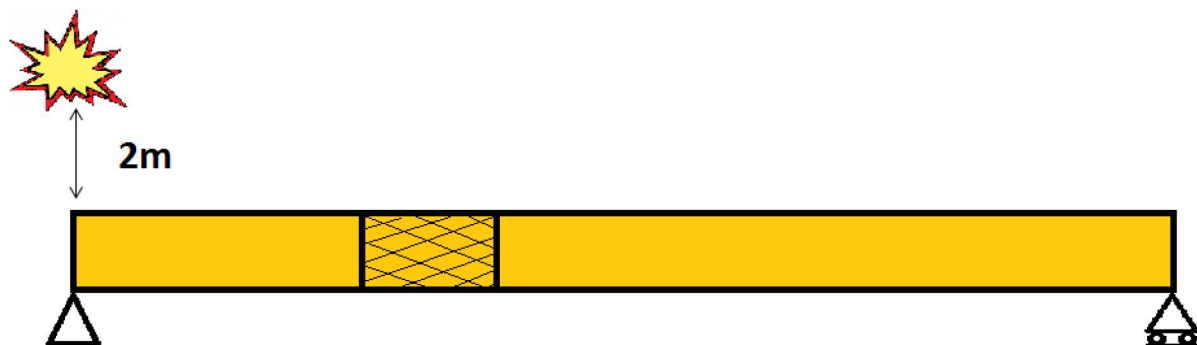


Figure 5.18: Load scenario

A beam with a section with a reduced bending stiffness has a lower stiffness, but the same mass as the reference beam. This results in larger deflections, since there is less resistance. If the stiffness decreases and the mass remains equal the beam will have a longer fundamental period.

In Figure 5.19 and Figure 5.20 the maximum occurring deformation and stresses at each location of the beam are presented.

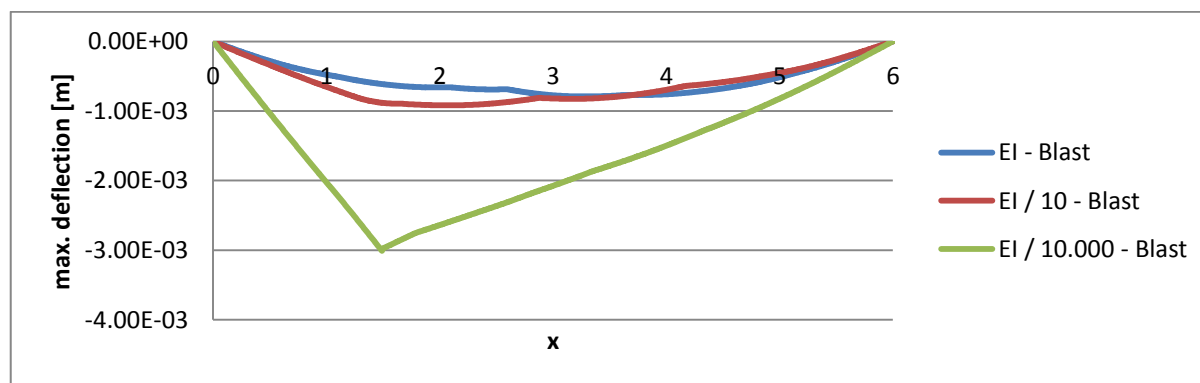


Figure 5.19: Maximum deflection at each point of the beam (at different points in time) .

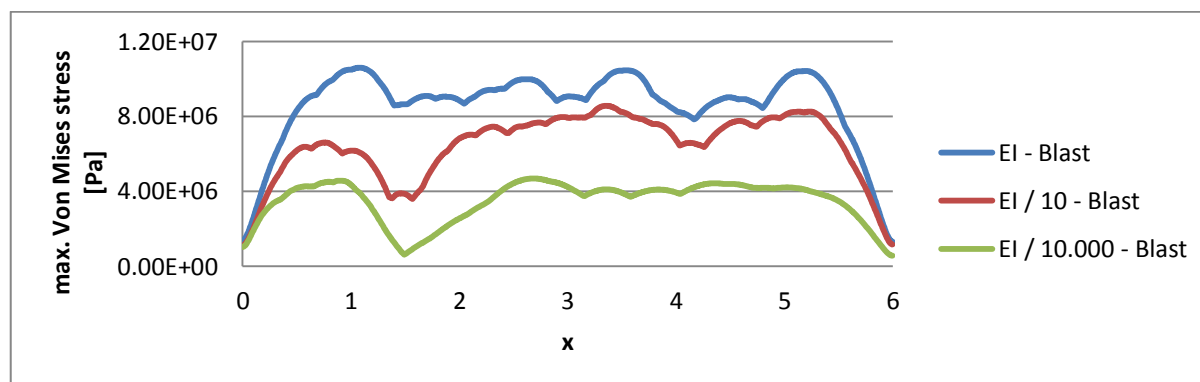


Figure 5.20: Maximum von Mises Stress at each point of the beam (at different points in time).

It can be observed that the maximum deflections are slightly larger and the stresses are decreased by 20% in case 1 . In case 2 a plastic hinge has been formed.

In the examined cases a section has been given a reduced bending stiffness during the whole loading process, while from the dynamic analyses (Chapter 7) it was observed that the stresses fluctuate very fast. It is therefore hard to estimate how much the bending stiffness would decrease. Depending on the yield strength and on the ductility of the material these differences may as well be smaller or greater as presented in Figure 5.19 and Figure 5.20.

5.5 Summary

The amount of plasticity that will occur due to an arbitrary blast wave is not known in advance. Therefore, to determine the influence of plasticity on the weightfactors, a yielded area has been predefined. This yielded area has a rectangular section with a decreased bending stiffness. The width and the bending stiffness of the rectangular section have been varied to represent different amounts of plasticity.

For a beam with a section with decreased bending stiffness at 1 or 2 locations the “plastic” weightfactors have analytically been determined. The equivalent uniform loads obtained by multiplying the “plastic” weightfactors with a local uniform load have been compared with the equivalent uniform load obtained with the “elastic” weightfactors. The effect of the “plastic” weightfactors on the equivalent load is small in case the section(s) with decreased bending stiffness is/are around midspan. When the section with decreased bending stiffness is at $x=0.25 \cdot l$ the

difference between the elastic and plastic equivalent uniform load became larger. However, when there are two sections with decreased bending stiffness, at $x=0.25 \cdot l$ and $x=0.75 \cdot l$, the difference between the elastic and plastic equivalent uniform load is small.

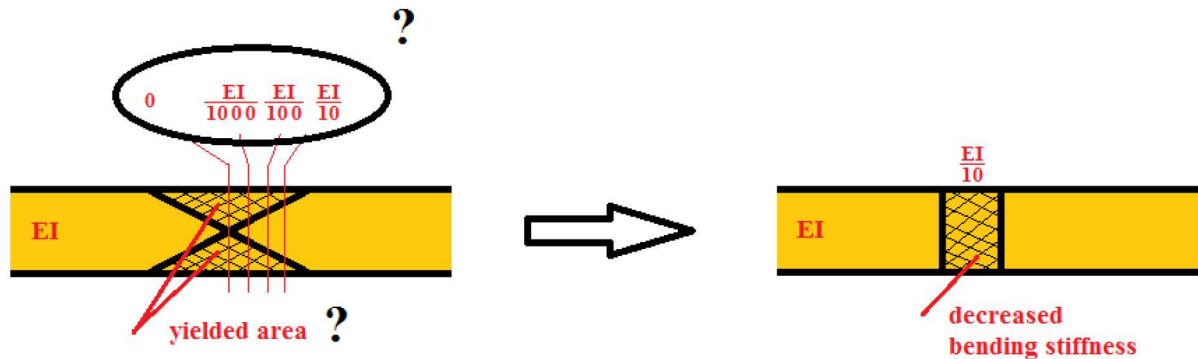


Figure 5.21: Simplification of the decreased bending stiffness due to yielding

In most cases the loading time due to a close-in blast is much shorter than the natural period of a beam and most plastic deformation occurs after the loading period. In this case the “elastic” weightfactors are usable. However, when the ratio between the load duration and fundamental period of the beam becomes larger, yielding might occur before the loading has finished. If this happens large errors might be obtained of the estimated deflections.

The calculated “plastic” weightfactors might be used for beams with discontinuous cross sections, since in this case the bending stiffness is reduced as well.

To verify if the statements made above hold for blast waves, in this research dynamic calculations have been done for different ratios between the Blast load duration and the fundamental period of the beam. This is described in Chapter 7.

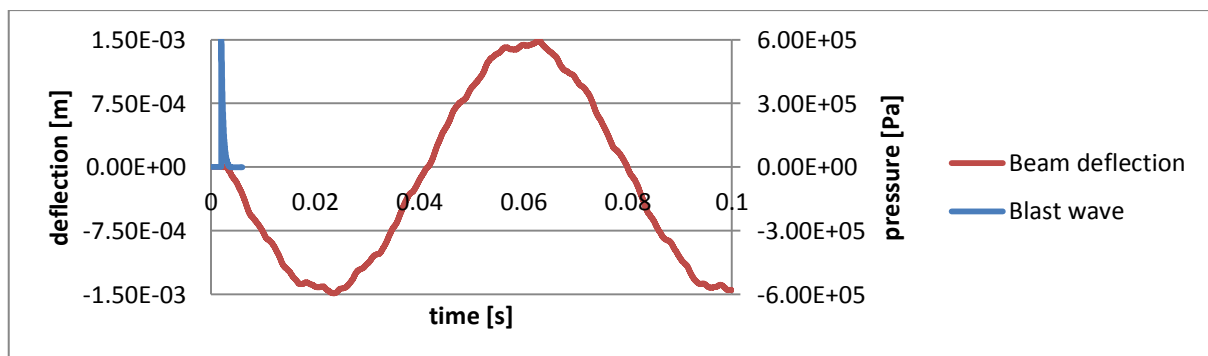


Figure 5.22: Comparison between the duration of a blast load of 1kg TNT equivalent with a stand-off of 2m and the fundamental period of a 6m long beam.

Part III
Accuracy of the LS-DYNA estimations

Chapter 6

Accuracy of the static deflection of a linear-elastic beam

When a non-uniform load is translated to a uniform load an approximation is made. The accuracy of the obtained deflection depends on in how many parts the beam has been split to determine the equivalent uniform load. In this chapter it has been investigated how accurate the weightfactors are for different fictive non-uniform static load distributions and in how many parts the beam needs to be split to obtain an accurate result. It has also been investigated what the influence of the boundary conditions are on the accuracy of the obtained estimations with the equivalent uniform load.

This study has been done for static loading to explicitly focus on the accuracy of the weightfactors on estimating the deflection at midspan (i.e., to see if the load has been caught correctly). In case of dynamic loading several other factors such as higher vibration modes and the ratio between the load duration and the fundamental period may influence the accuracy of the estimations. The influence of these other factors have been investigated in Chapter 7.

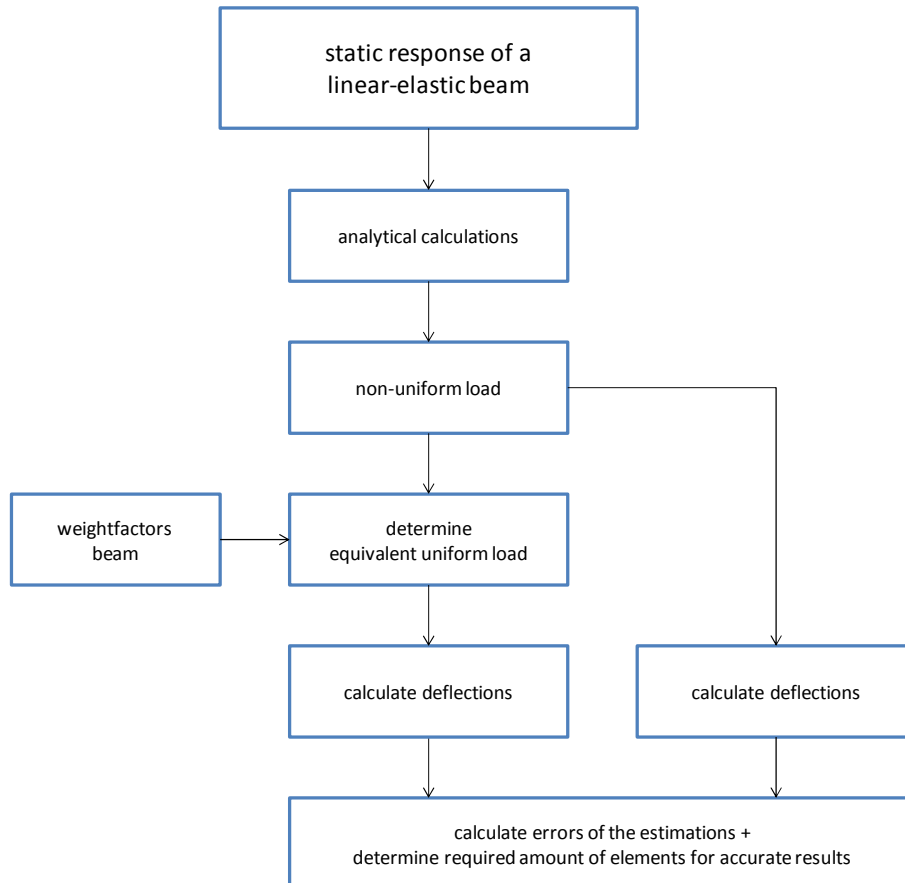


Figure 6.1: Flowchart Chapter 6

6.1 Example calculation

Using the weightfactors a non-uniform load distribution can be translated to an equivalent uniform load distribution.

- First the load is simplified by splitting the load in a certain amount of parts and assuming the load to be uniformly distributed over these parts. The uniform load will have the value of the non-uniform load at the centre of the corresponding part. See Figure 6.2
- The equivalent uniform load is then obtained by summing the product of the uniform loads and the corresponding weightfactors. See Figure 6.3.

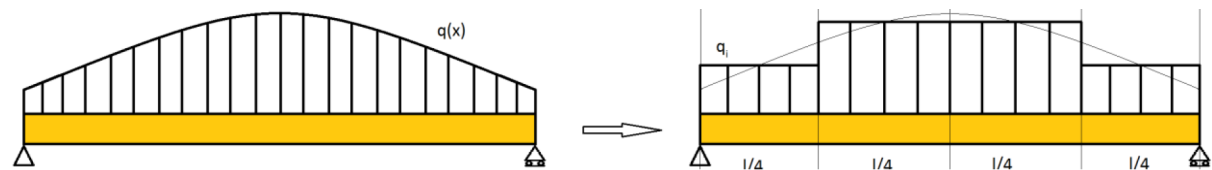


Figure 6.2: Simplification of a non-uniformly distributed load

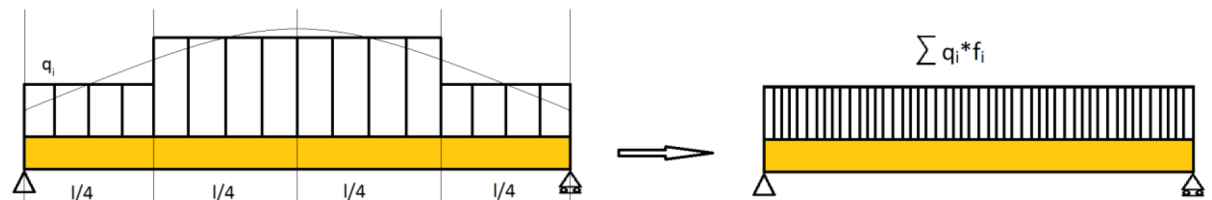


Figure 6.3: Translation to equivalent uniform load

Since an equivalent uniformly distributed load has been determined, now the deflection at midspan can easily be calculated using the standard formulas for a uniformly loaded beam:

$$w\left(x = \frac{l}{2}\right) = \sum_{i=1}^{\frac{l}{\Delta x}} \frac{5 q_i f_i l^4}{384 EI} \quad \text{for simply supported beams} \quad (6.1)$$

$$w\left(x = \frac{l}{2}\right) = \sum_{i=1}^{\frac{l}{\Delta x}} \frac{q_i f_i l^4}{384 EI} \quad \text{for fixed beams} \quad (6.2)$$

Where:

- q_i the value of the non-uniform load at the middle of part i
- f_i the weightfactor for part i
- Δx the size of the parts
- EI the bending stiffness
- l the length of the beam

For a sinusoidal load of half a period the approximated deflection is compared to the exact deflection. See Table 6.1. It can be seen that by dividing the beam in 4 parts an accurate result of the deflection at midspan is obtained.

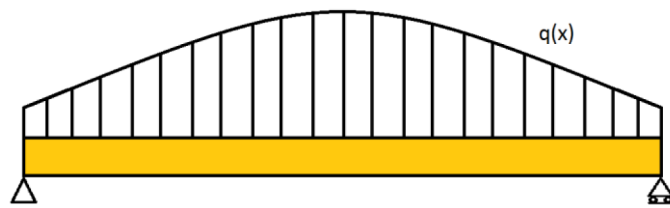


Figure 6.4: Simply supported beam loaded by a load in the form of a half of a sine period plus 1

Load formula	$W \cdot \left(1 + \sin\left(\frac{\text{Pi} \cdot x}{l}\right) \right)$
part size (Δx)	$l * 1/4$
Approximation of the deflection of a simply supported beam	$\frac{5}{384} \frac{\left(\frac{57}{80} W \left(1 + \sin\left(\frac{3}{8} \pi\right) \right) + \frac{23}{80} W \left(1 + \sin\left(\frac{1}{8} \pi\right) \right) \right) l^4}{EI}$
Approximation of the deflection of a fixed beam	$\frac{1}{6144} \frac{W l^4 \left(3 \sin\left(\frac{1}{8} \pi\right) + 13 \sin\left(\frac{3}{8} \pi\right) + 16 \right)}{EI}$
Exact solution of the deflection of a simply supported beam	$\frac{1}{384} \frac{W l^4 (5 \pi^4 + 384)}{EI \pi^4}$
Exact solution of the deflection of a fixed beam	$\frac{1}{384} \frac{W l^4 (\pi^4 - 96 \pi + 384)}{EI \pi^4}$
Relative Error for the simply supported beam	-1.126%
Relative Error for the fixed beam	-1.128%

Table 6.1: Relative error which has been caused due to simplification of the load

Where:

W the maximum value of the non-uniform load $q(x)$.

$$\text{Relative error} = \frac{w_{\text{approximate}} - w_{\text{exact}}}{w_{\text{exact}}} \cdot 100 \% \quad (6.3)$$

$w_{\text{approximate}}$ approximated deflection [m]

w_{exact} exact deflection [m]

6.2 Boundary conditions

In this subchapter the difference in accuracy of the deflection of an at two sides fixed beam and a simply supported beam have been investigated. The accuracy of the deflection at midspan has been investigated for a load which has the form of a half period of a sine function distributed over a part, h , of the beam. To calculate the equivalent uniform load the beam has been split into 4 parts.

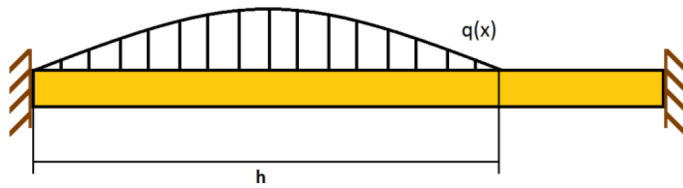


Figure 6.5: Fixed beam, partly loaded by a load in the form of a half of a sine period

In Table 6.2 an overview of the relative error is given for different ways of spreading the load. When the load is spread over a fifth of the beam only one part covers the load and large errors are obtained. If the load is spread over a tenth of the beam the load is not caught and a deflection of 0 is obtained.

h/l	rel. error fixed [%]	rel. error pinned [%]
10/10	-2.788	-2.555
9/10	-3.505	-3.559
8/10	-1.905	-1.264
7/10	-2.689	-1.728
6/10	-6.800	-6.699
5/10	11.072	6.475
4/10	-16.617	-15.619
3/10	0.260	5.961
2/10	189.131	121.947
1/10	-100.000	-100.000

Table 6.2: Accuracy of the deflection at midspan. $\Delta x = l/4$

For the situation that the load is distributed over 1 tenth and 1 fifth of the beam it is investigated how the accuracy changes if the beam is split in more parts. The results are presented in Figure 6.6 and Figure 6.7. It is notable that increasing the amount of parts does not always result in a better estimation of the deflection at midspan. The accuracy of the load depends on how the parts fit in the load and the value of the load at the middle of the parts (which is random).

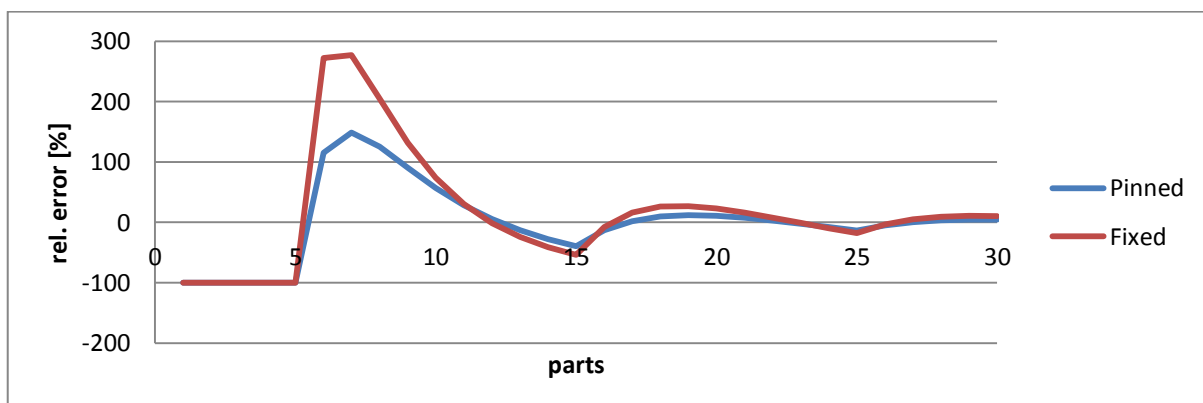


Figure 6.6: Accuracy of a $T/2$ sine load spread over $h = l/10$. Load division into 1 to 30 parts

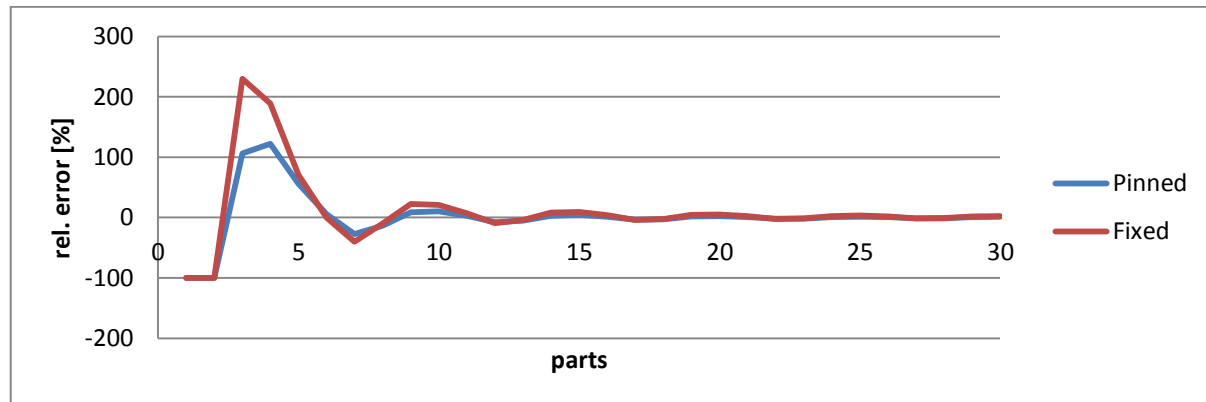


Figure 6.7: Accuracy of a $T/2$ sine load spread over $h = l/5$. Load division into 1 to 30 parts

6.2.1 Conclusion

The accuracy of the estimated deflection, for this load scenario, is slightly higher for the simply supported beam compared to the fixed beam. It can be concluded that the errors are random, but similar for the two different boundary conditions.

6.3 Accuracy of the deflection of different load types

Depending on the location and mass of an explosion, different load distributions are obtained. See Figure 7.4 and Figure 7.5. Several parts of the pressure of a beam subjected to blast loading can be approximated by a certain part of a sine function. The accuracy of the estimations of the elastic deflection at midspan have been investigated for different static load distributions in the form of a fraction of a sine period (see Figure 6.8):

- Load in the form of a half of a sine period
- Load in the form of a quarter of a sine period
- Load in the form of a sixth of a sine period
- Load in the form of a twelfth of a sine period
- A triangular load distribution

The load is spread over a part of the beam between $x=0$ and $x=h$.

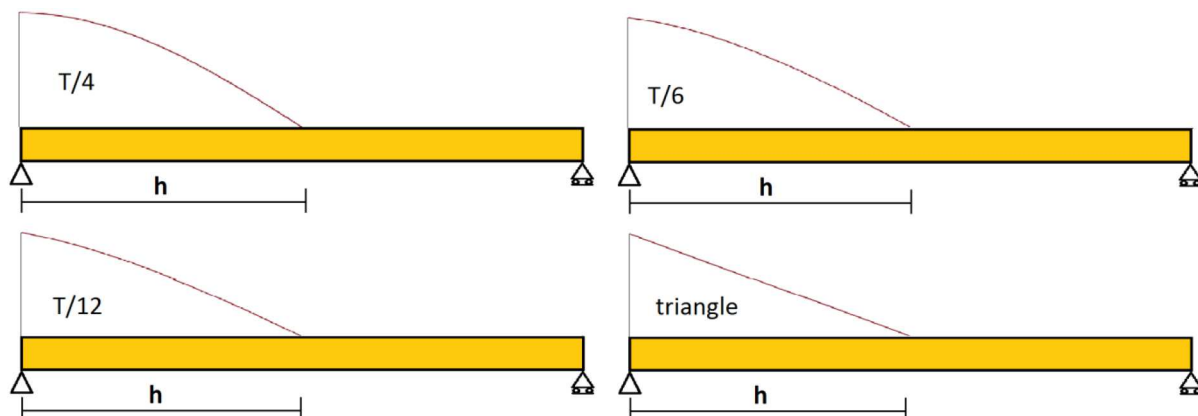


Figure 6.8: Different load types

In Table 6.3 an overview of the relative error is given for distributing the different loads over different parts (h) of the beam). The beam is divided into 4 parts. The colour of each cell indicates the accuracy respectively to the estimations of the other load distributions in the corresponding row. Red being less accurate and green the most accurate. No useful conclusions can be made from these results. It can't be said that one load is approximated more accurate than the other, since no colour pattern can be found

h/l	Rel. error [%] for sine T/2	Rel. error [%] for sine T/4	Rel. error [%] for sine T/6	Rel. error [%] for sine T/12	Rel. error [%] for triangle
1	-2.555	-0.612	-0.448	-0.342	0.000
0.9	-3.559	-0.988	-0.776	-0.639	-0.199
0.8	-1.264	0.757	0.944	1.065	1.464
0.7	-1.728	1.038	1.284	1.444	1.963
0.6	-6.699	-1.264	-0.826	-0.546	0.348
0.5	6.475	8.537	8.757	8.900	9.375
0.4	-15.619	-2.316	-1.369	-0.773	1.073
0.3	5.961	18.677	19.330	19.720	20.813
0.2	121.947	82.930	79.752	77.715	71.196
0.1	-100.000	-100.000	-100.000	-100.000	-100.000

Table 6.3: Relative error obtained by splitting a simply supported beam into 4 parts

To obtain a clearer overview of the accuracies of the different load distributions the load is divided into 2, 3 and 4 parts. See Table 6.4, Table 6.5 and Table 6.6 respectively.

h/l	Rel. error [%] for sine T/2	Rel. error [%] for sine T/4	Rel. error [%] for sine T/6	Rel. error [%] for sine T/12	Rel. error [%] for triangle
1	-10.314	-2.094	-1.510	-1.143	0.000
0.9	-6.022	-1.518	-1.160	-0.930	-0.199
0.8	-5.886	-0.860	-0.455	-0.196	0.631
0.7	1.056	4.352	4.653	4.848	5.479
0.6	-6.699	-1.264	-0.826	-0.546	0.348
0.5	6.475	8.537	8.757	8.900	9.375
0.4	8.281	9.858	10.044	10.167	10.577
0.3	6.782	8.631	8.833	8.966	9.406
0.2	10.419	11.458	11.606	11.706	12.043
0.1	10.911	11.832	11.972	12.066	12.387

Table 6.4: Relative error obtained by splitting a simply supported beam such that the load is covered by 2 parts

h/l	Rel. error [%] for sine T/2	Rel. error [%] for sine T/4	Rel. error [%] for sine T/6	Rel. error [%] for sine T/12	Rel. error [%] for triangle
1	-4.482	-1.038	-0.758	-0.578	0.000
0.9	-3.559	-0.988	-0.776	-0.639	-0.199
0.8	-1.264	0.757	0.944	1.065	1.464
0.7	-5.105	-1.921	-1.663	-1.498	-0.967
0.6	1.505	2.861	3.007	3.104	3.427
0.5	2.617	3.655	3.778	3.860	4.138
0.4	1.092	2.475	2.617	2.710	3.019
0.3	4.029	4.696	4.791	4.856	5.079
0.2	4.421	4.991	5.080	5.140	5.348
0.1	4.646	5.162	5.247	5.304	5.504

Table 6.5: Relative error obtained by splitting a simply supported beam such that the load is covered by 3 parts

h/l	Rel. error [%] for sine T/2	Rel. error [%] for sine T/4	Rel. error [%] for sine T/6	Rel. error [%] for sine T/12	Rel. error [%] for triangle
1	-2.555	-0.612	-0.448	-0.342	0.000
0.9	-2.404	-0.723	-0.583	-0.492	-0.199
0.8	-0.716	0.536	0.657	0.735	0.995
0.7	-0.357	0.702	0.806	0.874	1.100
0.6	0.059	1.001	1.096	1.159	1.367
0.5	1.426	2.030	2.104	2.153	2.322
0.4	1.894	2.373	2.437	2.481	2.631
0.3	0.826	1.578	1.658	1.712	1.891
0.2	2.448	2.788	2.842	2.879	3.007
0.1	2.576	2.885	2.937	2.972	3.096

Table 6.6: Relative error obtained by splitting a simply supported beam such that the load is covered by 4 parts

6.3.1 Conclusion

When the load is divided into more parts it becomes clear how the course from less accurate to more accurate is divided over the different load distributions. It can be seen that if the load is distributed over 70% of the beam or less, the deflection of a beam subjected to a half period of a sinusoidal load is more accurate than the deflection of a beam subjected to a triangular load (with a transition for the load distributions in between). However, when the load is distributed over a larger part, it is the contrary.

6.4 Summary

In this chapter it has analytically been determined how accurate the weightfactors are for different fictive non-uniform static load distributions and in how many parts the beam needs to be split to obtain accurate results. It has also been investigated what the influence of the boundary conditions are on the accuracy of the equivalent uniform load.

This study has been done for static loading to explicitly focus on the accuracy of the weightfactors on estimating the deflection at midspan (i.e., to see if the load has been caught correctly). In case of dynamic loading several other factors such as higher vibration modes and the ratio between the load

duration and the fundamental period may influence the accuracy of the estimations. The influence of these factors have been investigated in Chapter 7.

Boundary conditions

From the analytical calculations for different boundary conditions it resulted that when a load in the form of a half of a sine period is divided into a few parts to calculate an equivalent uniform load the deflection at midspan of a simply supported beam is more accurate than the deflection of a fixed beam. The error however is random and the accuracy of other load scenarios will therefore be different.

When more elements are used the difference between the accuracy of the different boundary conditions becomes negligible. It can be assumed that if a beam is divided into enough parts, independent of the boundary conditions, accurate estimations of the deflection at midspan of a statically loaded beam may be obtained.

Different load cases

When the loading is distributed over a small part of the beam it is harder to catch the load correctly. The beam needs to be divided into a large enough amount of parts to obtain an accurate estimation of the deflection at midspan. There is a random factor which influences the accuracy of the estimations. The influence of the random factor depends on 1. how the load fits inside the parts and 2. the amount of parts covering the load.

The error of the estimated deflection at midspan can be both negative (underestimation) and positive (overestimation). For the investigated load cases it holds that when the beam is divided in an amount of parts such that the load is covered by two three or four parts, an approximate maximum relative error of the estimation of the deflection at midspan of respectively 12%, 5.5% and 3% is obtained. See Table 6.4, Table 6.5 and Table 6.6.

In Table 6.7 the load scenarios which satisfy different maximum allowed absolute errors of the estimated deflection at midspan are presented.

	Load covered by 2 parts	Load covered by 3 parts	Load covered by 4 parts
	h/l	h/l	h/l
max 1%	-	-	-
max 2%	-	0.80	0.6 to 0.8
max 3%	-	0.80	0.3 to 1
max 4%	-	0.4 and 0.6 and 0.8 to 0.9	0.1 to 1
max 5%	-	0.4-0.6 and 0.8-1	0.1 to 1
max 6%	-	0.1 to 1	0.1 to 1
max 7%	0.6 to 0.8	0.1 to 1	0.1 to 1
max 8%	0.6 to 0.9	0.1 to 1	0.1 to 1
max 9%	0.6 to 0.9	0.1 to 1	0.1 to 1
max 10%	0.6 to 0.9	0.1 to 1	0.1 to 1

Table 6.7: Load scenarios which satisfies different maximum allowed errors of the estimated deflection at midspan

The final purpose of the weightfactors is to translate a non-uniform blast load to an equivalent uniform load. For blast loading the size of the loaded part of the beam and the distribution varies in

time, this makes it hard to tell in how many parts the beam needs to be divided in. If the pressure distribution of a blast load is known a rough estimation of the needed amount of elements can be made.

Chapter 7

Accuracy of the Dynamic Response of a Beam

In this chapter the accuracy of the weightfactors has been determined for dynamic (blast) loading. To do this the deflections and stresses of a beam subjected to the equivalent uniform load have been compared with the deflections and stresses of a beam subject to non-uniform blast loading. The dynamic calculations have been done using FE software LS-DYNA.

To determine the scope in which the weightfactors can be applied, the following parameters have been varied:

- The yield strength of the beam: to introduce different amounts of yielding
- Location of the explosive: to introduce different amounts of non-uniformity and asymmetry of the load
- Mass of the explosive: to introduce different load distributions
- Ratio between fundamental period and Load duration: large load durations may cause yielding while the beam is still being loaded (affects the validity of the weightfactors)

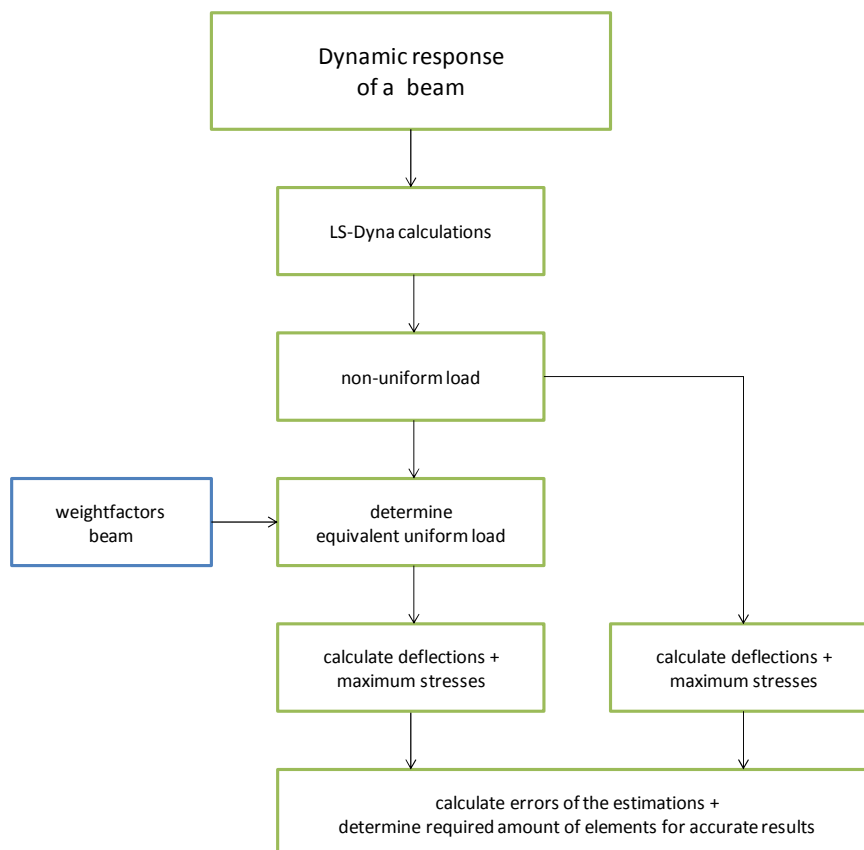


Figure 7.1: Flowchart Chapter 7

7.1 Determine pressure due to blast load

LS-DYNA has been used to determine the pressure on a beam subjected to a blast wave. Clearing effects and reflected waves are not taken into account. The pressure on the beam has been determined for explosions at the following locations (x,z) and of the following masses (m).

- $x=0 \cdot l$
- $x=1/8 \cdot l$
- $x=1/4 \cdot l$
- $x=3/8 \cdot l$
- $x=1/2 \cdot l$

- $z = 1\text{m}$
- $z = 2\text{m}$
- $z = 3\text{m}$

- $m = 1\text{ kg TNT equivalent}$
- $m = 5\text{ kg TNT equivalent}$ (only at 1 and 2 meters height)
- $m = 10\text{ kg TNT equivalent}$ (only at 3 meters height and above the centre of the beam)
- $m = 20\text{ kg TNT equivalent}$ (only at 3 meters height and above the centre of the beam)
- $m = 100\text{ kg TNT equivalent}$ (only at 3 meters height and above the centre of the beam)

Location of the explosive along the length of the beam

In Figure 7.2 an overview is given of the pressure over the length of a beam subjected to an explosion 3 meters above the centre of a beam of 6m length. Every line represents the pressure at a different point in time. The explosion takes place above the centre of the beam, therefore the blast wave reaches the centre of the beam first. Over time the blast wave reaches the remaining part of the beam. The distance from the explosion to the boundaries is larger than the distance from the explosion to the centre, therefore a smaller peak pressure closer to the boundaries is obtained. See Figure 7.2 and Figure 7.3.

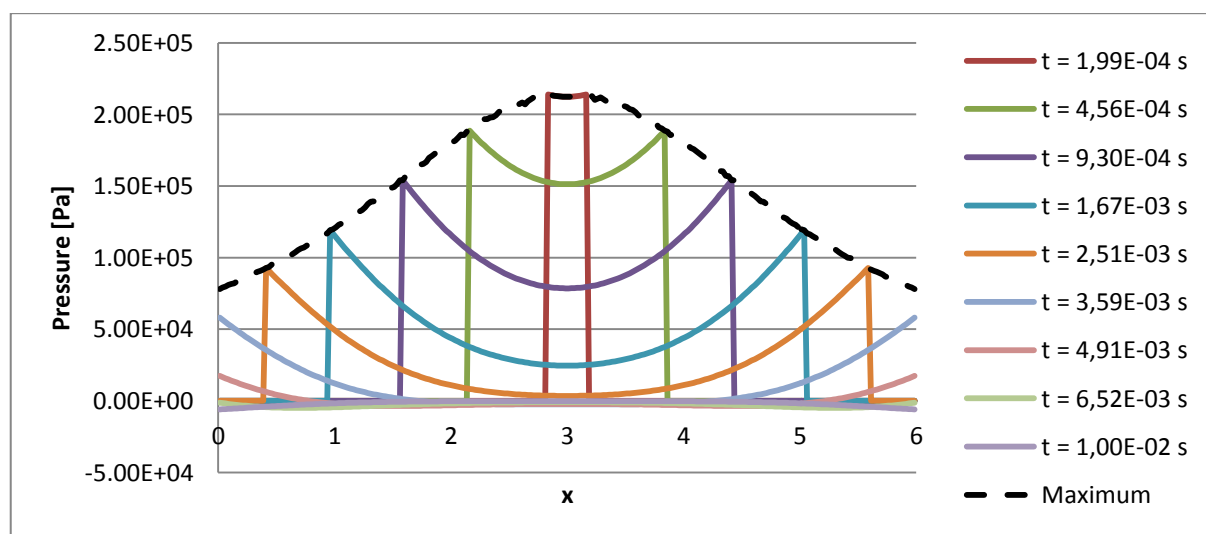


Figure 7.2: Pressure distribution over the length of a 6m long beam subjected to an explosion of 1kg TNT equivalent at 3m above the centre

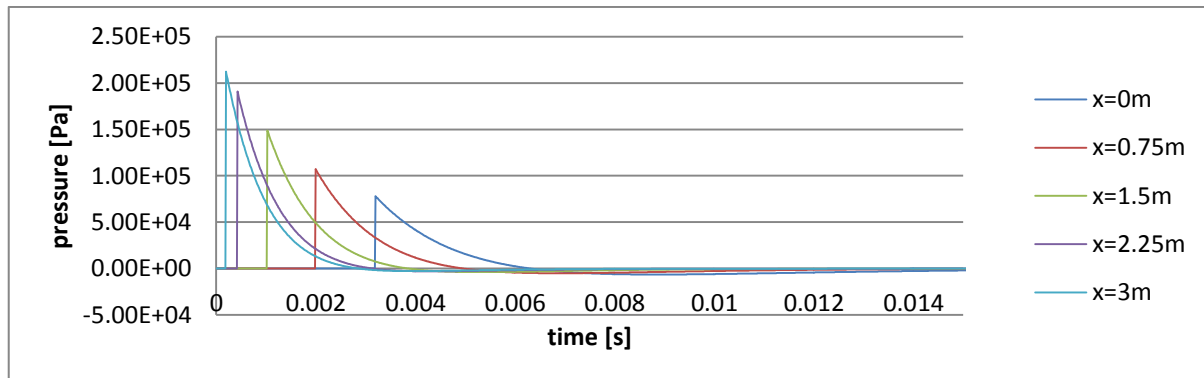


Figure 7.3: Pressure propagation at different locations on a 6m long beam for an explosion of 1kg TNT equivalent at 3m above the centre

In Figure 7.4 the pressure over the length of a beam subjected to an explosion 3 meters above different locations along the length of a beam of 6m length is presented. It can be seen that the load will be moved if the x-location of the explosive changes. If the explosion takes place closer to the boundaries the blast load becomes more non-uniformly distributed, since the difference between the maximum and minimum load on the beam becomes larger.

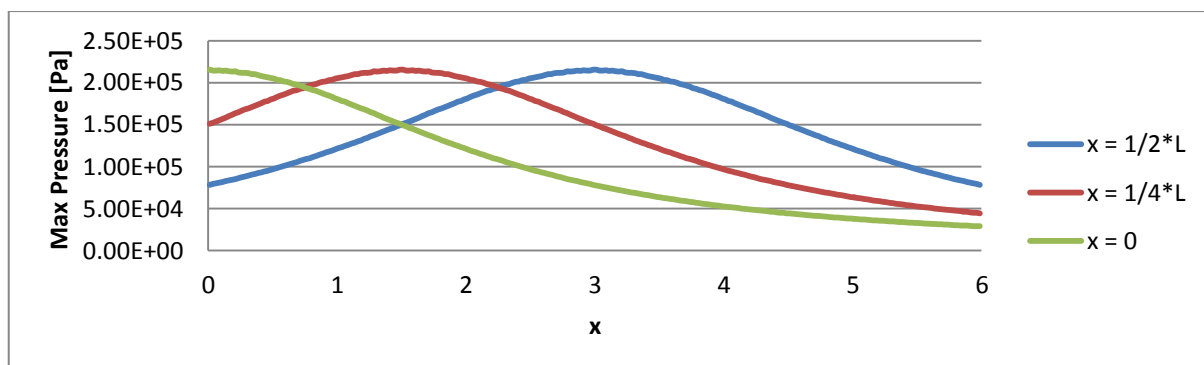


Figure 7.4: Maximum pressure over the length of a 6m long beam subjected to an explosion of 1 kg TNT equivalent at 3m height at different locations (x) along the length of the beam

Height of the explosive

Decreasing the distance of the explosive has a great influence on the (relative) pressure distribution on the beam. In Figure 7.5 it can be seen that if the location of the explosive is closer to the beam the beam will be loaded more locally. Therefore, if an equivalent load needs to be determined for an explosion closer to the beam, more parts are needed to catch the load correctly.

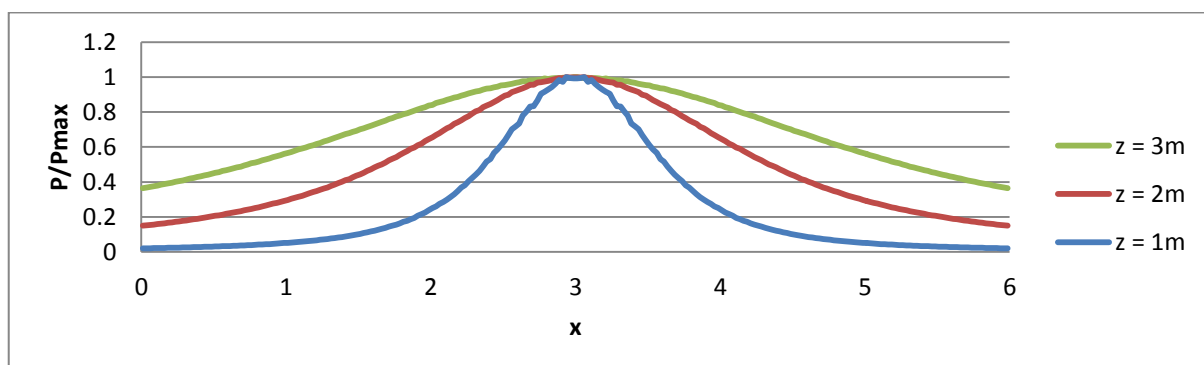


Figure 7.5: Relative pressure distribution over the length of a 6m long beam subjected to an explosion of 1kg TNT equivalent at different distances (z) above the centre of a beam with length 6m.

Mass of the explosive

In Figure 7.6 the maximum pressure on the beam due to an explosion of 20kg and 100kg TNT equivalent has been presented. In Figure 7.7 a slight difference in the relative pressure distribution can be seen for explosions of different masses. The small difference is caused by the non-linear relation between the scaled distance and the pressure. See equation (2.5) and (2.6).

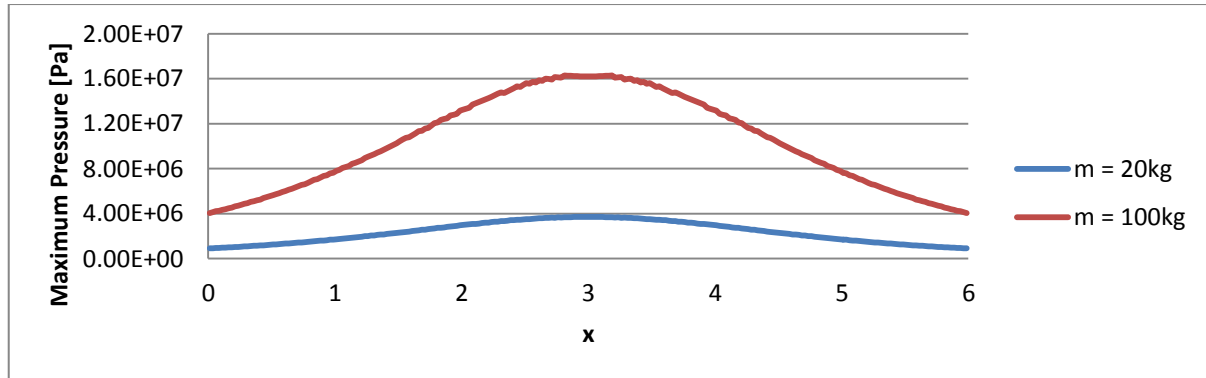


Figure 7.6: Absolute pressure distribution over the length of a beam subjected to an explosion of different masses at 3m above the centre of a 6m long beam.

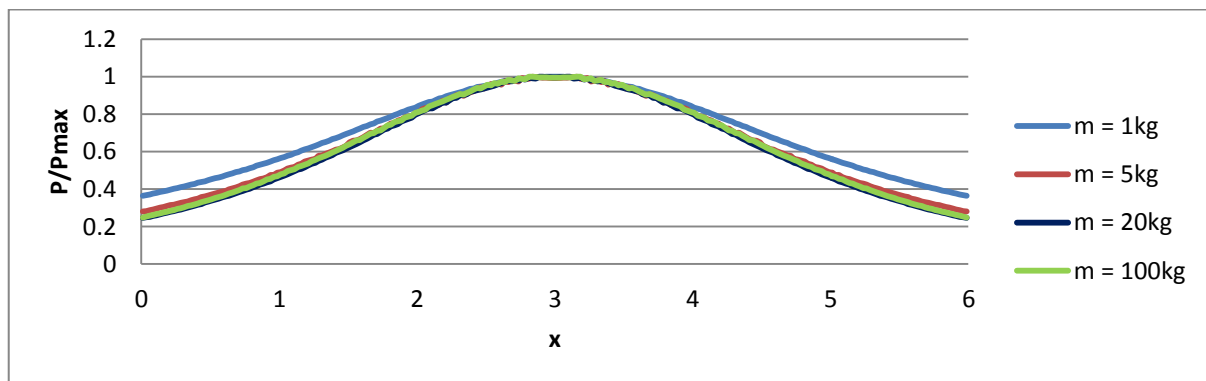


Figure 7.7: Relative pressure distribution over the length of a beam subjected to explosions of different TNT equivalent masses (m) at 3m above the centre of a 6m long beam.

7.2 Determine Equivalent uniform load

The data of the pressure on the beam can be used to calculate an equivalent uniform load. For a simply supported beam analyses have been carried out by splitting the beam into 10 and 240 parts. A calculation for 240 parts has been done to see how accurate the deflection of a beam subjected to the equivalent load eventually approaches the deflection of a beam subjected to a blast load.

To obtain a uniform equivalent load the pressure needs to be multiplied with the corresponding weightfactors and then summed. By doing this, an equivalent value of the uniform pressure over time is obtained. In Figure 7.8 the pressure curve is given for dividing the beam in a different amount of parts. It can be seen that the curve of the equivalent load has more peaks if the beam is subdivided into more parts. The peaks become smaller if the amount of parts increases. Resulting in an almost fluent line for dividing into 240 parts.

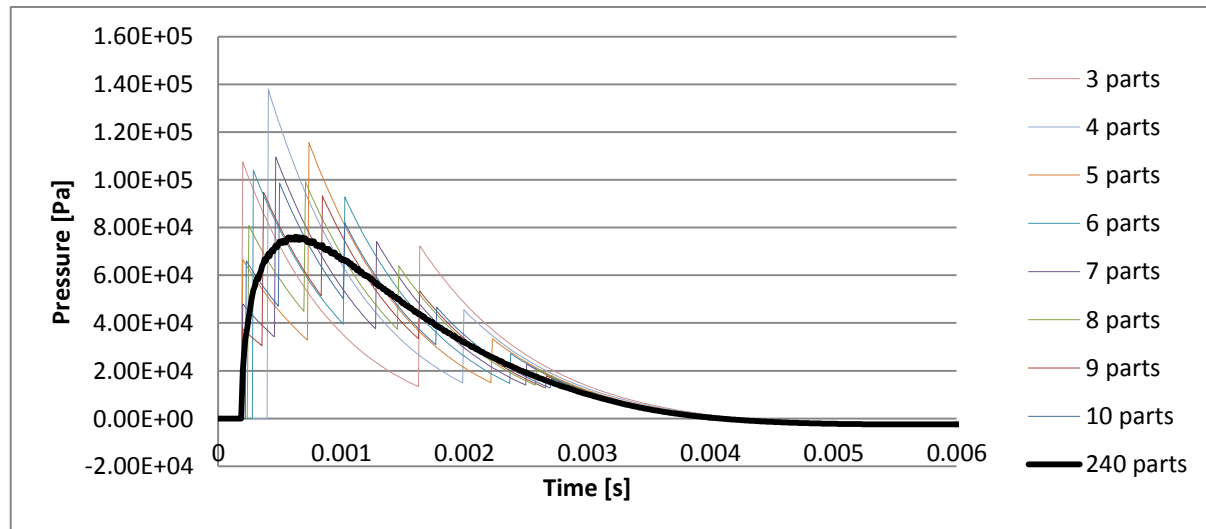


Figure 7.8: Equivalent uniform load for an explosion of 1kg TNT equivalent at 3m above the centre of the bottom surface of a 6 meters long beam

7.2.1 Impulse

It has been investigated if, by looking at the size of the impulse, it can be determined if the beam has been split into enough parts. The impulse of a load is determined as the integral of the pressure over time multiplied by the area on which the pressure acts. In Table 7.1 and Table 7.2 the ratio between the impulse of the equivalent load and the impulse of the blast load is presented for explosions at different locations. If the impulse is calculated for the equivalent uniform loads, which are obtained by splitting the beam into different amounts of parts, it can be seen that the impulse approaches a certain value.

	Blast	3 parts	10 parts	15 parts	240 parts
$x=0.50*I$	1	1.44835	1.24289	1.27506	1.28374
$x=0.375*I$	1	1.05665	1.22479	1.21762	1.22833
$x=0.25*I$	1	0.95766 ¹	1.07230	1.06685	1.07698
$x=0.125*I$	1	1.00744	0.88016	0.87293	0.88327
$x=0$	1	0.81402	0.76403	0.75509	0.75642

Table 7.1: Ratio between the impulse of the equivalent load and the impulse of the blast of 1kg TNT equivalent at 1 meter height above different locations along the length of the beam.

	Blast	3 parts	10 parts	15 parts	240 parts
$x=0.50*I$	1	1.16160	1.16757	1.16961	1.17198
$x=0.375*I$	1	1.11339	1.14868	1.15061	1.15147
$x=0.25*I$	1	1.05485	1.09974	1.09292	1.09894
$x=0.125*I$	1	1.03126	1.03298	1.02512	1.03507
$x=0$	1	0.92755	0.93850	0.92697	0.93957

Table 7.2: Ratio between the impulse of the equivalent load and the impulse of the blast of 1kg TNT equivalent at 2 meter height above different locations along the length of the beam.

In Table 7.1 and Table 7.2 it can be seen that if the explosion takes place closer to midspan, larger ratio's between the impulse of the equivalent load and blast load are obtained. The reason for this is that the weightfactors are larger in the middle than at the ends of the beam. See Figure 7.9.

¹ This value deviates from the decreasing trend. In the other column the ratio between the impulses decreases if the explosion takes place closer to the boundary conditions

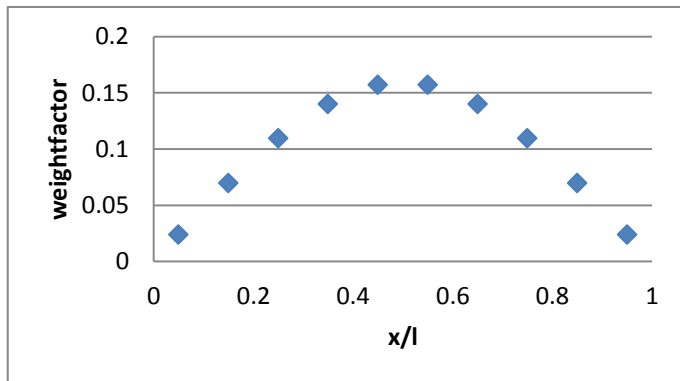


Figure 7.9: weightfactors for a simply supported beam split into 10 parts

Peak pressure, impulse and the decay of the pressure in time are three important aspects of a blast wave which influence the response of a structural element. The dominant aspect may vary for different scenarios. For the investigated cases it may be assumed that if the impulse of the equivalent load is close to the impulse of the equivalent load obtained with 240 elements, the beam has been split into enough parts. However, this has only been verified using FE analyses, for SDOF calculations different results may be obtained.

In Table 7.1 and Table 7.2 it can be seen that the impulse of the equivalent load obtained by splitting the beam into 10 or 15 parts is close to the impulse of the equivalent load obtained by splitting the beam into 240 parts, except for one case. An explosion of 1kg TNT at 1m above $x=0.50 \cdot l$. This is as well the only case where a difference in the deflection at midspan due to splitting the beam into 10 or 15 parts can be observed. See Figure 7.10.

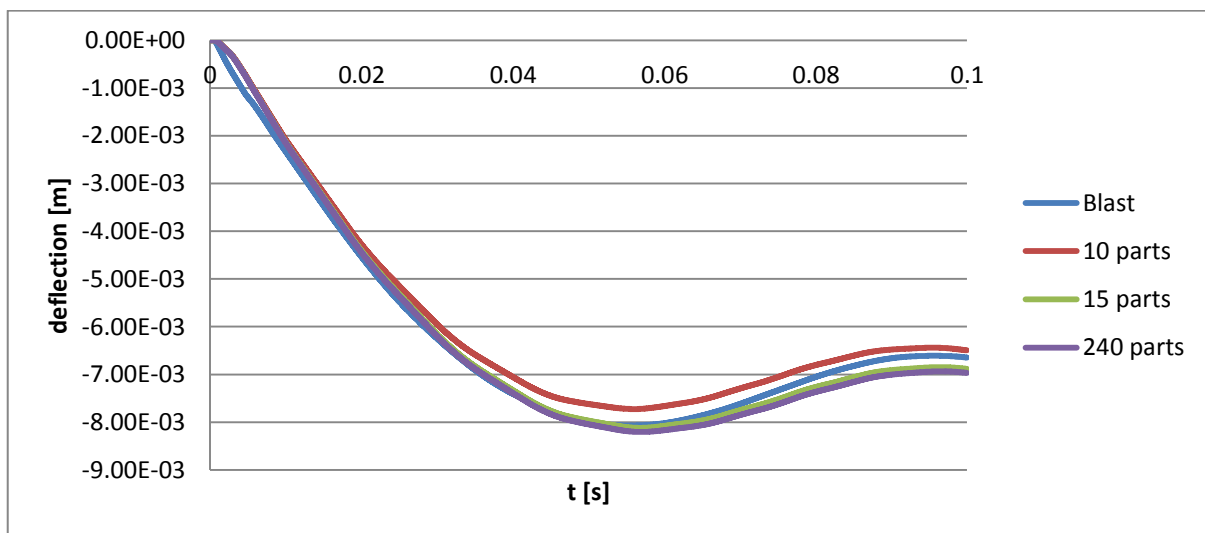


Figure 7.10: Deflection at midspan of a beam with yield strength 2.85E6Pa due to an explosion at 2 meters above $x=0.50 \cdot l$. Lines for 15 and 240 parts overlap each other

7.3 Accuracy of the Linear-Elastic Response

To determine the accuracy of the uniform equivalent load, the deflection at midspan and the maximum occurring bending stresses of a beam subjected to the equivalent uniform load have been compared with the deflection at midspan and the maximum occurring bending stresses of a beam

subjected to the non-uniform blast load. For both load distributions the analyses are performed using LS-DYNA. The FE model is described in appendix D.

The following parameters have been varied:

- Yield strength of the beam: influences the amount of yielding
- Location of the explosive: influences the amount of uniformity and asymmetry of the load. It has a relatively small influence on the load duration. See Figure 7.4 and Figure 7.5.

In Chapter 7.3 the accuracy of the response is investigated for linear-elastic deformation and in Chapter 7.4 for elastic-plastic deformation.

Density	7850 kg/m ³
Young's modulus	2.1E11 Pa
Poisson ration	0.0
Dimensions	0.2x0.2x6 m
Natural period	76.7 ms

Table 7.3: Properties of the investigated beam

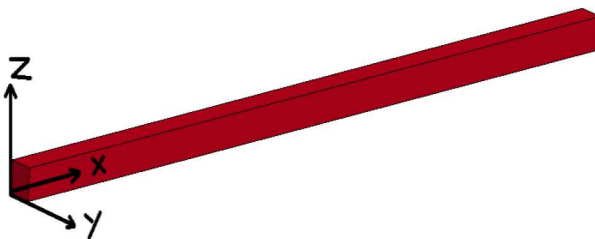


Figure 7.11: Coordinate system of the beam

7.3.1 Deflection at midspan

In Figure 7.12, Figure 7.13 and Figure 7.14 a comparison is made between the deflection at midspan of a beam subjected to equivalent uniform loads obtained by splitting a beam into different amount of parts and the deflection at midspan of a beam subjected to the actual non-uniform blast load. In the graphs it can be seen that the deflection at midspan is well estimated with the equivalent uniform load. For an explosion at a height of 3 meters above the investigated elastic beam it holds that creating an equivalent uniform load by splitting the beam in more than 10 parts doesn't increase the accuracy of the estimations. The same holds for explosions at 1 and 2 meter height.

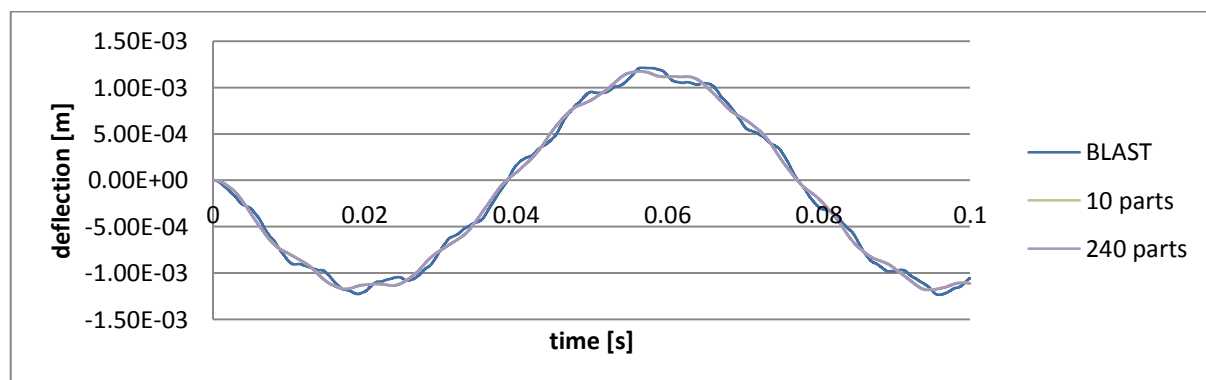


Figure 7.12: Deflection at midspan of a beam for an explosion 3 meters above $x=0.5 \cdot l$. The curve of 10 and 240 parts overlap each other

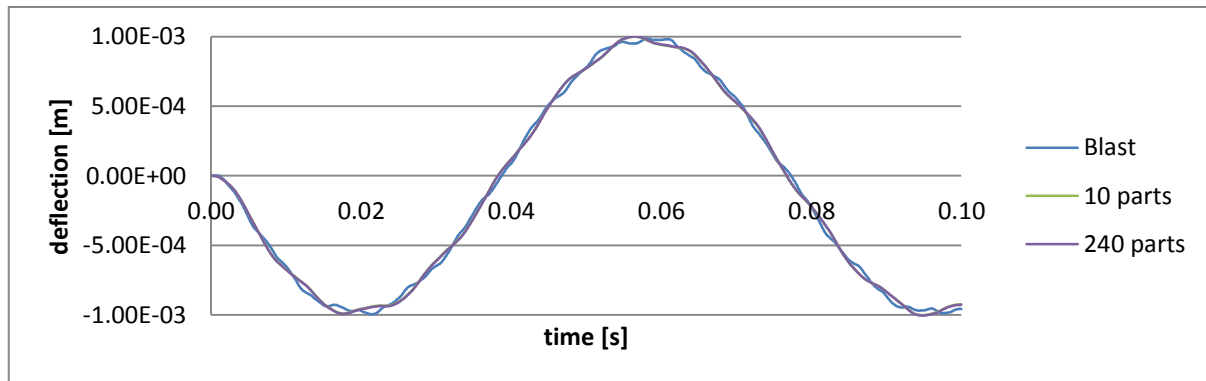


Figure 7.13: Deflection at midspan of a beam for an explosion at 3 meters above $x=0.25*l$. The curve of 10 and 240 parts overlap each other

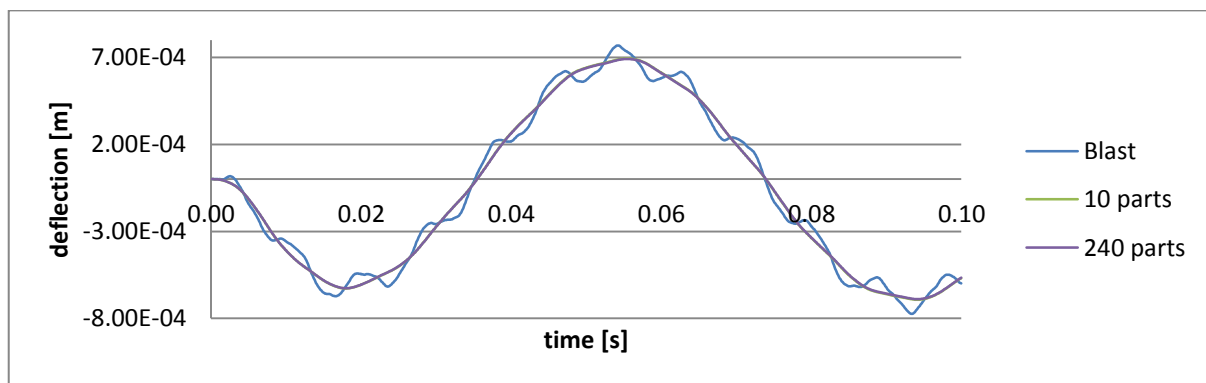


Figure 7.14: Deflection at midspan of a beam for an explosion at 3 meters above $x=0.00*l$. The curve of 10 and 240 parts overlap each other

Asymmetric deformation shapes are obtained in case of asymmetric load distributions. In Figure 7.15 the deformations shape of a beam subjected to an explosion of 1kg TNT equivalent at 2 meters above the left boundary is given at different points in time. It can be seen that for this case higher order vibration modes play an important role and that the maximum deformation, which is obtained at $t=1.83E-02$ s, can still occur around midspan ($0.57*l$ for this case).

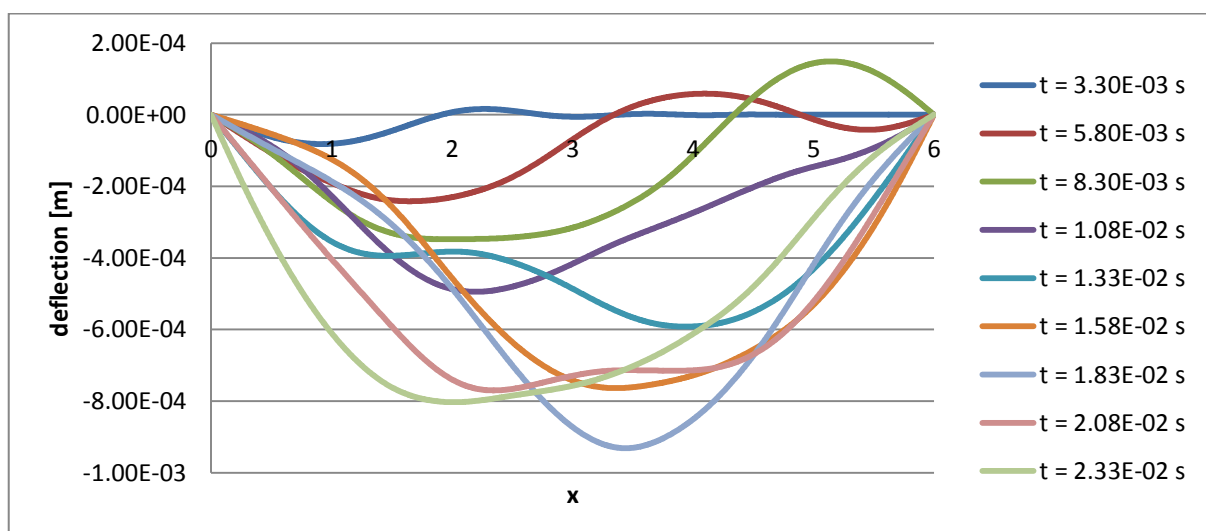


Figure 7.15: Deflection of a 6m long beam subjected to an explosion of 1kg TNT at 2 meters above $x=0$ at different time steps

7.3.2 Stresses

For explosions at 1, 2 and 3 meters height at different locations along the length of the beam the maximum Von Mises stresses due to the equivalent uniform load are compared with the maximum Von Mises stresses due to the non-uniform blast load. In Figure 7.16, Figure 7.17 and Figure 7.18 a few examples are presented of the maximum occurring Von Mises stresses in a beam subjected to an explosion at 3 meters above different locations along the length of the beam.

Explosion 3 meters above midspan

For the explosion at $x=0.50^*$ higher stresses were obtained with the non-uniform blast load (with a maximum at midspan) than with the equivalent uniform load. The maximum occurring bending stress due to the uniform load is 73% of the maximum occurring stress due to the blast load.

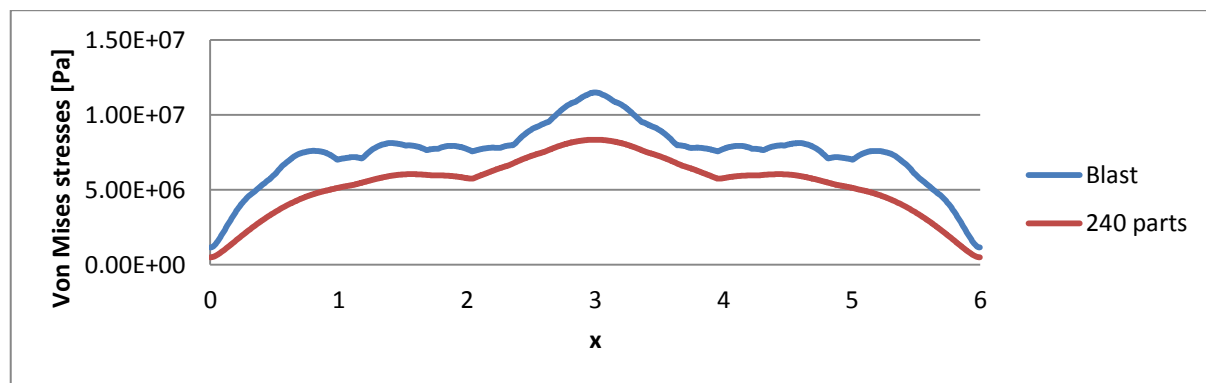


Figure 7.16: Maximum occurring Von Mises stresses over the length of the beam for an explosion 3 meters above $x=0.50^*$. The ratio between the maximum occurring stresses is 0.73. (using 240 parts)

Explosion 3 meters above a quarter of the beam

For the explosion at $x=0.25^*$ higher stresses were obtained with the non-uniform blast load (with a maximum at 0.39^*) than with the equivalent uniform load. The maximum occurring bending stress due to the uniform load is 71% of the maximum occurring stress due to the blast load.

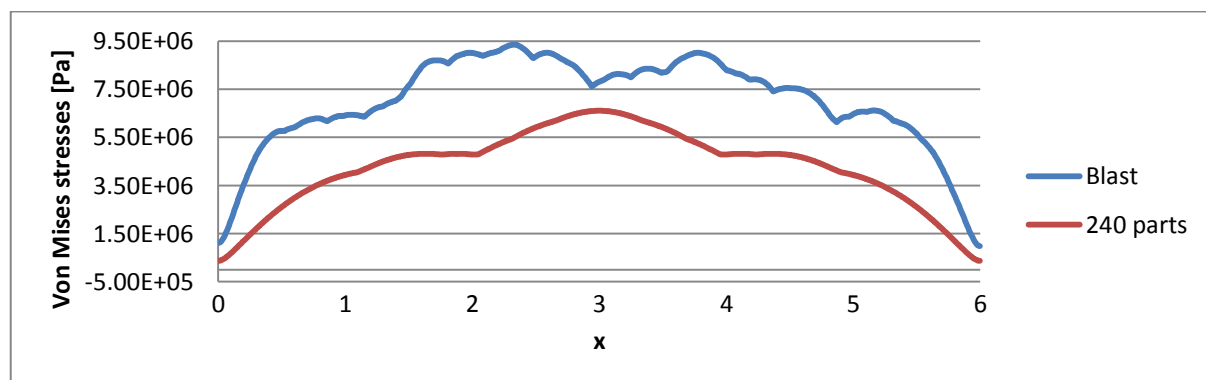


Figure 7.17: Maximum occurring Von Mises stresses over the length of the beam. for an explosion 3 meters above $x=0.25^*$. The ratio between the maximum occurring stresses is 0.71. (using 240 parts)

Explosion 3 meters above the left end of the beam

For the explosion at $x=0$ higher stresses were obtained with the non-uniform blast load (with a maximum at 0.18^*) than with the equivalent uniform load. The maximum occurring bending stress due to the uniform load is 38% of the maximum occurring stress due to the blast load

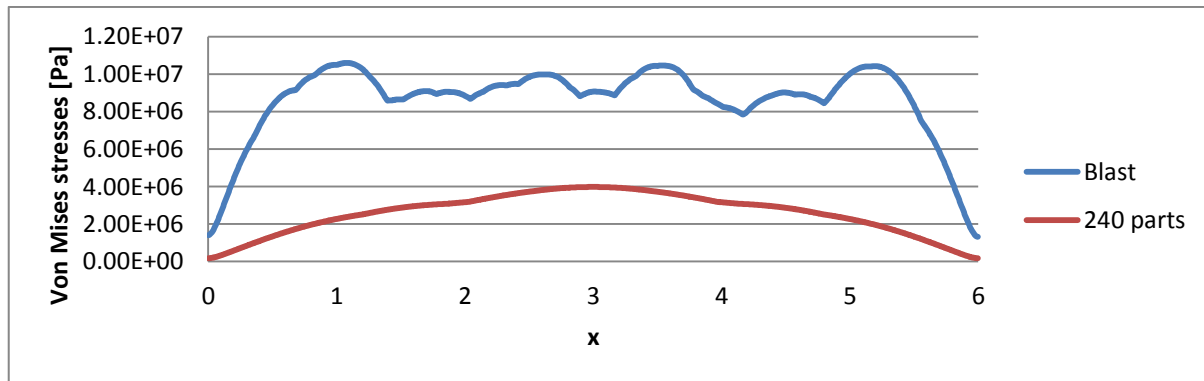


Figure 7.18: Maximum occurring Von Mises stresses over the length of the beam for an explosion 3 meters above $x=0$. The ratio between the maximum occurring stresses is 0.38. (using 240 parts)

In Table 7.4, for explosions at different locations, an overview is given of the obtained ratios between the maximum occurring bending stress of a beam subjected to the equivalent uniform load and the maximum occurring bending stress of a beam subjected to the non-uniform blast load. These ratios are obtained for a beam with properties as presented in Table 7.3. Different ratios between the maximum occurring bending stresses may be obtained for beams with different properties. The larger influence of higher order vibration modes for explosions closer to the boundaries and closer to the beam result in larger differences between the maximum occurring bending stresses.

	$x=0.000 \cdot l$	$x=0.125 \cdot l$	$x=0.250 \cdot l$	$x=0.375 \cdot l$	$x=0.500 \cdot l$
$z=1\text{m}$	0.25	0.36	0.54	0.60	0.64
$z=2\text{m}$	0.31	0.44	0.67	0.69	0.70
$z=3\text{m}$	0.38	0.53	0.71	0.72	0.73

Table 7.4: Ratio between maximum occurring Von Mises stresses due to the equivalent uniform load and the non-uniform blast load. (using 240 parts)

If the obtained ratios in Table 7.4 are compared with the ratio between the stressfactors and weightfactors in Chapter 3, it can be seen that much larger ratios are obtained for dynamic responses. With dynamic loading higher order vibration modes are introduced, which cause larger bending stresses.

7.4 Accuracy of the elastic - plastic response

In case of non-uniform/asymmetric loading high stresses might occur over the entire length of the beam, while it occurs mainly at midspan for a uniform load distribution (e.g. due to higher order vibration modes). If plasticity occurs this will influence the deflection shape of the beam. This makes it harder for the equivalent uniform load to correctly estimate the deflection at midspan. To determine the accuracy of the equivalent load in case of elastic-plastic deformation the following parameters have been varied:

- Yield strength of the beam: influences the amount of yielding
- Location of the explosion: influences the amount of uniformity and asymmetry of the load (and slightly the load duration). See Figure 7.4 and Figure 7.5.

- Mass of the explosive: influences the relative load distribution over the length of the beam and the load duration. See Figure 7.7
- Ratio between fundamental period and Load duration: large load durations may cause yielding while the beam is still being loaded (affects the validity of the weightfactors)

7.4.1 Deflection

In most cases the first maximum of the curve of the deflection at midspan is estimated well. The estimation for the second maximum is less accurate. See Figure 7.19 and Figure 7.20. The first maximum is often the largest deformation that will occur due to a blast wave (ignoring reflections) and therefore determinative for the prediction of the failure of a component. The highest priority is therefore to accurately estimate the first maximum. The second maximum has been ignored in this research.

Location of the explosive

An example of the deflection at midspan of a beam subjected to an explosion of 1 kg TNT 2 meters above $x=1/4*l$ and $x=1/8*l$ is presented in Figure 7.19 and Figure 7.20 respectively. The beam has a yield strength of $3.35e5$ Pa in both cases. For the case with an explosion above an eighth of the beam an error of -15.88% is obtained and in the case with an explosion above a quarter above the beam an error of -6.92% is obtained. It can be seen that if the explosion takes place closer to the boundaries, the accuracy may decrease.

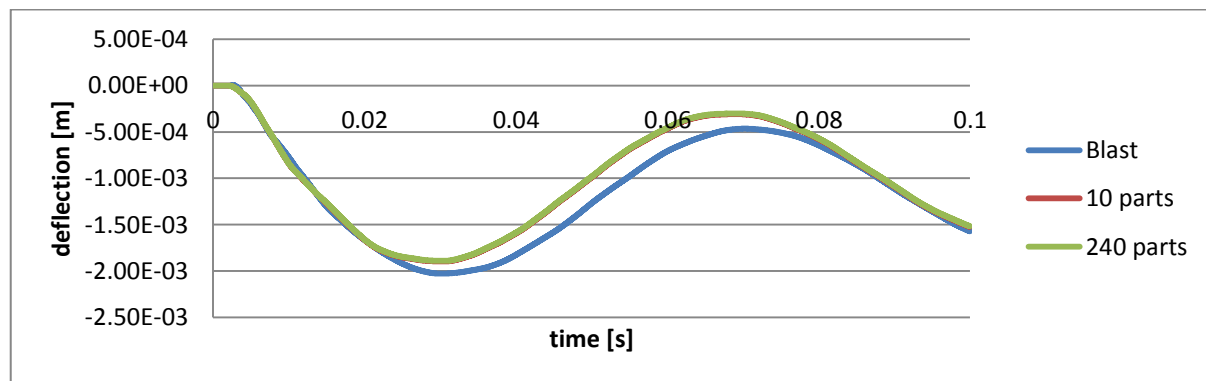


Figure 7.19: Deflection at midspan of a beam due to an explosion 2 meters above $x=1/4*l$. Yield strength = $3.35e6$ Pa. The curve of 10 and 240 parts overlap each other

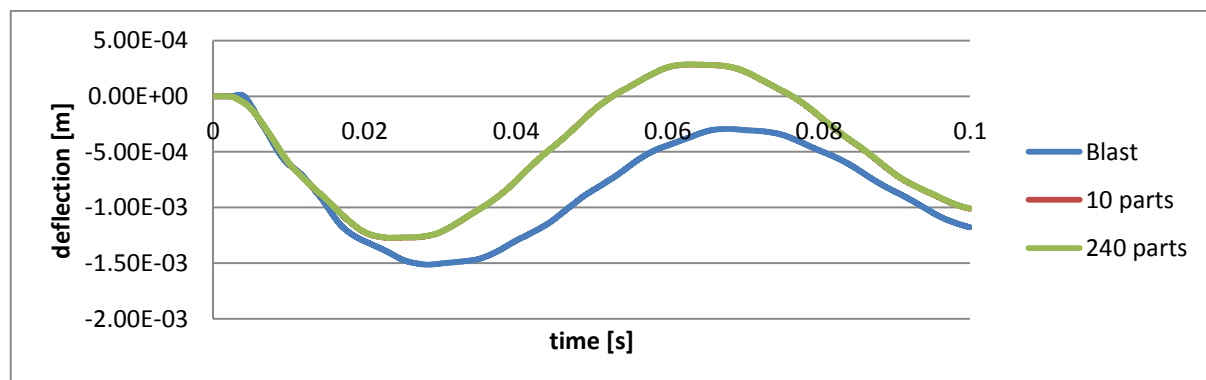


Figure 7.20: Deflection at midspan of a beam due to an explosion 2 meters above $x=1/8*l$. Yield strength = $3.35e6$ Pa. The curve of 10 and 240 parts overlap each other

Accuracy of the estimations

In Figure 7.21 all obtained errors are plotted against the ratio between the maximum obtained deformation of the beam subjected to blast loading and the elastic deformation limit of a static uniformly loaded beam ($w_{max,lsdyna(blast)}/w_{el}$). To obtain different ratios $w_{max,lsdyna(blast)}/w_{el}$ the yield strength of the beam has been varied between 2.35e8 Pa and 2.35e5 Pa.

$w_{max,lsdyna(blast)}$ = maximum deformation of a beam subjected to blast loading
 w_{el} = elastic deformation limit of a static uniformly loaded beam.
 Dependent on the yield strength of the beam

The relative error is defined as:

$$error_{lsdyna, uniform} = \frac{w_{max,lsdyna(uniform)} - w_{max,lsdyna(blast)}}{w_{max,lsdyna(blast)}} \cdot 100 [\%] \quad (7.1)$$

Where:

$w_{max,lsdyna(uniform)}$ = maximum obtained deflection at midspan using the equivalent uniform load (obtained with LS-DYNA)
 $w_{max,lsdyna(blast)}$ = maximum obtained deflection at midspan using the blast load (obtained with LS-DYNA)

In Figure 7.21 it can be seen that the errors are spread over region between -35% and +10%. The load scenarios have been categorized into four groups to obtain a clearer overview:

1. Explosions at 2m and 3m height above $x=1/4 \cdot l$, $3/8 \cdot l$ and $1/2 \cdot l$. See Figure 7.22.
2. Explosions at 1m height above $x=1/4 \cdot l$, $3/8 \cdot l$ and $1/2 \cdot l$. See Figure 7.27.
3. Explosions at 2m and 3m height above $x=0$ and $1/8 \cdot l$. See Figure 7.29.
4. Explosions at 1m height above $x=0$ and $1/8 \cdot l$. See Figure 7.32.

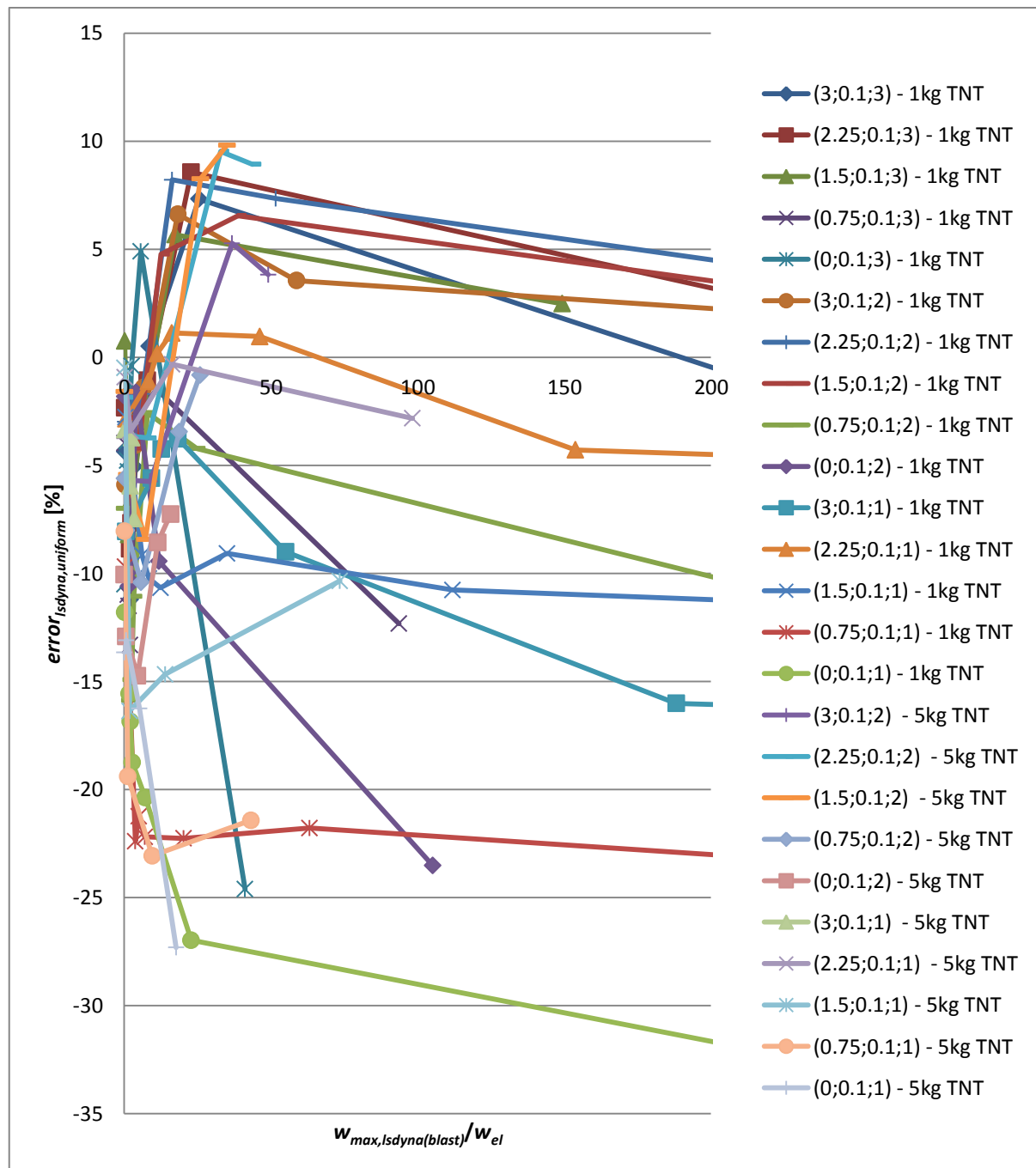


Figure 7.21: Relative error for explosions at different locations (x;y;z) and of different masses

Group 1: Explosions at 2m and 3m height above $x=1/4*l$, $3/8*l$ and $1/2*l$

In Figure 7.22 the relative errors of the deflection at midspan obtained with the equivalent uniform load are presented for explosions at 2 and 3 meters above the middle half part of the beam. A pattern can be observed. The pattern however does not coincide with the factors determined in Chapter 4.5, where a negative error has been obtained. An elucidation for this pattern will now be described.

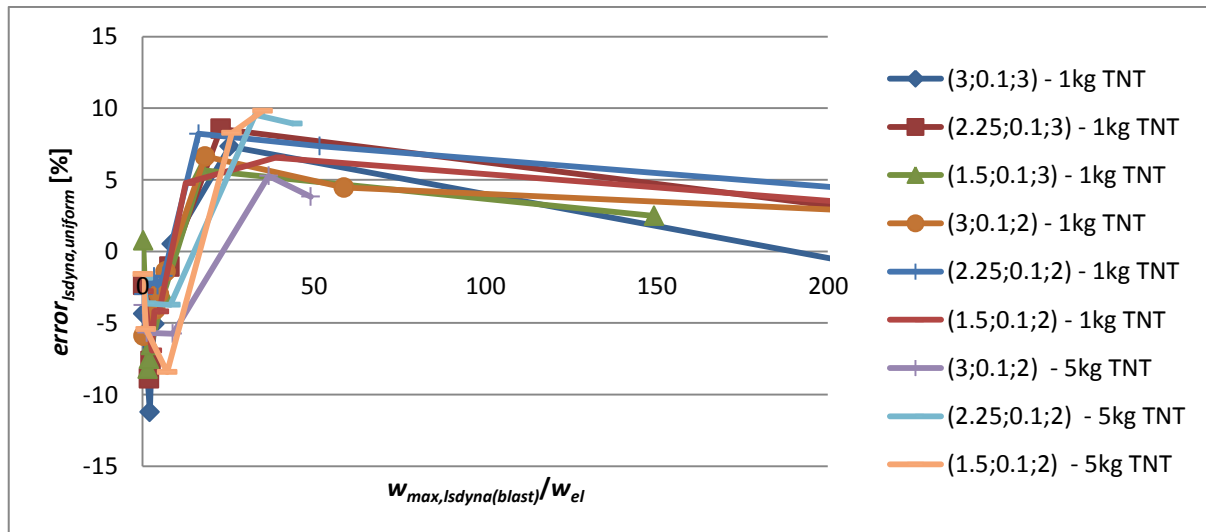


Figure 7.22: Obtained relative error of the estimated deflection at midspan for explosions at 2m and 3m height above $x=1/4 \cdot l$, $x=3/8 \cdot l$ and $x=1/2 \cdot l$.

In Figure 7.23 and Figure 7.24 the deformation of a linear elastic beam subjected to an explosion 2 meters above $x=0$ and the deformation of a linear elastic beam subjected to the equivalent uniform load are presented at different points in time. It can be seen that the deformation shape differs in time.

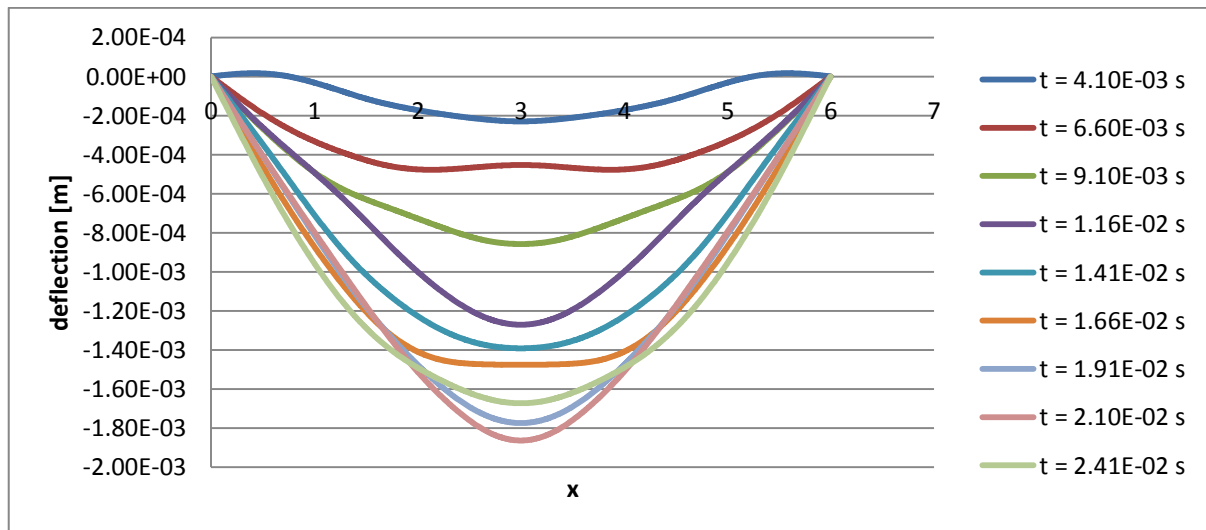


Figure 7.23: Elastic deflection shapes of a 6m long beam due to an explosion of 1kg TNT at 2 meters above $x=0$, at different points in time

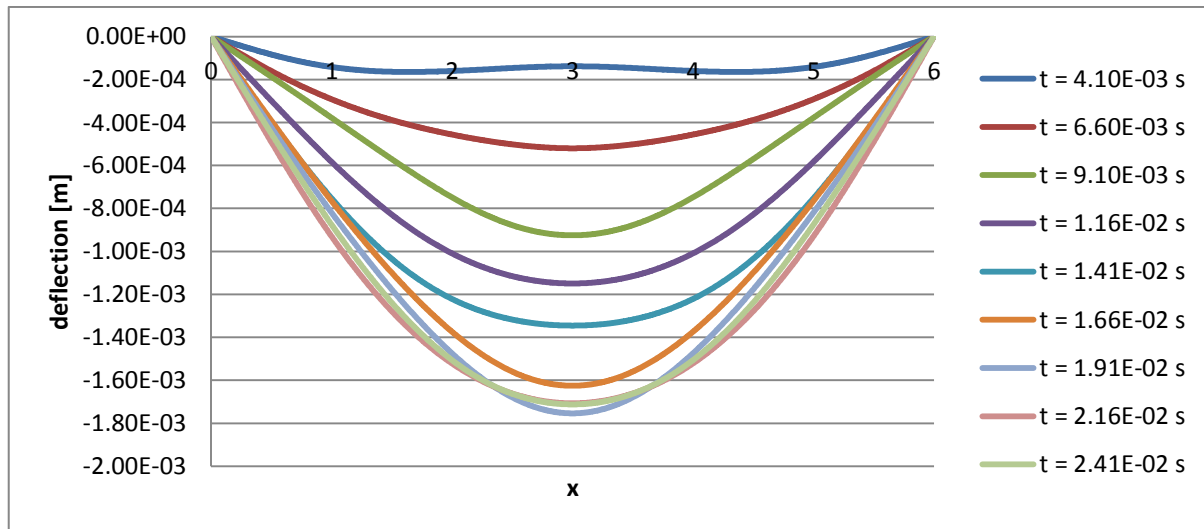


Figure 7.24: Elastic deflection shapes of a 6m long beam due to the equivalent uniform load for an explosion of 1kg TNT at 2 meters above $x=0$, at different points in time

The deformation shape at the moment that yielding occurs is decisive for the size of the maximum deflection at midspan. If the shape is close to its first mode, yielding will occur mainly at midspan. This will result in a reduction of the stiffness of the beam, and therefore large deformations are obtained. If yielding occurs at the moment the beam has a flat shape around midspan (due to higher order vibration modes), yielding will occur over a larger section. This results in a smaller reduction of the stiffness of the beam, and therefore smaller deformations are obtained compared to the case where yielding mainly occurs at midspan.

In Figure 7.25 and Figure 7.26 an example is presented for an explosion at 2m above the centre of a beam with a yield strength of $1.35E6$ Pa. In this case an error of 6.6% and a ratio $w_{max,Isdyna(blast)}/w_{el}$ of 18.8 are obtained. In the figures the deformation of a beam subjected to blast load and a beam subjected to the equivalent uniform load are presented.

If Figure 7.23 is compared with Figure 7.25 it can be seen that yielding has occurred at approximately $t=6.60E-03s$. At this point in time the elastic shape of a beam subjected to a blast load is flat around midspan. Therefore, the yielding has occurred over a large section of the beam, resulting in small deformations. If Figure 7.24 is compared with Figure 7.26 it can be seen that yielding has occurred at approximately $t=6.60E-03s$ as well. The shape of a linear-elastic beam subjected to the equivalent uniform load is close to the first mode at approximately $t=6.60E-03s$, this results in yielding over a small section at midspan. Larger deformations are obtained with the equivalent uniform load. The deformation at midspan has been overestimated for this scenario.

Between approximately $t=9.10E-03s$ and $t=2.41E-02s$ many different deformation shapes can be observed for both an elastic beam subjected to a blast load and an elastic beam subjected to the equivalent uniform load (Figure 7.23 and Figure 7.24). This results in a lot of fluctuations of the obtained error of the estimated deflection for low ratios of $w_{max,Isdyna(blast)}/w_{el}$. See Figure 7.22.

For larger ratios of $w_{max,Isdyna(blast)}/w_{el}$ the deflection is less overestimated with the equivalent uniform load. In Figure 7.24 it can be seen that the deflection shape of a beam subjected to the equivalent uniform load becomes flat around midspan at approximately $t=4.10E-03s$ (due to higher order

vibration modes). This results in yielding over a larger width. Smaller deformations are therefore obtained for beams with a lower yield strength.

The described progress of the deformation of a beam in time is similar for the scenarios where the explosion occurs at a height of 2 or 3 meters above the middle half part of the beam.

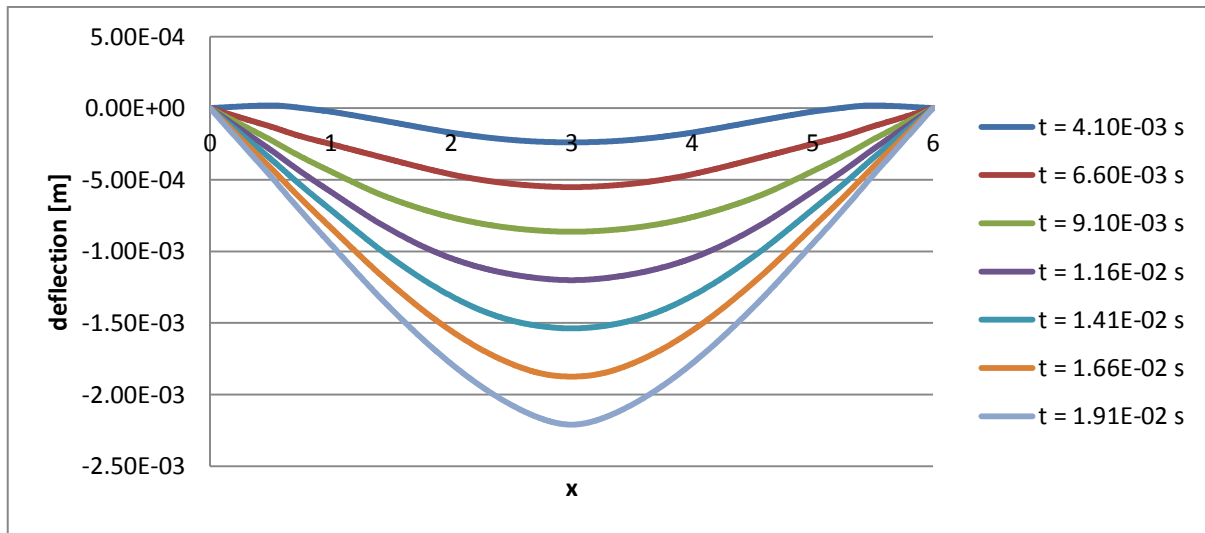


Figure 7.25: Elastic-plastic deflection shape of a 6m long beam subjected to an explosion 2m above the centre, at different points in time.

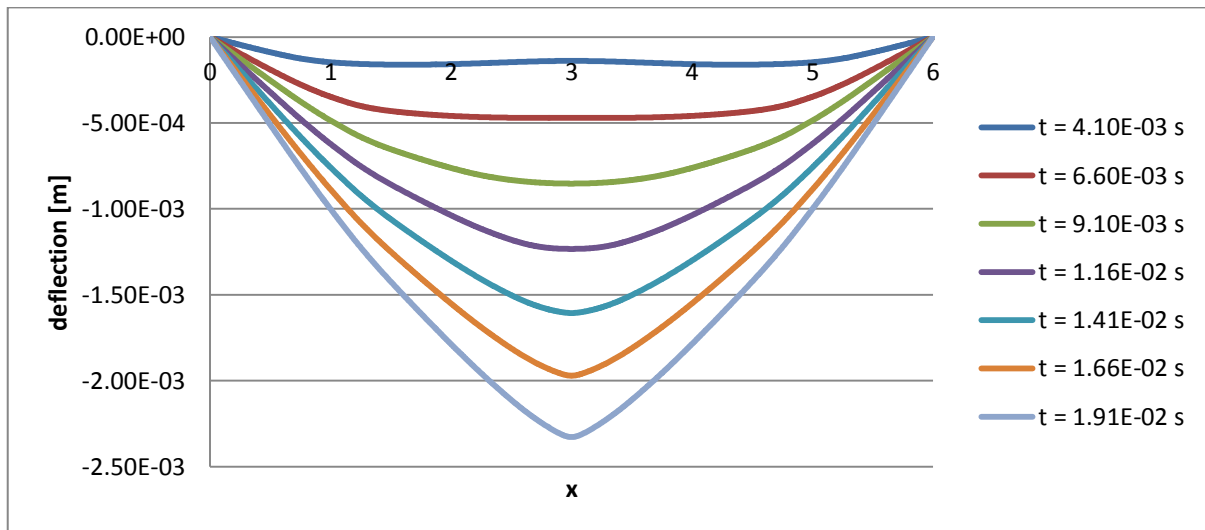


Figure 7.26: Elastic-plastic deflection shape of a 6m long beam subjected to the equivalent load for an explosion 2m above the centre, at different points in time.

Group 2: Explosions at 1m height above $x=1/4*l$, $3/8*l$ and $1/2*l$

In Figure 7.27 the relative errors of the deflection at midspan obtained with the equivalent uniform load are presented for explosions at 1 meter above the middle half part of the beam.

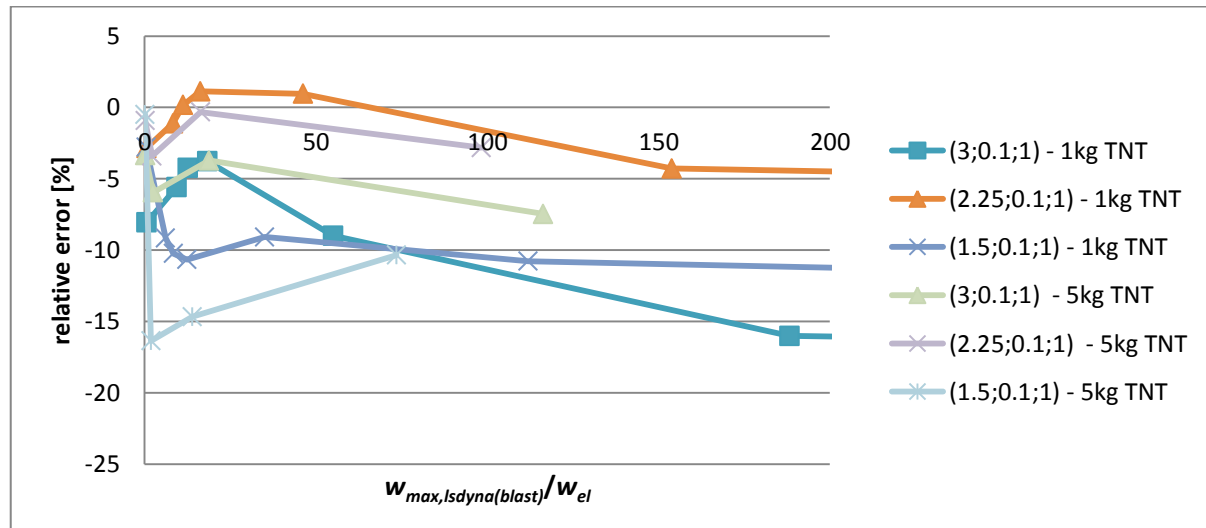


Figure 7.27: Obtained relative error of the estimated deflection at midspan for explosions at 1m height above $x=1/4*l$, $x=3/8*l$ and $x=1/2*l$.

For the different load scenarios different relations between the ratio $w_{max,Isdyna(blast)}/w_e$ and the obtained errors can be observed. The reason for this difference is that explosions in this region result in different fluctuating deformation shapes of the beam. This is caused by higher order vibration modes. Like it has been described for Group 1, the sign and magnitude of the error depends on the deformation shape of both the uniformly and non-uniformly loaded beam at the moment yielding starts to occur.

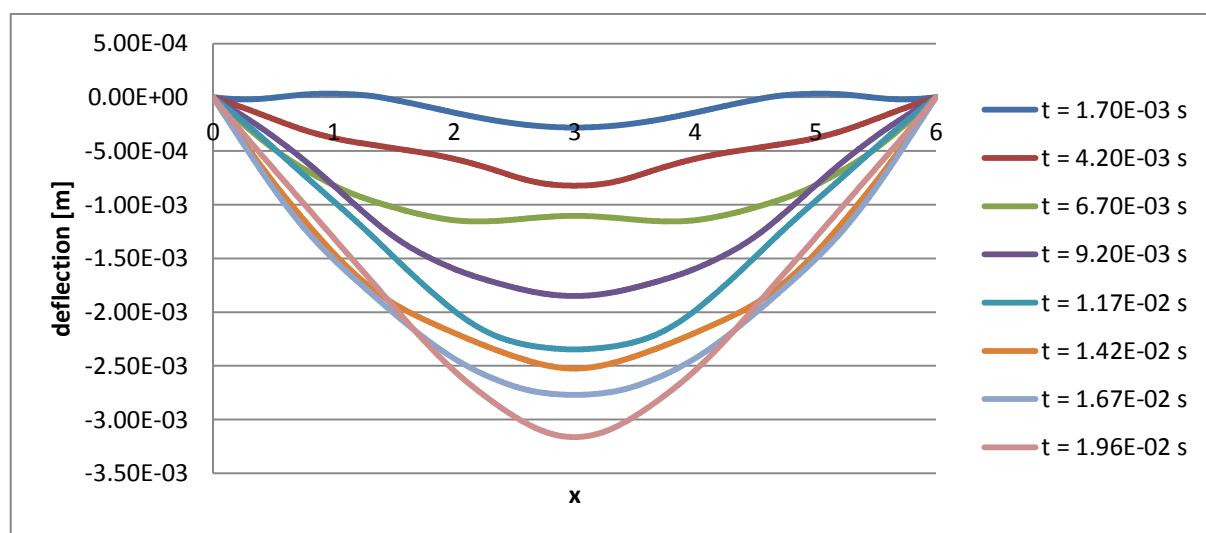


Figure 7.28: Elastic deflection shapes of a 6m long beam due to the equivalent uniform load for an explosion of 1kg TNT at 1 meter above $x=3m$, at different points in time

Group 3: Explosions at 2m and 3m height above $x=0$ and $1/8^*l$

In Figure 7.29 the relative errors of the deflection at midspan obtained with the equivalent uniform load are presented for explosions at 2 and 3 meters above $x=0$ and $x=1/8^*l$.

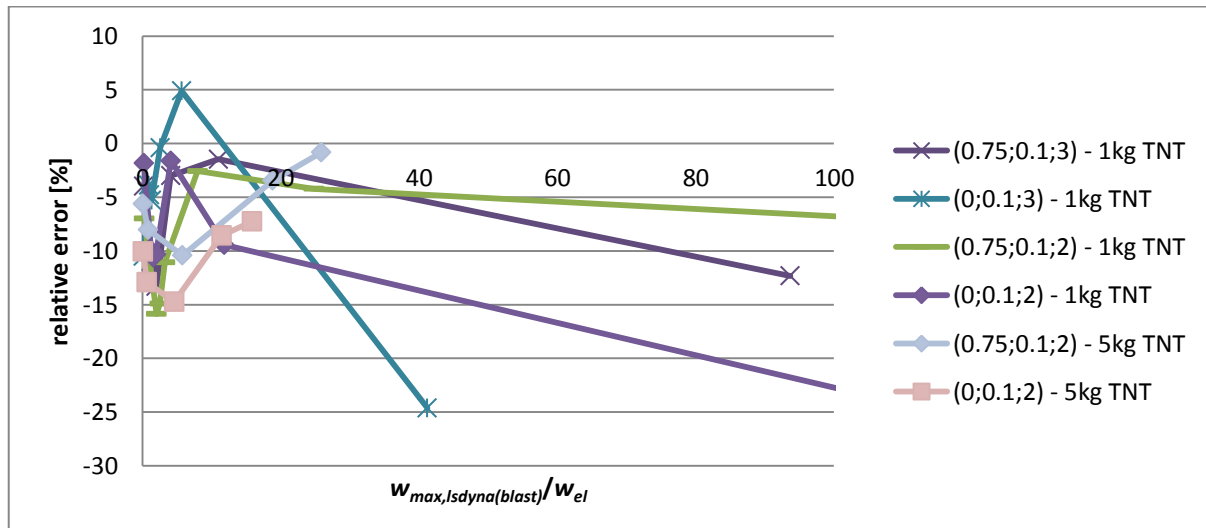


Figure 7.29: Obtained relative error of the estimated deflection at midspan for explosions at 2m and 3m height above $x=0$ and $x=1/8^*l$.

For the different load scenarios different relations between the ratio $w_{max,Isdyna(blast)}/w_e$ and the obtained errors can be observed. The reason for this difference is that explosions in this region result in different fluctuating deformation shapes of the beam. Like it has been described for Group 1, the sign and magnitude of the error depends on the deformation shape of both the uniformly and non-uniformly loaded beam at the moment yielding starts to occur. In Figure 7.31 the elastic-plastic deflection shape of a 6m long beam due to an explosion of 1kg TNT at 2 meters above $x=0$, at different points in time is presented. It can be seen that higher order vibration modes are damped and that the largest deflection occurs around midspan.

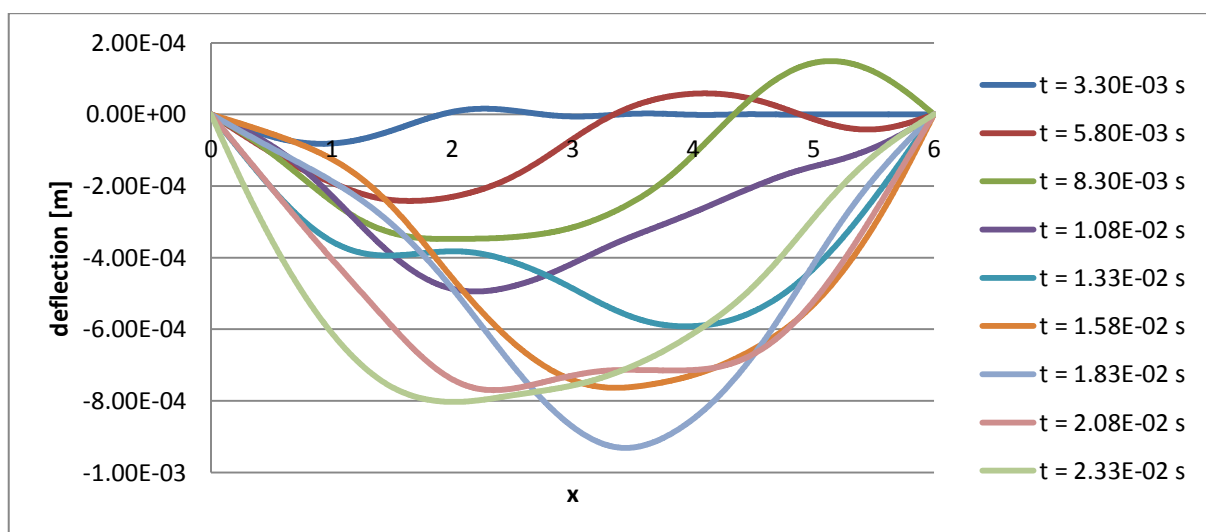


Figure 7.30: Elastic deflection shapes of a 6m long beam due to an explosion of 1kg TNT at 2 meters above $x=0$, at different points in time

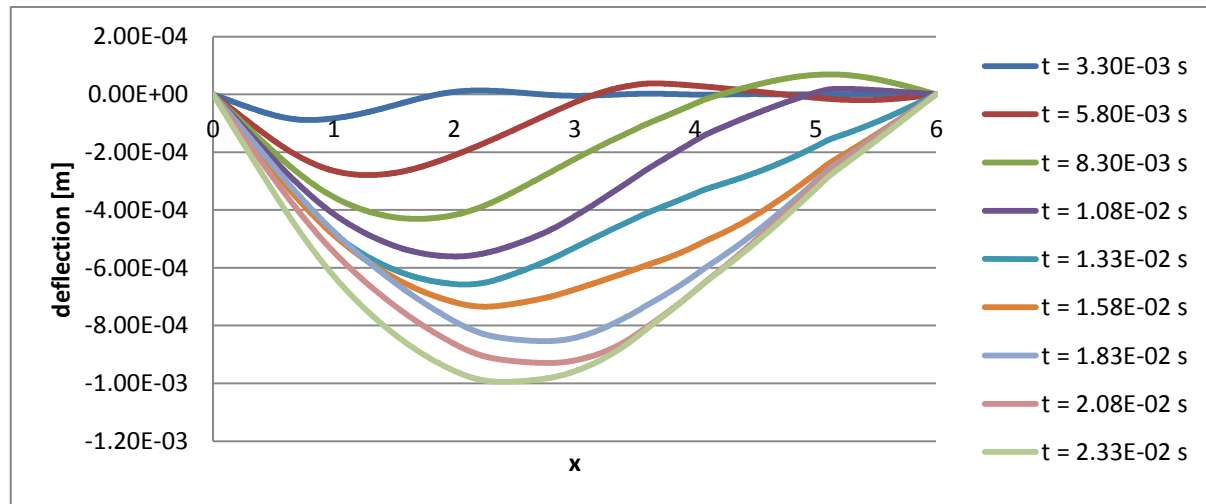


Figure 7.31: Elastic-plastic deflection shapes of a 6m long beam due to an explosion of 1kg TNT at 2 meters above $x=0$, at different points in time. $f_y = 2.35E6Pa$.

Group 4: Explosions at 1m height above $x=0$ and $1/8 \cdot l$

In Figure 7.32 the relative errors of the deflection at midspan obtained with the equivalent uniform load are presented for explosions at 1 meter above $x=0$ and $x=1/8 \cdot l$.

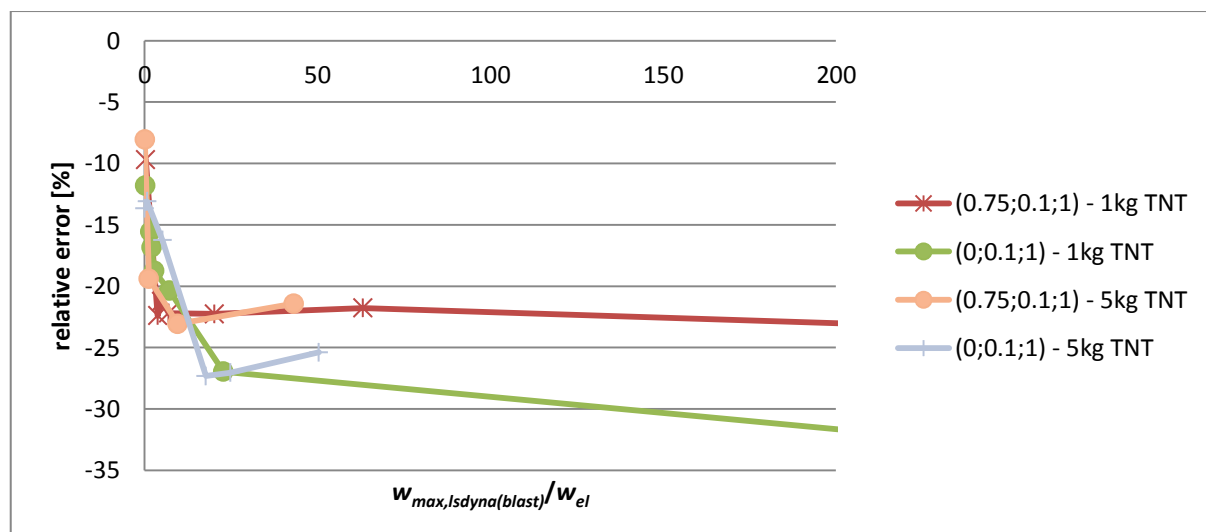


Figure 7.32: Obtained relative error of the estimated deflection at midspan for explosions at 1m height above $x=0$ and $x=1/8 \cdot l$.

Similar patterns for the load scenarios can be observed. Explosions at only two locations are being compared in Figure 7.32, therefore it might be a coincidence that the lines lie together.

Influence of the ratio between the load duration and the fundamental period

Usually blast waves have a very short duration time. This results that in most situations yielding occurs after a beam has been loaded. In this case the weightfactors are valid, since they are used for a linear-elastic beam. However for large ratios between the load duration and the fundamental period yielding occurs while the beam is still being loaded by the blast wave. The ratio between the load duration t_d and the fundamental period of the beam T_N , therefore affects the accuracy of the estimated deflections with the equivalent uniform load. It has been investigated for different ratio's

between the fundamental period of the beam and the load duration how accurate the deflections are estimated.

The beam with properties as presented in Table 7.5 has a fundamental period of 76.7ms. In the case the explosion takes place at 2 meters above the centre of the beam, the duration of the equivalent load is 4.5ms. For this scenario the ratio t_d/T_N has a value of 0.059. The stiffness of the beam has been varied to obtain different ratio's t_d/T_N . The following ratios have been examined:

Scenario	l [m]	E [Pa]	EI [Nmm]	t_d [ms]	T_N [ms]	t_d/T_N
1	6	2.1E11	2.80E+07	4.5	76.8	0.059
2	6	5.5E12	7.33E+08	4.5	15.0	0.30
3	6	6.1E13	8.13E+09	4.5	4.5	1.0
4	6	5.5E14	7.33E+10	4.5	1.5	3.0
5	6	6.1E15	8.13E+11	4.5	0.45	10.0

Table 7.5: Investigated scenario's with different t_d/T_N ratio's

The accuracy of the estimated deflections plotted against the ratio $w_{max,isdyna(blast)}/w_{el}$ are presented for each scenario in Figure 7.33 to Figure 7.35.

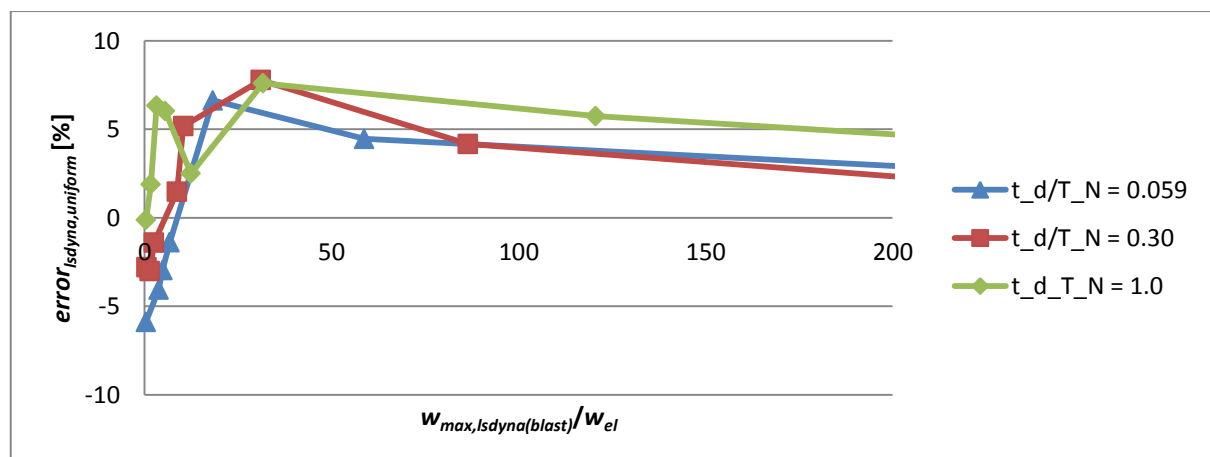


Figure 7.33: Accuracy of the estimated deflection with the equivalent uniform load for a ratio $td/TN \leq 1.0$.

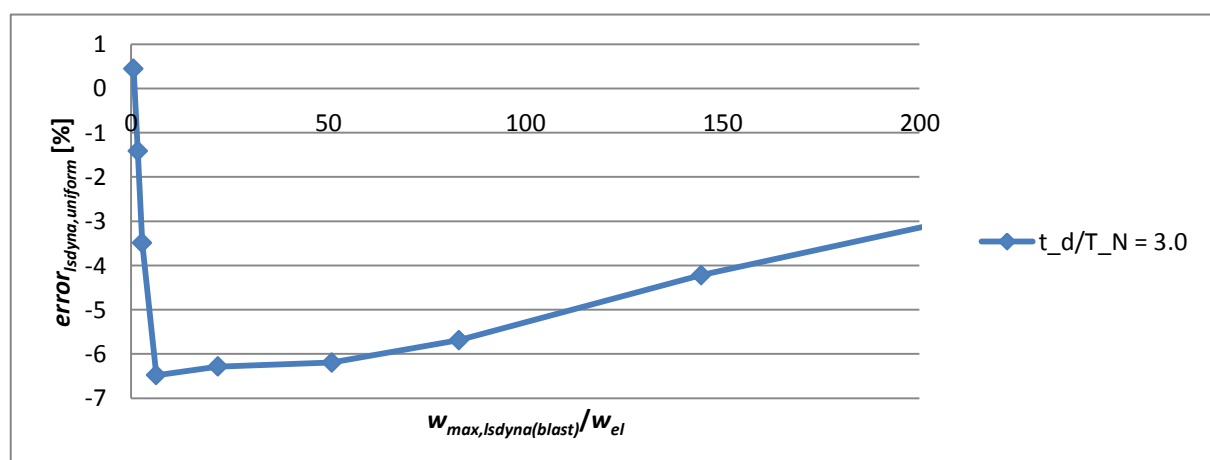


Figure 7.34: Accuracy of the estimated deflection with the equivalent uniform load for a ratio $td/TN = 3.0$.

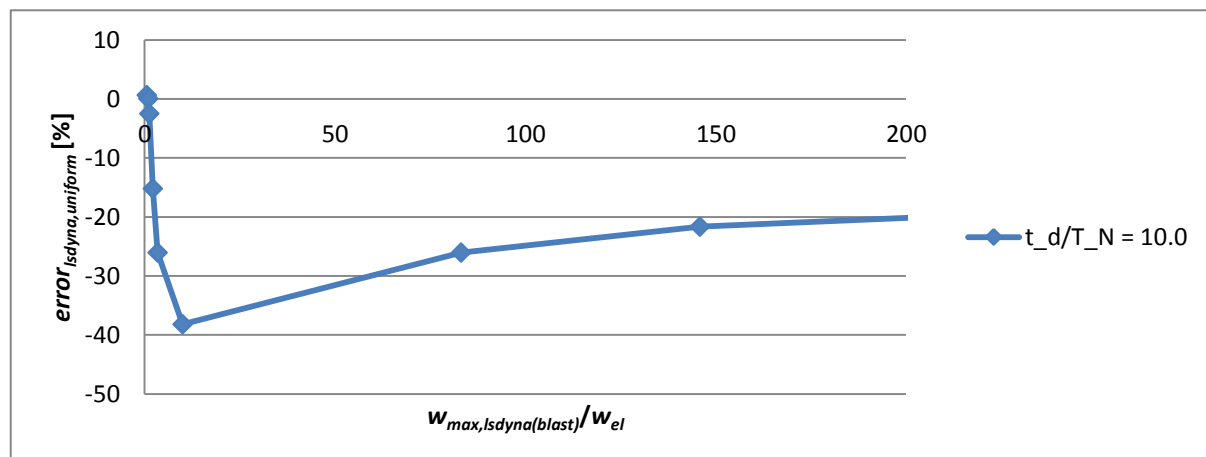


Figure 7.35: Accuracy of the estimated deflection with the equivalent uniform load for a ratio $t_d/T_N = 10.0$.

For a ratio t_d/T_N of 0.30 and 1.0 the same relation between the error and the ratio $w_{max,isdyna(blast)}/w_{el}$ can be observed as for a ratio t_d/T_N of 0.059 (Figure 7.33).

For a ratio t_d/T_N of 3.0 and 10.0 the error trends look similar, but different from a ratio t_d/T_N of ≤ 1.0 . For a ratio t_d/T_N of 3.0 and 10.0, in contrast to a ratio t_d/T_N of ≤ 1.0 , the deflection at midspan is underestimated with the equivalent uniform load. See Figure 7.36. From Chapter 5 it resulted that if plasticity occurs the weightfactors should increase at that location. Therefore, it makes sense that the deflection is underestimated for larger ratios t_d/T_N .

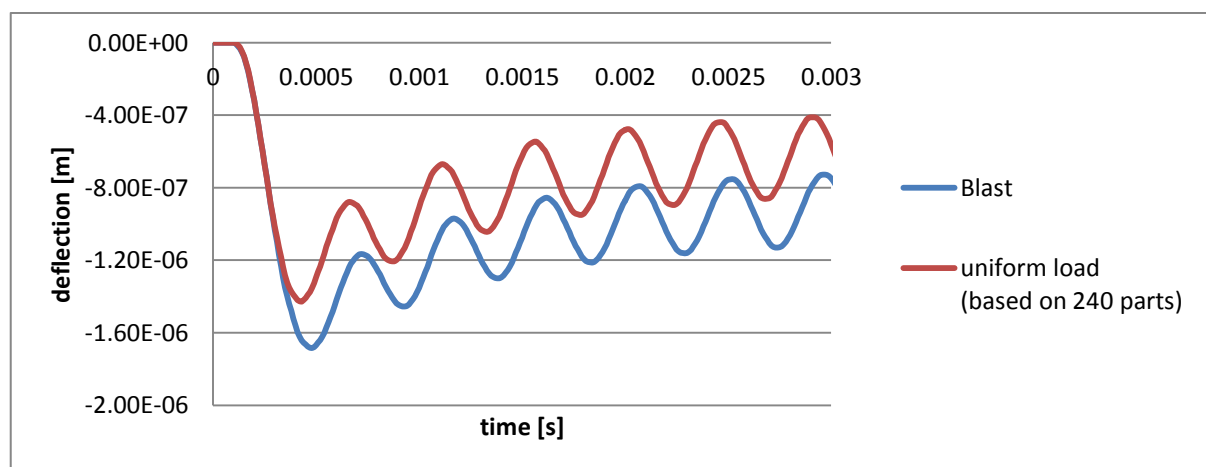


Figure 7.36: Deflection at midspan of a beam subjected to an explosion 2 meters above $x=0$. $f_{yd} = 1e8Pa$. $t_d/T_N = 10.0$.

Note that to obtain ratios t_d/T_N larger than 0.059 in this research unrealistically large values for the Young's modulus have been used. Steel has a Young's modulus in the order of $2E11Pa$. Even if the dimensions of the beam are varied a bending stiffness higher than $7.33E+08Nmm$ is not common for a beam with a length of 6m. For close-up explosions large ratios of t_d/T_N are not common. Large load durations are obtained for explosions far away and shorter fundamental periods are obtained for shorter beams. Both result in a more uniform load distribution. This investigation has been done to determine the appliance of the weightfactors.

7.4.2 Stresses

The size of the part of the beam where yielding has occurred has been underestimated for a beam subjected to the equivalent uniform load. This can be explained by the fact that in case of linear-elastic deformation the bending stresses are underestimated with the equivalent uniform load. In Figure 7.37 an example of the maximum occurring bending stresses over the length of the beam has been presented. In this example at 55% of the length of the beam subjected to the equivalent uniform load yielding has occurred and at 91% of the length of the beam subjected to blast load yielding has occurred. In this case the explosion was located at two meters above the left boundary and the beam had a yield strength of 2.35×10^6 Pa. In Figure 7.38 it can be seen that the stresses fluctuate a lot. Due to an explosion at $x=0$ yielding will occur close to the boundaries at first, but eventually when the higher order modes are damped around midspan only. This means that it depends on the ductility of the material when/if the beam would crack/fail.

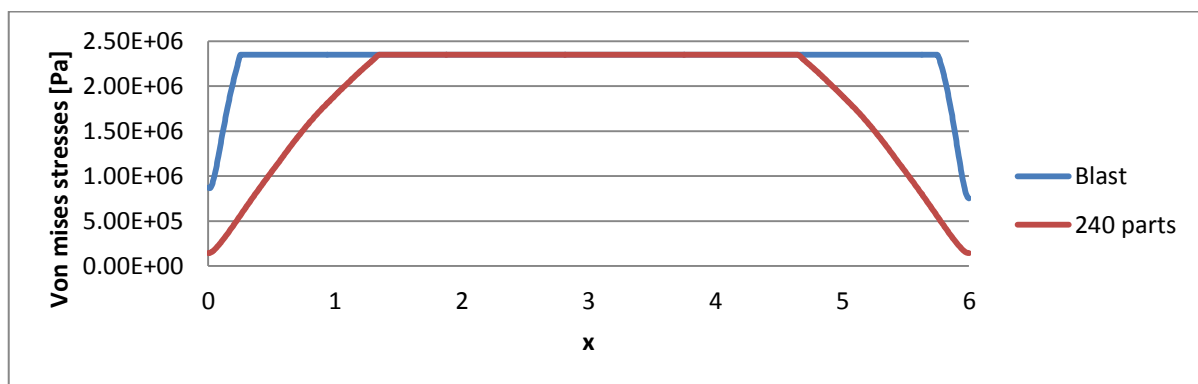


Figure 7.37: Maximum occurring Von Mises stresses over the length of a beam with a yielding strength of 2.35×10^6 Pa due to an explosion of 1kg TNT equivalent at $x=0$ m at two meter height

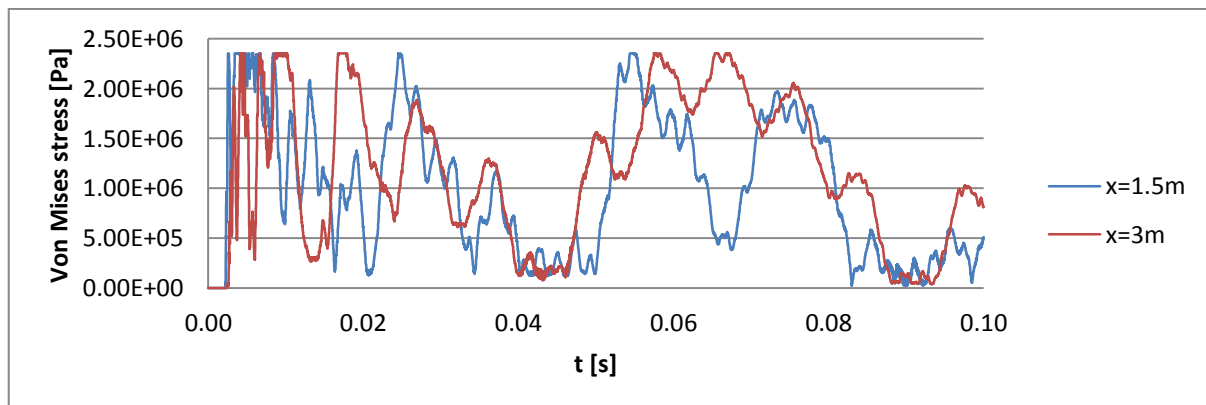


Figure 7.38: Von Mises stresses of a beam with a yielding strength of 2.35×10^6 Pa due to an explosion of 1kg TNT equivalent at $x=0$ m at two meters height

7.5 Conclusion

Load distribution

The accuracy of the estimations of the deflections and stresses are dependent on the relative pressure distributions which determines the amount of non-uniformity / asymmetry of the load. The relative pressure distribution on the beam is dependent on the location of the explosive (along the length and stand-off). The mass of the explosive has a minor influence.

Equivalent uniform load

An equivalent uniform load is obtained by splitting the beam into a certain amount of parts. The total impulse of the equivalent load approaches an asymptotic value if the beam has been split into more parts to determine the equivalent load. For the investigated cases it holds that if the impulse of the equivalent load is close to the impulse of the equivalent load obtained with 240 elements, enough parts have been used.

Accuracy of the Linear-Elastic Response

Deflection

With the equivalent load very accurate estimations of the deflection at midspan are obtained. An average error -5.0% is obtained with a maximum of -13.7%

Stresses

With the equivalent uniform load the maximum bending stresses are underestimated. For the investigated case the obtained ratios between the maximum stress due to the equivalent uniform load and the non-uniform blast load for explosions at different locations are presented in Table 7.4. It can be seen that the ratio becomes smaller if 1. the height of the explosion decreases and 2. if the explosion takes place closer to the boundaries. This is caused by the effect of higher order vibration modes.

Accuracy of the Elastic – Plastic Response

Deflection

It depends on the deflection shape at the moment yielding starts to occur, whether larger or smaller deformations will be obtained with the equivalent uniform load. If yielding occurs at the moment the shape of the beam is close to the first vibration mode large deformations are obtained and if yielding occurs at the moment the beam has a flat shape around midspan smaller deformations are obtained. The deflection shapes at different points in time are similar for explosions at 2 and 3 meters height above the middle half part of the beam, therefore a relation exists between the relative error of the estimated deflection at midspan and the ratio between the maximum deflection and the elastic deformation limit of a static uniformly loaded beam ($w_{max,lsdyna(blast)}/w_{el}$). See Figure 7.22. For explosions close to the boundaries and for explosions at a height of 1 meter different deflection shapes are obtained which result in different relations between the relative error and $w_{max,lsdyna(blast)}/w_{el}$. See Figures 7.27, Figure 7.29 and Figure 7.32.

Usually blast waves have a very short duration time. Therefore, yielding occurs beyond the loading phase. In this case the weightfactors are valid, since the beam is still in the linear-elastic regime. However for large ratios between the load duration t_d and the fundamental period T_N yielding occurs while the beam is still being loaded by the blast wave. For a ratio t_d/T_N of 0.059, 0.30 and 1.0 the same relation between the error and the ratio $w_{max,lsdyna(blast)}/w_{el}$ is obtained. See Figure 7.33. For a ratio t_d/T_N of 3.0 and 10.0, in contrast to a ratio t_d/T_N of ≤ 1.0 , the deflection at midspan is mostly underestimated with the equivalent uniform. From Chapter 5 it resulted that if plasticity occurs the weightfactors should increase at that location. Therefore, it makes sense that the deflection is underestimated for larger ratios t_d/T_N .

Stresses

The size of the yielded part of a beam has been underestimated for a beam subjected to the equivalent uniform load. See Figure 7.37. This can be explained by the fact that in case of linear-elastic deformation the bending stresses (in the higher order vibration modes) are underestimated with the equivalent uniform load. In Figure 7.38 it can be seen that the stresses fluctuate a lot. This means that it depends on the ductility of the material when/if the beam would crack/fail.

Part IV

Accuracy of the SDOF estimations

Chapter 8

SDOF calculations

A single degree of freedom (SDOF) model has been used to approach the response of a simply supported beam. In contrast to LS-DYNA with the SDOF model higher order vibration modes are not taken into account. With the SDOF model the response is assumed to be in the first vibration mode. Higher order vibration modes play an important role when a beam is subjected to blast load as has been seen in Chapter 7. In this chapter it has been investigated how large the differences between the deflections obtained with the two methods are.

To determine the accuracy of the SDOF model, first the estimated deflections obtained with the SDOF model have been compared with the estimated deflections obtained with LS-DYNA using the equivalent uniform load and second they have been compared with the deflections obtained with LS-DYNA using the actual non-uniformly distributed blast load.

In this study the influence of the following parameters has been examined:

- Yield strength of the beam
- Location of the explosive

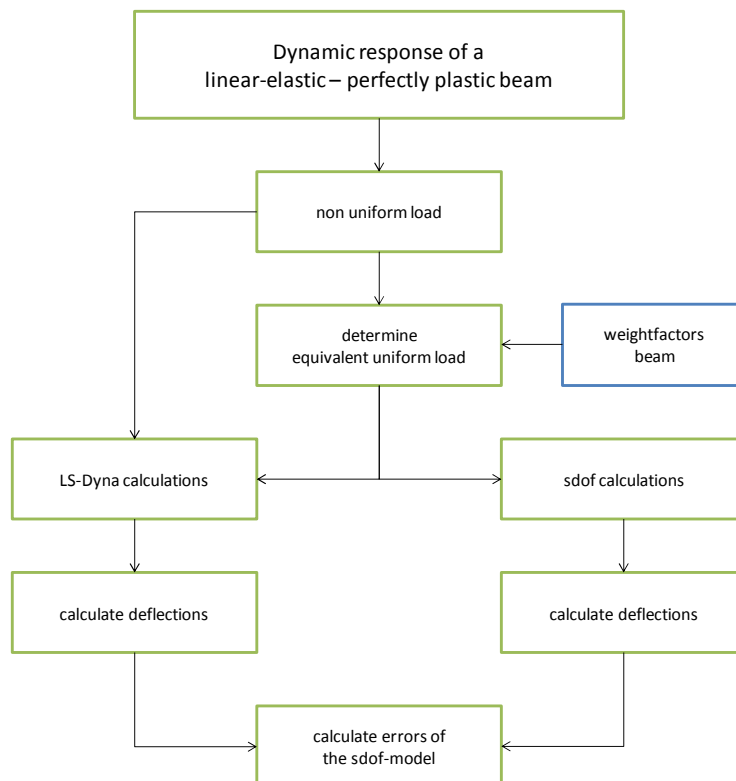


Figure 8.1: Flowchart Chapter 8

8.1 Beam properties

Calculations have been done for a simply supported beam with the same properties as in chapter 7:

Cross-section:	0.2x0.2m
Length:	6m
Young's modulus:	2.1E11 Pa
Mass density:	7850 kg/m ³
Yield strength:	various values
fundamental period:	76.7ms

8.2 Input

The SDOF model is used to schematize a uniformly loaded simply supported beam as a mass spring system (Figure 8.2). To perform SDOF calculations the model requires the load-mass factor, the total mass of the beam, the total load as function of time and a resistance-deflection function.

The equation of motion of the equivalent mass-spring-system is as follows:

$$K_{LM}M \left(\frac{d^2}{dt^2} x(t) \right) + R(x) = F(t) \quad (8.1)$$

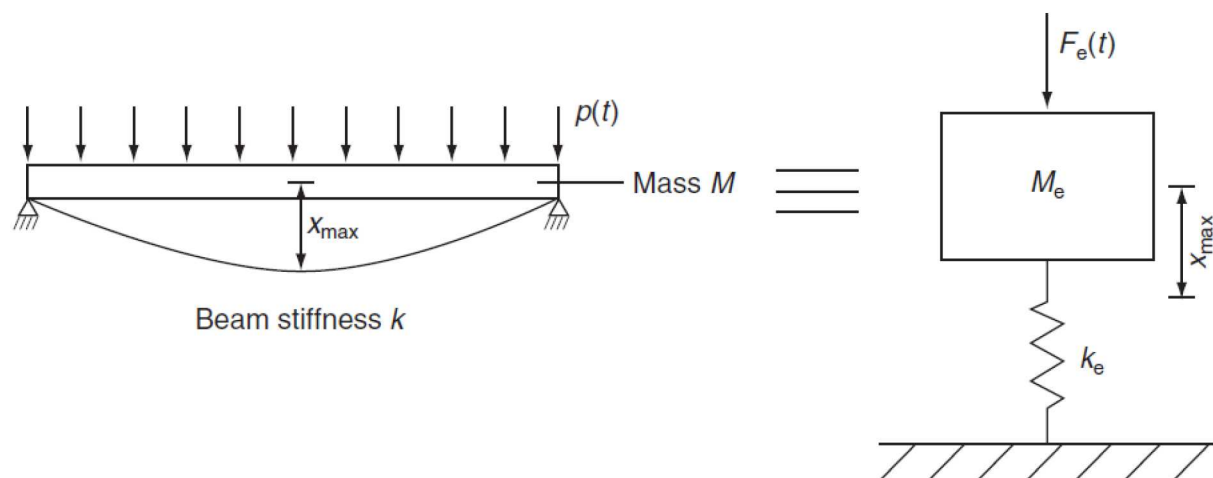


Figure 8.2: Equivalent mass spring system

8.2.1 Load-mass factor

The load-mass factor is dependent on the assumed deformation shape (Chapter 3). For the analyses an average is used between the load-mass factor for an static uniformly loaded elastic beam and the load-mass factor for a beam with a hinge at midspan. See Figure 8.3 and Equation (8.2).

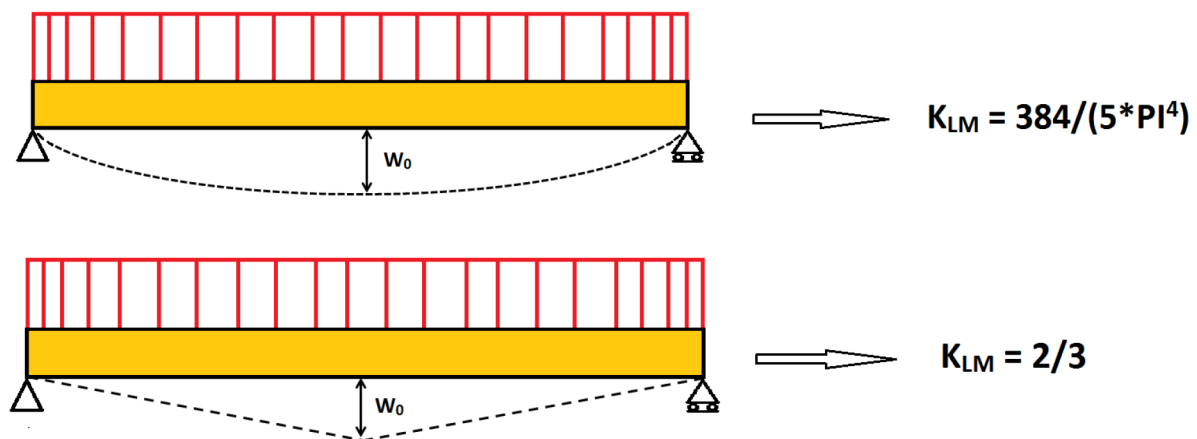


Figure 8.3: Load-mass factor in the elastic and plastic regime.

$$K_{LM} = \left(\frac{384}{5\pi^4} + \frac{2}{3} \right) \cdot \frac{1}{2} \approx 0.7275 \quad (8.2)$$

In the real situation the vibration shape changes in time due to the influence of higher vibration modes and plasticity. The load-mass factor should therefore actually not be a constant value.

8.2.2 Resistance-deflection function

The resistance-deflection function can be determined with standard static calculation formulas using dynamic material strengths. However, for simplicity the dynamic strength factors are neglected in both LS-DYNA and SDOF calculations. To compute calculations for a simply supported beam the resistance-deflection curve is simplified as a bilinear curve.

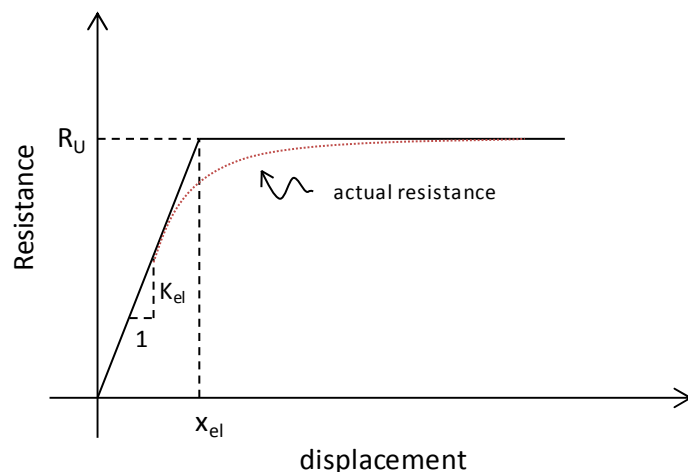


Figure 8.4: Resistance-displacement curve for a simply supported homogenous beam

For a simply supported beam it holds that:

$$\text{Plastic moment capacity:} \quad M_P = W_{pl} \cdot f_{yd} \quad (8.3)$$

$$\text{Maximum resistance:} \quad R_U = \frac{8 \cdot M_P}{l} \quad (8.4)$$

$$\text{Elastic stiffness: } K_{el} = \frac{384}{5} \frac{EI}{l^3} \quad (8.5)$$

$$\text{Elastic deflection limit: } x_{el} = \frac{R_U}{K_{el}} \quad (8.6)$$

The actual resistance-deflection curve of a simply supported beam lies lower than the bilinear curve and therefore the SDOF model would act stiffer than in the real situation.

8.2.3 Load

The equivalent uniform load determined as described in Chapter 7 has been used as input for the SDOF model. For explosions of 1kg TNT equivalent at a height of 1, 2 and 3m at the following locations along the length of the beam the accuracy with the SDOF model has been determined:

- $x=0$
- $x=1/8 \cdot l$
- $x=1/4 \cdot l$
- $x=3/8 \cdot l$
- $x=1/2 \cdot l$

8.3 Errors of the obtained deflections

It has been investigated how the accuracy of the estimated deflection at midspan is influenced by the location of the explosive. The deflections obtained with the SDOF model are first compared with the deflections obtained with a uniform equivalent load in LS-DYNA and second with the deflection obtained with a non-uniform Blast load in LS-DYNA.

8.3.1 SDOF response versus LS-DYNA response using the equivalent uniform load

In Figure 8.5 the obtained relative errors are plotted against the ratio between the maximum obtained deflection and the elastic deflection limit of a static uniformly loaded beam ($w_{max,SDOF}/w_{el}$). The relative error is defined as:

$$error_{sdof, uniform} = \frac{w_{max, sdof} - w_{max, lsdyna(uniform)}}{w_{max, lsdyna(uniform)}} \cdot 100 \quad (8.7)$$

Where:

$w_{max,SDOF}$ = maximum obtained deflection with the SDOF model.

An increase of the error can be observed for larger ratios $w_{max,SDOF}/w_{el}$. In Chapter 7.4.1 it has been seen that for larger ratios $w_{max,lsdyna(blast)}/w_e$ the influence of higher order vibration modes on the maximum deflection at midspan became larger. This resulted in larger plastic zones and therefore smaller deflections were obtained. With the SDOF model higher order vibrations modes are neglected and therefore larger maximum deformations at midspan are obtained.

Errors have been obtained of the same order as in previous research (0-30%), where the accuracy of the SDOF method has been analysed for uniform load distributions [12].

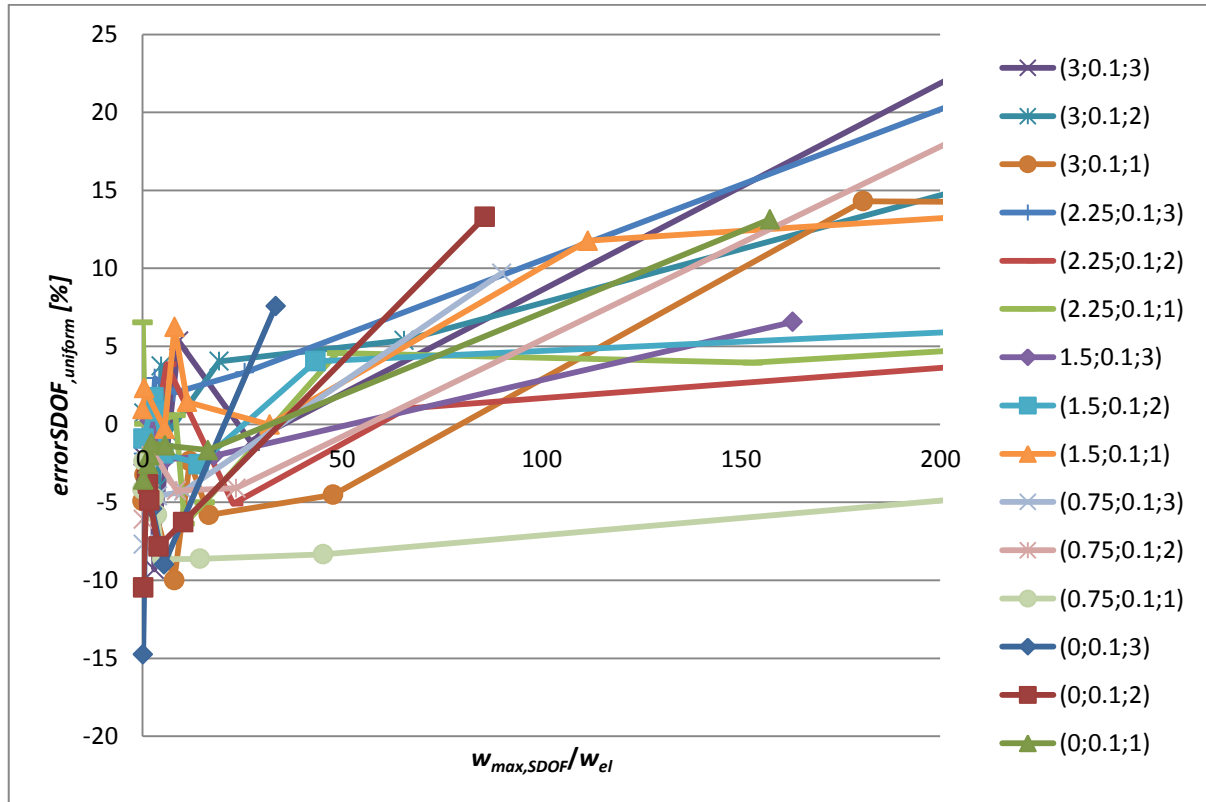


Figure 8.5: Relative error of the estimated deflection obtained with the SDOF model compared to the deflections obtained with the uniform load in LS-DYNA for explosions at different locations (x;y;z)

In Figure 8.6 to Figure 8.8 examples are presented of the estimated deflections with the SDOF model for an explosion at 2 meter above $x=1/2 \cdot l$, $x=1/4 \cdot l$ and $x=1/8 \cdot l$ of the 6m long beam. It can be seen that the deflection due to the uniform load in LS-DYNA is in these cases accurately approximated with the SDOF model. In Figure 8.9 the scenario with the lowest accuracy in the 0 to 200 $w_{max,SDOF}/w_{el}$ range has been presented. In this case the ratio $w_{max,SDOF}/w_{el}$ has a value of 181 and an error of 14.3% has been obtained.

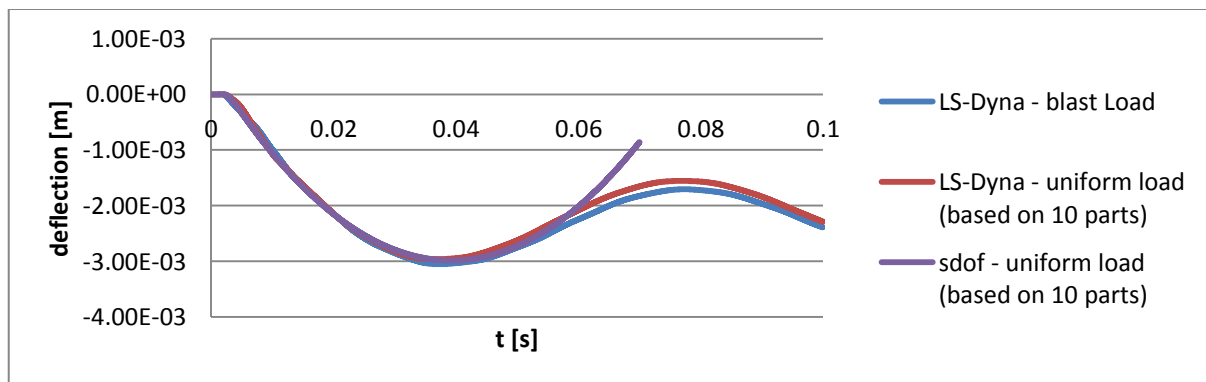


Figure 8.6: Deflection at midspan of a beam with yield strength 2.85E6Pa due to an explosion at 2 meters above $x=0.50 \cdot l$.

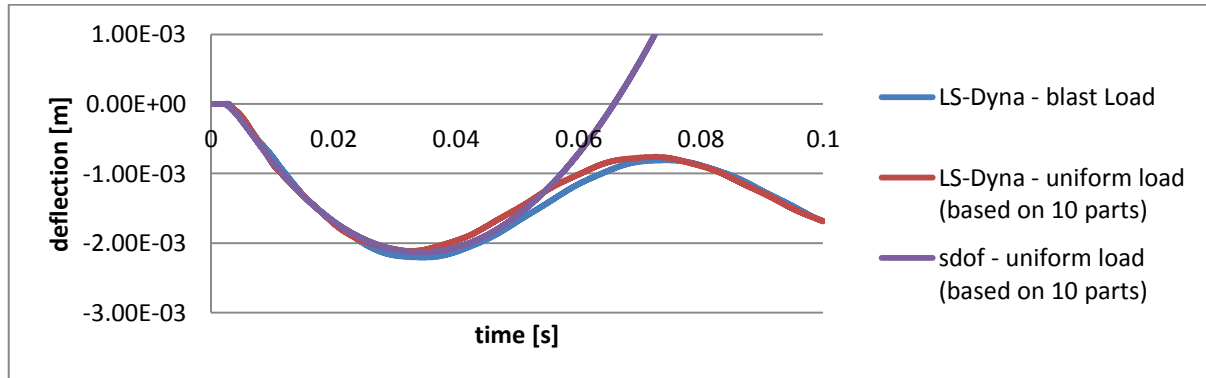


Figure 8.7: Deflection at midspan of a beam with yield strength 2.85E6Pa due to an explosion at 2 meters above $x=0.25*I$.

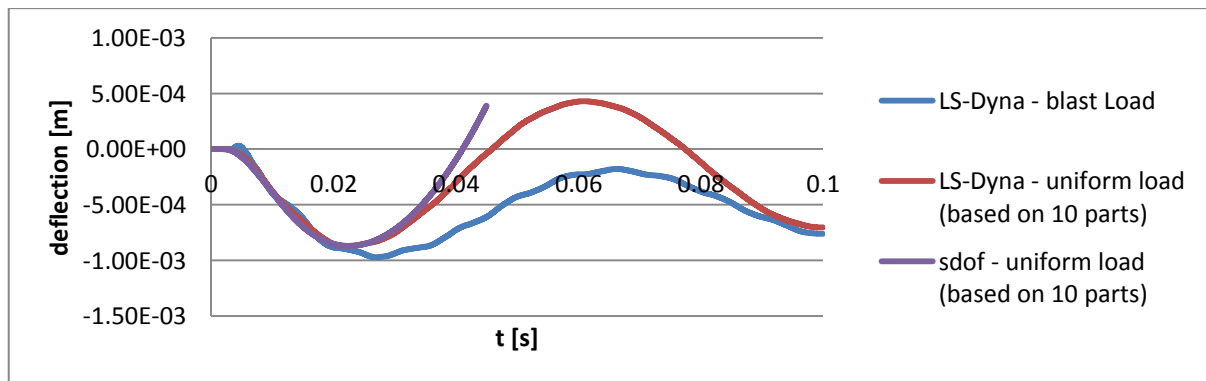


Figure 8.8: Deflection at midspan of a beam with yield strength 2.85E6Pa due to an explosion at 2 meters above $x=0.125*I$.

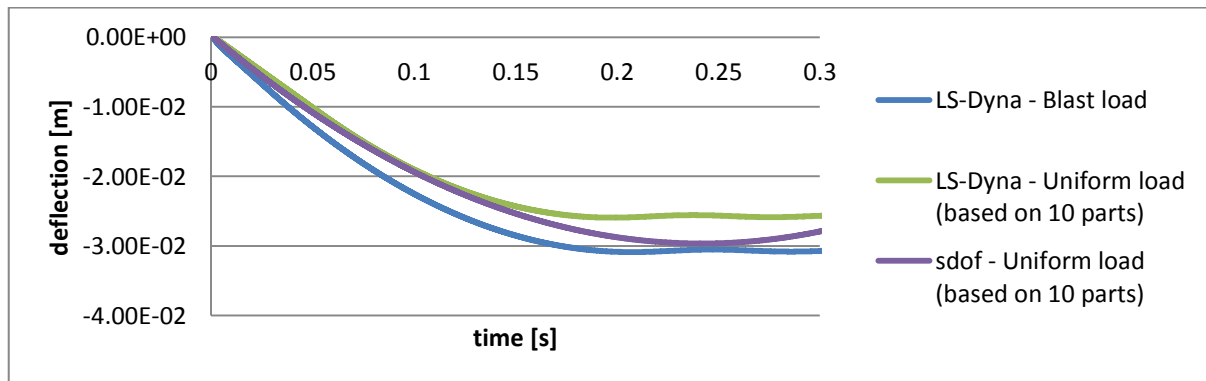


Figure 8.9: Deflection at midspan of a beam with yield strength 7.35E5Pa due to an explosion at 1 meters above $x=0.5*I$.

8.3.2 SDOF response versus LS-DYNA response using the non-uniform blast load

In Figure 8.10 all obtained relative errors are plotted against the ratio between the maximum obtained deflection and the elastic deformation limit of a static uniformly loaded beam ($w_{max,SDOF}/w_{el}$).

The relative error is calculated as:

$$error_{s dof, blast} = \frac{w_{max, sdof} - w_{max, lsdyna(blast)}}{w_{max, lsdyna(blast)}} \cdot 100 \quad (8.8)$$

$$error_{s dof, blast} = \frac{error_{lsdyna, uniform} \cdot error_{s dof, uniform}}{100} + error_{lsdyna, uniform} + error_{s dof, uniform} \quad (8.9)$$

In Figure 8.10 it can be seen that the errors are spread over region between -30% and +30%. The load scenarios have been categorized into four groups to obtain a clearer overview:

1. Explosions at 2m and 3m height above $x=1/4l$, $3/8l$ and $1/2l$. See Figure 8.11.
2. Explosions at 1m height above $x=1/4l$, $3/8l$ and $1/2l$. See Figure 8.12.
3. Explosions at 2m and 3m height above $x=0$ and $1/8l$. See Figure 8.13.
4. Explosions at 1m height above $x=0$ and $1/8l$. See Figure 8.14.

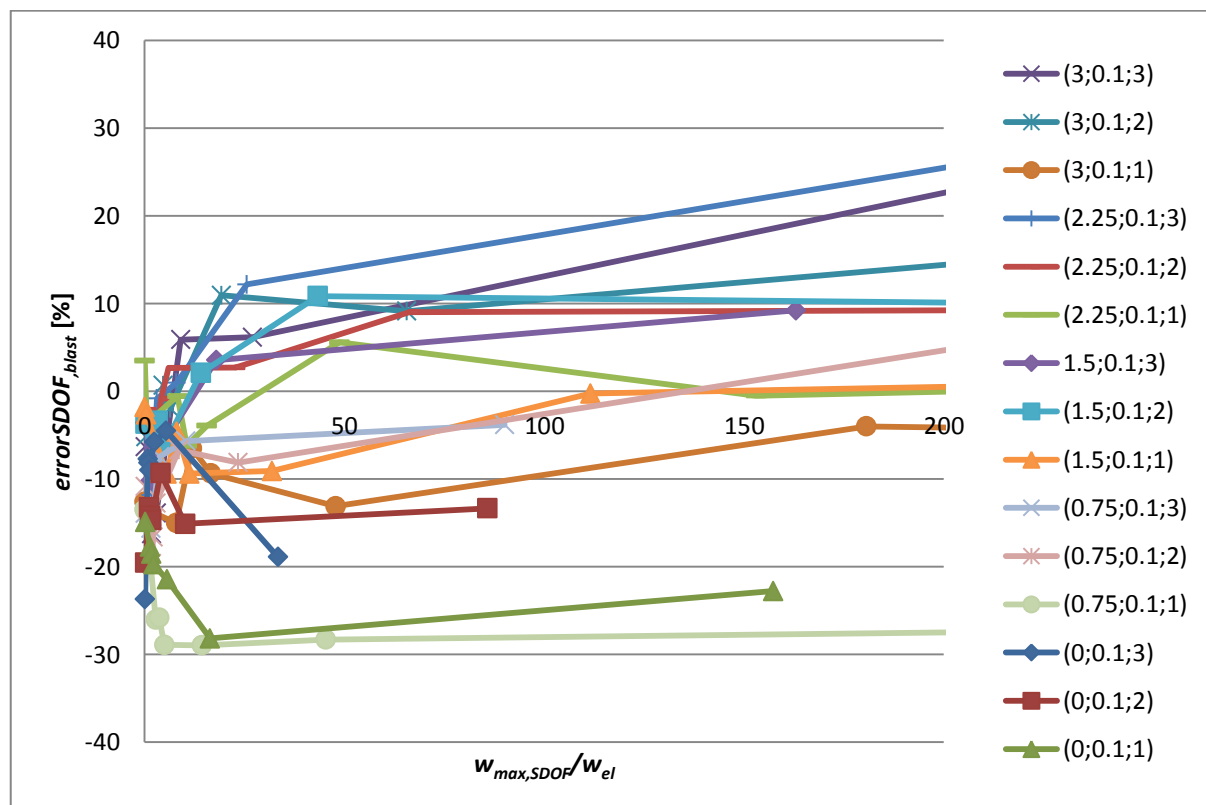


Figure 8.10: Relative error of the estimated deflection obtained with the SDOF model compared to the deflections obtained with the blast load in LS-DYNA for explosions at different locations ($x;y;z$)

In Figure 8.11 the relative errors of the deflection at midspan are presented for explosions at 2 and 3 meters height above the middle half part of the beam. Like in Chapter 7, for this group a relation between the obtained error and $w_{max,SDOF}/w_{el}$ can be observed. For group 2 to 4 the errors are presented in Figure 8.12, Figure 8.13 and Figure 8.14 respectively. For the same reasons as in Chapter 7, there is no trend.

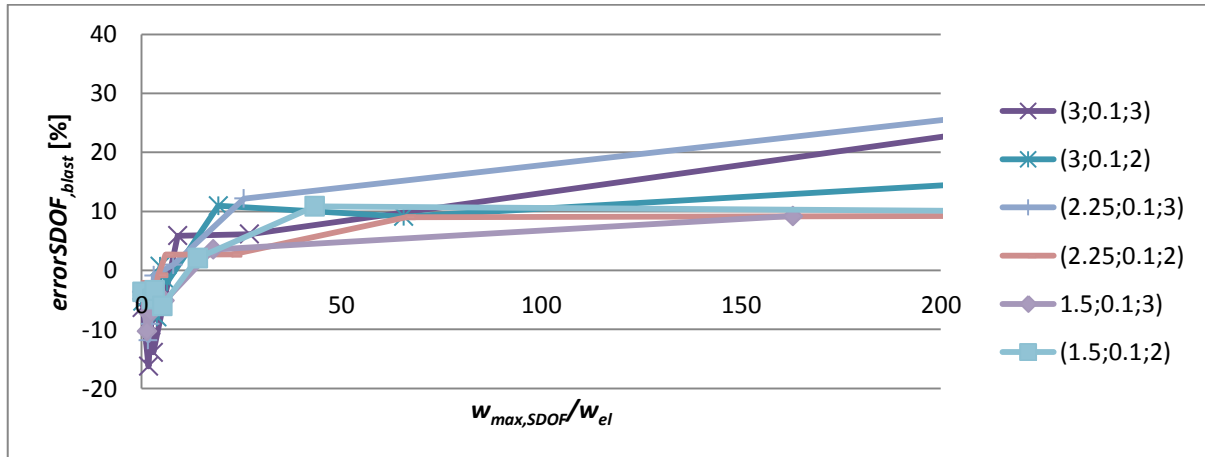


Figure 8.11: Relative error of the estimated deflection obtained with the SDOF model compared to the deflections obtained with the blast load in LS-DYNA for explosions at 2m and 3m height above $x=1/4^*$, $3/8^*$ and $1/2^*$

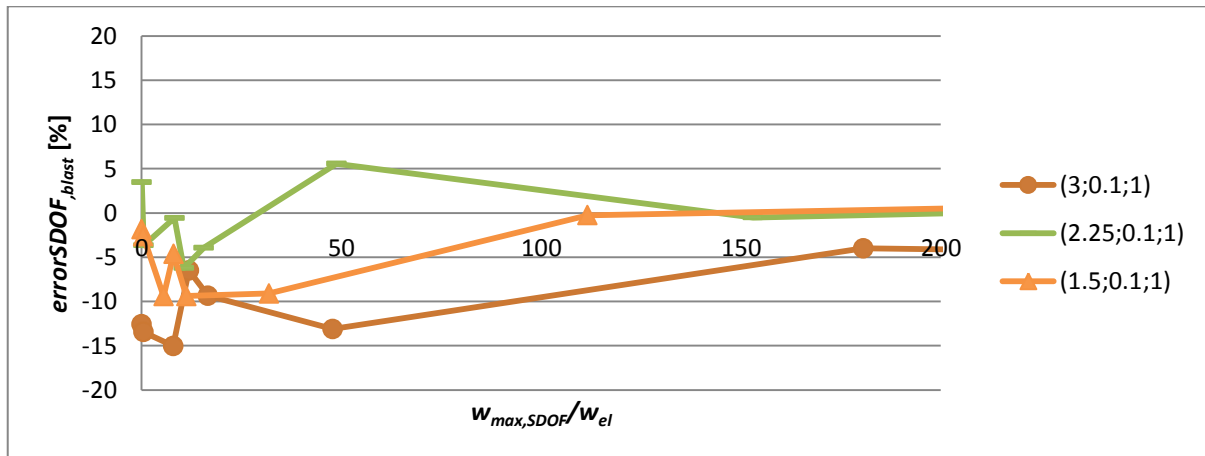


Figure 8.12: Relative error of the estimated deflection obtained with the SDOF model compared to the deflections obtained with the blast load in LS-DYNA for explosions at 1m height above $x=1/4^*$, $3/8^*$ and $1/2^*$

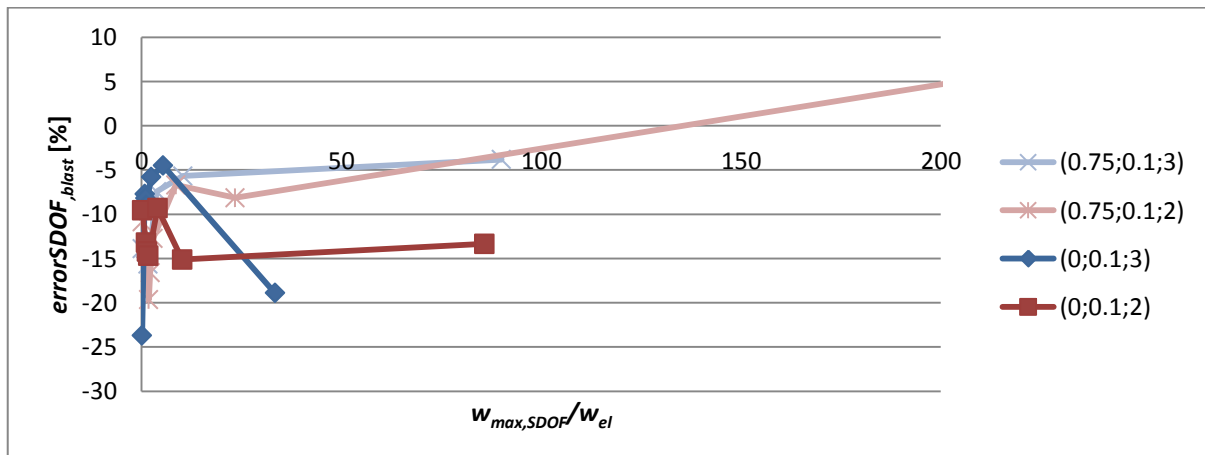


Figure 8.13: Relative error of the estimated deflection obtained with the SDOF model compared to the deflections obtained with the blast load in LS-DYNA for explosions at 2m and 3m height above $x=0$ and $x=1/8^*$

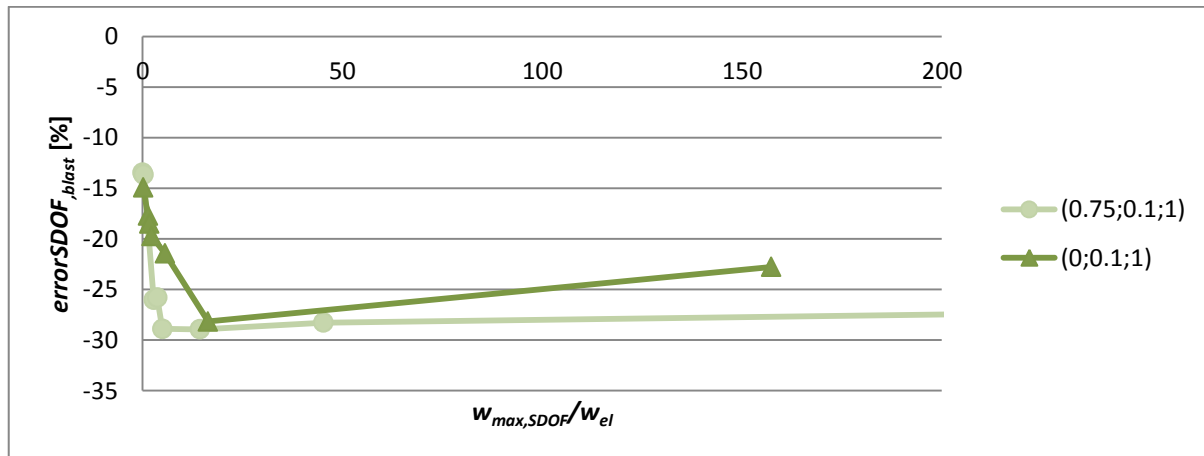


Figure 8.14: Relative error of the estimated deflection obtained with the SDOF model compared to the deflections obtained with the blast load in LS-DYNA for explosions at 1m height above $x=0$ and $1/8 \cdot l$

8.4 Conclusion

Errors of the obtained deflections

To determine the accuracy of the SDOF model, first the estimated deflections obtained with the SDOF model have been compared with the estimated deflections obtained with LS-DYNA using the equivalent uniform load and second they have been compared with the deflections obtained with LS-DYNA using the actual non-uniformly distributed blast load.

SDOF response versus LS-DYNA response using the equivalent uniform load

Using the SDOF model the maximum deflections at midspan of a beam is accurately estimated. The obtained errors lie between - 15% and +25%. The deflection is more overestimated for larger ratios between the maximum obtained deflection and the elastic deformation limit of a static uniformly loaded beam ($w_{max,SDOF}/w_{el}$). This is caused by the influence of higher order vibration modes on the obtained maximum deflection with LS-DYNA. See Chapter 7.

SDOF response versus LS-DYNA response using the non-uniform blast load

For the scenarios the explosion takes place 2 or 3 meters above the middle half part of the beam a relation between the obtained error ($error_{SDOF,blast}$) and the ratio between the maximum obtained deflection and the elastic deformation limit of a static uniformly loaded beam ($w_{max,SDOF}/w_{el}$) could be observed. See Figure 8.11. For the explosions at the remaining locations no trend between $error_{SDOF,blast}$ and $w_{max,SDOF}/w_{el}$ exists. This is caused by the different deformation shapes at different points in time. See Chapter 7.

Part V

Conclusions and recommendations

Chapter 9

Conclusions and recommendations

9.1 Conclusions

To model the response of a structural element subjected to explosions, single degree of freedom (SDOF) systems can be used. It only takes seconds to perform an SDOF calculation. This is a lot faster than finite element analyses. The SDOF method is therefore a powerful method to perform vulnerability analyses in which hundreds of scenarios need to be analysed.

To perform an SDOF calculation a representative load as function of time is needed. Usually the value of the non-uniform load at one single location on the beam is chosen as representative load. For non-uniform or asymmetric load distributions this might result in inaccurate estimations.

In this report an approach has been presented to translate an arbitrary non-uniformly distributed load acting on an elastic-plastic simply supported beam to an equivalent uniform load. For this translation factors have analytically been determined. The factors are dependent on the geometry and boundary conditions of the structural element. To determine the model capabilities and the accuracy of the estimations, the obtained response of a beam using the SDOF model has been compared with the obtained response using finite element software.

Cause of the error of the estimations

The midpoint deflection of a simply supported beam has been estimated with an SDOF model. The error of the estimations are caused by the several simplifications of the SDOF model. The main reasons why errors occur are 1. translating a non-uniform or asymmetric load to a uniform load and 2. assuming deformation in the first vibration mode. For both causes errors of the same order have been obtained.

Order of the error of the estimations

The equivalent uniform load is based on the value of the non-uniform load at several locations. These locations are at the centre of the parts in which the beam is divided. To catch the load correctly the beam must be divided into enough parts. It holds that the more local the load is, the more parts are necessary. For the investigated 6 meter long beam it resulted that for explosions at 2 meter or higher the beam needs to be divided into 10 parts and for explosions at 1 meter height the beam needs to be divided into 15 parts. Dividing the beam into more parts is not necessary, since it does not increase the accuracy of the estimations. Using the determined factors an accurate estimations can be made of the deflection at midspan of a simply supported beam subjected to a non-uniform blast load. Errors have been obtained in the range of -23% to +7% in case of elastic deformation and in the range of -29% to +33% in case of elastic-plastic deformation. The order of the obtained errors are consistent with the basic errors of the SDOF method itself.

Load regime in which the translation factors are recommended to be used

For the investigated beam with a length of 6 meters, the extension of the SDOF model is especially useful for explosions at 2 or 3 meters height above the middle half part of the beam, since a relation

has been found between the error of the estimated deflection and the maximum deformation. For explosions closer to the boundaries and explosions at a distance of 1 meter the factors are still usable, however larger errors (up to 30%) have been obtained in this regime.

Explosions with a distance larger than 3 meter have not been investigated. In this regime the load distribution becomes more uniformly distributed and therefore the translation factors are still useful. Explosions with a distance smaller than 1 meter have not been investigated either. In this case the load becomes too locally distributed and dividing the beam into a huge amount of parts would be necessary to calculate the equivalent uniform load correctly.

9.2 Recommendations

Simulating the response of an structural element subjected to uniform load distributions using an SDOF method introduces errors, which are in the order of 0-30%. Using the factors determined in this research the SDOF method can be used for asymmetrically/non-uniformly distributed loads as well, without increasing the basic errors of the SDOF method.

For explosions at a height of 2 and 3 meter above the middle half part of the beam a relation has been found with the error of the estimated deflections and the maximum deflection. For this regime the estimated maximum deflection might be corrected to reduce the error. If the scenarios are scaled (beam dimensions, distance explosions, etc.) it is likely that errors of the same order will be obtained, since the relative load distribution on the beam remains similar. However, this has not been investigated and further research could be beneficial.

With the SDOF model failure is based on a maximum allowed deformation. Currently the maximum allowed deformations are based on symmetric loading. Using the equivalent uniform load smaller bending stresses have been obtained compared to using non-uniform blast loading. Therefore, it is recommended to perform follow-up research on investigating at what deformation elements subjected to non-uniform and asymmetric load distributions fail.

Chapter 10

References

- [1] Strehlow, R.A., Baker W.E.; *The Characterization and Evaluation of Accidental Explosions*; Pergamon Press., Pro 9. Energy Combust. Sci. 2:27-60, Great Britain, 1976.
- [2] Baker, W.E., Cox, P.A., Westine, P.S., Kulesz, J.J., Strehlow, R.A.; *Explosion Hazards and Evaluation*; Elsevier Science Publishers B.V., The Netherlands, 1983.
- [3] LS-DYNA®; *Keywords user's Manual*; USA, 2014
- [4] Cormie, D., Mays, G., Smith, P.; *Blast effects on building*; ICE Publishing, England, 1995
- [5] Biggs, J.M.; *Introduction to structural dynamics*; McGraw-Hill, United States Of America, 1964.
- [6] TM 5-1300; *Structures to resist the effects of accidental explosions*; Departments of the Army, the Navy, and the Air Force, TM 5-1300, NAVFAC P-397, AFR 88-22, United States of America, 1990.
- [7] Spijkers J.M.J., Vrouwenvelder A.W.C.M., Klaver E.C.; *Structural Dynamics CT 4140 Part 1 - Structural Vibrations*; TU Delft, The Netherlands, 2005.
- [8] Morison, C.M.; *Dynamic response of walls and slabs by single-degree-of-freedom analysis—a critical review and revision*; Elsevier Science Publishers B.V., International Journal of Impact Engineering 32:1214-1247, The Netherlands, 2006.
- [9] U.S. Army Corps of Engineers; *Methodology Manual for the Single-Degree-of-Freedom Blast Effects Design Spreadsheets*; U.S. Army Corps of Engineers, United States Of America, 2008.
- [10] Gannon, J.C., Marchand, K.A., Williamson, E.B.; *Approximation of blast loading and single degree-of-freedom modelling parameters for long span girders*; WIT Press., Transactions on The Built Environment 87, England, 2006.
- [11] Timoshenko, S.P., Woinowsky-Krieger, S.; *Theory of Plates and Shells*; McGraw-Hill, United States of Amerika, 1959.
- [12] Rosendal, F.J.J., van Wees, R.M.M.; *Onderzoek naar de nauwkeurigheid van de l -massa-veer methode Deel 1: zakking en oplegreactie*; TNO, Nederland, 1994.

Part VI

Appendices

> # A. Load-mass factors

> Parameters

- > w = deflection at midspan [m]
- > q = load [N/mm]
- > l = beam length [m]
- > A = crosssectional area [m²]
- > EI = bending stiffness [N/mm²]
- > k = stiffness [N/m]
- > ω = fundamental frequency [rad/s]
- > m = total mass [kg]
- > K_{LM} = load – mass factor [m]

> # A1. Load-mass factor for a simply supported beam

$$> w := \frac{5}{384} \cdot \frac{q \cdot l^4}{EI} :$$

$$> k := \frac{q \cdot l}{w} :$$

$$> \omega := \pi^2 \cdot \text{sqrt} \left(\frac{EI}{\text{rho} \cdot A \cdot l^4} \right) :$$

$$> m := l \cdot \text{rho} \cdot A :$$

$$> K_{LM} := \text{evalf} \left(\frac{k}{m} \cdot \frac{1}{\omega^2}, 5 \right)$$

$$K_{LM} := 0.78843$$

(1)

> # A2. Load-mass factor of a fixed beam

$$> w := \frac{1}{384} \cdot \frac{q \cdot l^4}{EI} :$$

$$> k := \frac{q \cdot l}{w} :$$

```
> ω := 4.730040744862702·sqrt( $\frac{EI}{\rho \cdot A \cdot l^4}$ ):
```

```
> m := l·rho·A:
```

```
>
```

```
>
```

```
>  $K_{LM} := \text{evalf}\left(\frac{k}{m} \cdot \frac{1}{\omega^2}, 5\right)$ 
```

```
 $K_{LM} := 0.76716$ 
```

(2)

```
>
```

```
>
```

> # B. Weightfactors

> Parameters

> C	=	amount of parts [-]
> h	=	size of the parts [m]
> l	=	beam length [m]
> a	=	distance from the load to the left support [m]
> b	=	distance from the load to right support [m]
> q	=	load [N/mm]
> R_1	=	left support reaction force [N]
> R_2	=	right support reaction force [N]
> EI	=	bending stiffness [N/mm ²]
> w	=	deflection [m]
> M_A	=	left support moment [Nm]
> M_B	=	right support moment [Nm]
> l_x	=	plate width in x - direction [m]
> l_y	=	plate width in y - direction [m]
> DD	=	bending stiffness [N/mm ²]
> ax	=	load between $x = a1$ and $x = a2$ [m]
> by	=	load between $y = b1$ and $y = b2$ [m]
> f	=	weightfactors [-]

> # B1. Weightfactors for a simply supported beam divided into 10 parts

$$> C := 10 :$$

$$> h := \frac{l}{C} :$$

$$> b1 := l - h - a : b2 := l - h :$$

```

> R11 :=  $\frac{q \cdot h \cdot \left(\frac{h}{2} + b1\right)}{l}$  : R12 :=  $\frac{q \cdot h \cdot \left(\frac{h}{2} + b2\right)}{l}$  :
> R21 :=  $q \cdot h - R11$  : R22 :=  $q \cdot h - R12$  :
> w11 :=  $x \rightarrow -\frac{1}{EI} \cdot \left(\frac{1}{6} \cdot R11 \cdot x^3 + c11 \cdot x + c21\right)$  : w12 :=  $x \rightarrow \text{simplify}\left(-\frac{1}{EI} \cdot \left(\frac{1}{6} \cdot R12 \cdot x^3 - \frac{1}{24} \cdot x^4 \cdot q + c12 \cdot x + c22\right)\right)$  :
> w21 :=  $x \rightarrow \left(-\frac{1}{EI} \cdot \left(\frac{1}{6} \cdot R11 \cdot x^3 - \frac{1}{24} \cdot (x - a)^4 \cdot q + d11 \cdot x + d21\right)\right)$  : w22 :=  $x \rightarrow \text{simplify}\left(-\frac{1}{EI} \cdot \left(-\frac{1}{6} \cdot R22 \cdot x^3 + \frac{1}{2} \cdot R22 \cdot l \cdot x^2 + d12 \cdot x + d22\right)\right)$  :
> w31 :=  $x \rightarrow \text{simplify}\left(-\frac{1}{EI} \cdot \left(-\frac{1}{6} \cdot R21 \cdot x^3 + \frac{1}{2} \cdot R21 \cdot l \cdot x^2 + e11 \cdot x + e21\right)\right)$  :
>
>
> eq11 :=  $w11(x) = w21(x)$  : eq11 :=  $\text{subs}(x = a, eq11)$  : eq12 :=  $w12(x) = w22(x)$  : eq12 :=  $\text{subs}(x = h, eq12)$  :
> eq21 :=  $\text{diff}(w11(x), x) = \text{diff}(w21(x), x)$  : eq21 :=  $\text{subs}(x = a, eq21)$  : eq22 :=  $\text{diff}(w12(x), x) = \text{diff}(w22(x), x)$  : eq22 :=  $\text{subs}(x = h, eq22)$  :
> eq31 :=  $w21(x) = w31(x)$  : eq31 :=  $\text{subs}(x = a + h, eq31)$  : eq32 :=  $w12(x) = 0$  : eq32 :=  $\text{subs}(x = 0, eq32)$  :
> eq41 :=  $\text{diff}(w21(x), x) = \text{diff}(w31(x), x)$  : eq41 :=  $\text{subs}(x = a + h, eq41)$  : eq42 :=  $w22(x) = 0$  : eq42 :=  $\text{subs}(x = l, eq42)$  :
> eq51 :=  $w11(x) = 0$  : eq51 :=  $\text{subs}(x = 0, eq51)$  :
> eq61 :=  $w31(x) = 0$  : eq61 :=  $\text{subs}(x = l, eq61)$  :
> sol11 :=  $\text{solve}(\{eq11, eq21, eq31, eq41, eq51, eq61\}, \{c11, c21, d11, d21, e11, e21\})$  :
>  $\text{assign}(sol11)$  : sol12 :=  $\text{solve}(\{eq12, eq22, eq32, eq42\}, \{c12, c22, d12, d22\})$  :
>  $\text{assign}(sol12)$  :
>
>
> a :=  $i \cdot h$  :
> w1 :=  $w31\left(\frac{l}{2}\right)$  : # for i from 1 to  $\frac{l}{2 \cdot h} - 1$ 
> w2 :=  $w22\left(\frac{l}{2}\right)$  : # for i is 0
> w3 :=  $w11\left(\frac{l}{2}\right)$  : # for i from  $\frac{l}{2 \cdot h}$  to  $\frac{l}{h} - 2$ 
> w5 :=  $w21\left(\frac{l}{2}\right)$  : # for i is uneven
>
>
> w_uniform :=  $\frac{5}{384} \cdot \frac{q \cdot l^4}{EI}$  :
>
>
> F_factor1 :=  $\frac{w2}{w\_uniform}$  : F_factor2 :=  $\frac{w1}{w\_uniform}$  : F_factor3 :=  $\frac{w3}{w\_uniform}$  : F_factor4 :=  $\frac{w5}{w\_uniform}$  :

```

$$:= F_factor1 : F_factor5 := \frac{w5}{w_uniform} :$$

>

$$> f := Matrix\left(\frac{l}{h}, 1\right) :$$

> if type $\left(\frac{1}{h}, \text{even}\right) = \text{false}$ then;

$$f(1) := \text{subs}(i=0, F_factor1);$$

for i from 1 to $\left(\frac{l}{h} - 1\right) \cdot \frac{1}{2} - 1$ do $f(i+1) := F_factor2$ end do;

$$f\left(\frac{l}{2 \cdot h} + \frac{1}{2}\right) := \text{subs}\left(i = \frac{l}{2 \cdot h} - \frac{1}{2}, F_factor5\right) :$$

for i from $\left(\frac{l}{h} + 1\right) \cdot \frac{1}{2}$ to $\frac{l}{h} - 2$ do $f(i+1) := F_factor3$ end do;

$$f\left(\frac{1}{h}\right) := \text{subs}\left(i = \frac{l}{h} - 1, F_factor4\right);$$

end if :

>

> if type $\left(\frac{1}{h}, \text{even}\right) = \text{true}$ then;

$$f(1) := \text{subs}(i=0, F_factor1);$$

for i from 1 to $\frac{l}{2h} - 1$ do $f(i+1) := F_factor2$ end do;

for i from $\frac{l}{2h}$ to $\frac{l}{h} - 2$ do $f(i+1) := F_factor3$ end do;

$$f\left(\frac{1}{h}\right) := \text{subs}\left(i = \frac{l}{h} - 1, F_factor4\right);$$

end if :

>

> $W := Matrix(C, 1)$:for i from 1 to C do $W[i] := f(i)$ end do;

$$W_1 := \frac{149}{6250}$$

$$W_2 := \frac{87}{1250}$$

$$W_3 := \frac{137}{1250}$$

$$W_4 := \frac{7}{50}$$

$$W_5 := \frac{981}{6250}$$

$$W_6 := \frac{981}{6250}$$

$$W_7 := \frac{7}{50}$$

$$W_8 := \frac{137}{1250}$$

$$W_9 := \frac{87}{1250}$$

$$W_{10} := \frac{149}{6250}$$

(1)

B2. Weightfactors for a fixed beam divided into 10 parts

C := 10 : # amount of parts

h := $\frac{l}{C}$:

M_A1 := $\frac{q}{l^2} \cdot \text{int}(x \cdot (l-x)^2, x=a..a+h)$: M_A2 := $\frac{q}{l^2} \cdot \text{int}(x \cdot (l-x)^2, x=0..h)$:

M_B1 := $\frac{q}{l^2} \cdot \text{int}(x^2 \cdot (l-x), x=a..a+h)$: M_B2 := $\frac{q}{l^2} \cdot \text{int}(x^2 \cdot (l-x), x=0..h)$:

b1 := l - h - a : b2 := l - h :

R₁₁ := $\frac{q \cdot h \cdot \left(\frac{h}{2} + b1\right)}{l}$: R₁₂ := $\frac{q \cdot h \cdot \left(\frac{h}{2} + b2\right)}{l}$:

R₂₁ := q · h - R₁₁ : R₂₂ := q · h - R₁₂ :

w11 := x → simplify $\left(-\frac{1}{EI} \cdot \left(\frac{1}{6} \cdot R_{11} \cdot x^3 + c11 \cdot x + c21\right)\right)$: w12 := x → simplify $\left(-\frac{1}{EI} \cdot \left(\frac{1}{6} \cdot R_{12} \cdot x^3 - \frac{1}{24} \cdot x^4 \cdot q + c12 \cdot x + c22\right)\right)$:

w21 := x → simplify $\left(-\frac{1}{EI} \cdot \left(\frac{1}{6} \cdot R_{11} \cdot x^3 - \frac{1}{24} \cdot (x-a)^4 \cdot q + d11 \cdot x + d21\right)\right)$: w22 := x → simplify $\left(-\frac{1}{EI} \cdot \left(-\frac{1}{6} \cdot R_{22} \cdot x^3 + \frac{1}{2} \cdot R_{22} \cdot l \cdot x^2 + d12 \cdot x + d22\right)\right)$:

w31 := x → simplify $\left(-\frac{1}{EI} \cdot \left(-\frac{1}{6} \cdot R_{21} \cdot x^3 + \frac{1}{2} \cdot R_{21} \cdot l \cdot x^2 + e11 \cdot x + e21\right)\right)$:

eq11 := w11(x) = w21(x) : eq11 := subs(x=a, eq11) : eq12 := w12(x) = w22(x) : eq12 := subs(x=h, eq12) :

eq21 := diff(w11(x), x) = diff(w21(x), x) : eq21 := subs(x=a, eq21) : eq22 := diff(w12(x), x) = diff(w22(x), x) : eq22 := subs(x=h, eq22) :

eq31 := w21(x) = w31(x) : eq31 := subs(x=a+h, eq31) : eq32 := w12(x) = 0 : eq32 := subs(x=0, eq32) :

```

> eq41 := diff(w21(x), x) = diff(w31(x), x) : eq41 := subs(x = a + h, eq41) : eq42 := w22(x)
= 0 : eq42 := subs(x = l, eq42) :
> eq51 := w11(x) = 0 : eq51 := subs(x = 0, eq51) :
> eq61 := w31(x) = 0 : eq61 := subs(x = l, eq61) :
> soll := solve({eq11, eq21, eq31, eq41, eq51, eq61}, {c11, c21, d11, d21, e11, e21}) :
assign(soll) : sol2 := solve({eq12, eq22, eq32, eq42}, {c12, c22, d12, d22}) :
assign(sol2) :
>
> a := i · h :
>
> w1 := w31( $\frac{l}{2}$ ) -  $\frac{(M_{A1} + M_{B1}) \cdot l^2}{16 \cdot EI}$  : # for i from 1 to  $\frac{l}{2 \cdot h} - 1$ 
> w2 := w22( $\frac{l}{2}$ ) -  $\frac{(M_{A2} + M_{B2}) \cdot l^2}{16 \cdot EI}$  : # for i is 0
> w3 := w11( $\frac{l}{2}$ ) -  $\frac{(M_{A1} + M_{B1}) \cdot l^2}{16 \cdot EI}$  : # for i from  $\frac{l}{2 \cdot h}$  to  $\frac{l}{h} - 2$ 
> w5 := w21( $\frac{l}{2}$ ) -  $\frac{(M_{A1} + M_{B1}) \cdot l^2}{16 \cdot EI}$  : # for i is uneven
>
> w_uniform :=  $\frac{1}{384} \cdot \frac{q \cdot l^4}{EI}$  :
>
> F_factor1 :=  $\frac{w2}{w\_uniform}$  : F_factor2 :=  $\frac{w1}{w\_uniform}$  : F_factor3 :=  $\frac{w3}{w\_uniform}$  : F_factor4
:= F_factor1 : F_factor5 :=  $\frac{w5}{w\_uniform}$  :
>
> f := Matrix( $\frac{l}{h}, 1$ ) :
> if type( $\frac{l}{h}$ , even) = false then;
f(1) := subs(i = 0, F_factor1);
for i from 1 to  $(\frac{l}{h} - 1) \cdot \frac{1}{2} - 1$  do f(i + 1) := F_factor2 end do;
f( $\frac{l}{2 \cdot h} + \frac{1}{2}$ ) := subs( $i = \frac{l}{2 \cdot h} - \frac{1}{2}$ , F_factor5) :
for i from  $(\frac{l}{h} + 1) \cdot \frac{1}{2}$  to  $\frac{l}{h} - 2$  do f(i + 1) := F_factor3 end do;
f( $\frac{l}{h}$ ) := subs( $i = \frac{l}{h} - 1$ , F_factor4);
end if :
>
> if type( $\frac{l}{h}$ , even) = true then;
f(1) := subs(i = 0, F_factor1);

```



```

for  $i$  from 1 to  $\frac{l}{2h} - 1$  do  $f(i + 1) := F\_factor2$  end do;
for  $i$  from  $\frac{l}{2h}$  to  $\frac{l}{h} - 2$  do  $f(i + 1) := F\_factor3$  end do;
 $f\left(\frac{1}{h}\right) := \text{subs}\left(i = \frac{l}{h} - 1, F\_factor4\right)$ ;
end if :

```

```

>  $W := \text{Matrix}(C, 1)$  : for  $i$  from 1 to  $\frac{1}{h}$  do  $W[i] := f(i)$  end do

```

$$W_1 := \frac{9}{1250}$$

$$W_2 := \frac{11}{250}$$

$$W_3 := \frac{1}{10}$$

$$W_4 := \frac{39}{250}$$

$$W_5 := \frac{241}{1250}$$

$$W_6 := \frac{241}{1250}$$

$$W_7 := \frac{39}{250}$$

$$W_8 := \frac{1}{10}$$

$$W_9 := \frac{11}{250}$$

$$W_{10} := \frac{9}{1250}$$

(2)

```

> # B3. Weightfactors for a 4-sided simply supported plate
    divided into 5x5 parts

```

```

> #weightfactors are dependent on ratio lx/ly

```

```

> lx := 1 :

```

```

> ly := 1 :

```

```

>  $DD := \frac{E \cdot t^3}{12 \cdot (1 - \nu^2)}$  :

```

```

> C := 5 :
> terms := 100 : #amount of terms Navier solution
>
> hx :=  $\frac{lx}{C}$  : hy :=  $\frac{ly}{C}$  :
>
> xx :=  $\frac{hx}{2} + i \cdot hx$  :
> yy :=  $\frac{hy}{2} + j \cdot hy$  :
>
> a := a2 - a1 :
> a12 :=  $\frac{1}{2} (a1 + a2)$  :
> b := b2 - b1 :
> b12 :=  $\frac{1}{2} (b1 + b2)$  :
>
>
>  $a_{mn} := \frac{16 \cdot q}{\pi^2 \cdot (2 \cdot m - 1) \cdot (2 \cdot n - 1)} \cdot \sin\left(\frac{(2 \cdot m - 1) \cdot \pi \cdot a12}{lx}\right) \cdot \sin\left(\frac{(2 \cdot n - 1) \cdot \pi \cdot b12}{ly}\right)$ 
>  $\cdot \sin\left(\frac{(2 \cdot m - 1) \cdot \pi \cdot a}{2 \cdot lx}\right) \cdot \sin\left(\frac{(2 \cdot n - 1) \cdot \pi \cdot b}{2 \cdot ly}\right) :$ 
>
>  $w := (x, y) \rightarrow \frac{1}{\pi^4 \cdot DD} \sum_{m=1}^{termsterms} \sum_{n=1}^{termsterms} \frac{a_{mn}}{\left(\frac{(2 \cdot m - 1)^2}{lx^2} + \frac{(2 \cdot n - 1)^2}{ly^2}\right)^2} \cdot \sin\left(\frac{(2 \cdot m - 1) \cdot \pi \cdot x}{lx}\right)$ 
>  $\cdot \sin\left(\frac{(2 \cdot n - 1) \cdot \pi \cdot y}{ly}\right) :$ 
>
>  $f := Matrix\left(\frac{lx}{hx}, \frac{ly}{hy}, [ ]\right) :$  for  $i$  from 0 to  $\frac{lx}{hx} - 1$  do for  $j$  from 0 to  $\frac{ly}{hy} - 1$  do  $f[i + 1, j$ 
>  $+ 1]$ 
>  $:= \left( subs\left(\left\{ a1 = i \cdot hx, a2 = (i + 1) \cdot hx, b1 = j \cdot hy, b2 = (j + 1) \cdot hy, x = \frac{lx}{2}, y = \frac{ly}{2} \right\},$ 
>  $w(x, y) \right) \right) / \left( subs\left(\left\{ b1 = 0, b2 = ly, a1 = 0, a2 = lx, x = \frac{lx}{2}, y = \frac{ly}{2} \right\}, w(x, y) \right) \right) ;$  end do
> end do;  $f := simplify(evalf(f), size);$ 

```

$$f := \begin{bmatrix} 0.008218023901 & 0.02232265150 & 0.02827729710 & 0.02232265148 & 0.008218023805 \\ 0.02232265150 & 0.06196141308 & 0.08015469713 & 0.06196141303 & 0.02232265146 \\ 0.02827729710 & 0.08015469713 & 0.1069730671 & 0.08015469721 & 0.02827729715 \\ 0.02232265148 & 0.06196141303 & 0.08015469721 & 0.06196141286 & 0.02232265143 \\ 0.008218023805 & 0.02232265146 & 0.02827729715 & 0.02232265143 & 0.008218023841 \end{bmatrix}$$

(3)

> # C. Ratio between maximum bending stresses due to locally loaded beam and uniform loaded beam.

> Parameters

> h	=	size of the parts [m]
> l	=	beam length [m]
> a	=	distance from the load to the left support [m]
> q	=	load [N/mm]
> A_v	=	left support reaction force [N]
> w	=	deflection [m]
> M	=	bending moment [Nm]
> M_{max}	=	maximum bending moment, partially loaded beam [Nm]
> $M_{uniform}$	=	maximum bending moment, uniformly loaded beam [Nm]
> V	=	shearforce [N]
> x_{Mmax}	=	x location of maximum moment [m]
> $Ratio$	=	$M_{uniform}/M_{max}$

$$> A_v := \frac{q \cdot h \cdot \left(l - a - \frac{h}{2} \right)}{l} : \# \text{ left support load}$$

$$> M := A_v \cdot x - \frac{1}{2} q \cdot (x - a)^2 : \# \text{ moment distribution}$$

$$> V := \text{diff}(M, x) : \# \text{ shear force distribution}$$

$$> x_{Mmax} := \text{solve}(V = 0, x) : \# \text{ location with maximum bending moment}$$

$$> M_{max} := \text{subs}(x = x_{Mmax}, M) : \#$$

$$> M_{uniform} := \frac{1}{8} \cdot q \cdot l^2 : \#$$

$$> Ratio := \text{simplify}\left(\frac{M_{uniform}}{M_{max}}, \text{size}\right) : f_{stress, max} = Ratio$$

$$f_{stress, max} = \frac{l^4}{(h - 2l)(h + 2a)(-2l + 2a + h)h}$$

(1)

> "a = 0"; $f_{stress, max} = subs(a = 0, Ratio);$

$$f_{stress, max} = \frac{l^4}{(h - 2l)^2 h^2} \quad (2)$$

> "a = $\frac{1}{2}(l - h)$ "; $f_{stress, max} = subs(a = \frac{1}{2}(l - h), Ratio);$

$$f_{stress, max} = -\frac{l^2}{(h - 2l)h} \quad (3)$$

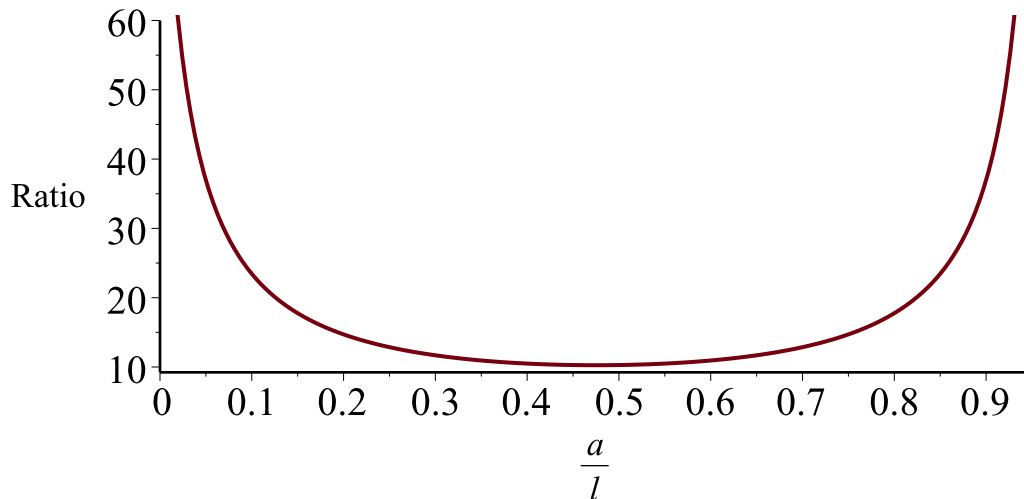
> "h = $\frac{l}{20}$ "; $f_{stress, max} = simplify(subs(h = \frac{l}{20}, Ratio), size)$

$$f_{stress, max} = -\frac{160000 l^2}{39(l + 40a)(-39l + 40a)} \quad (4)$$

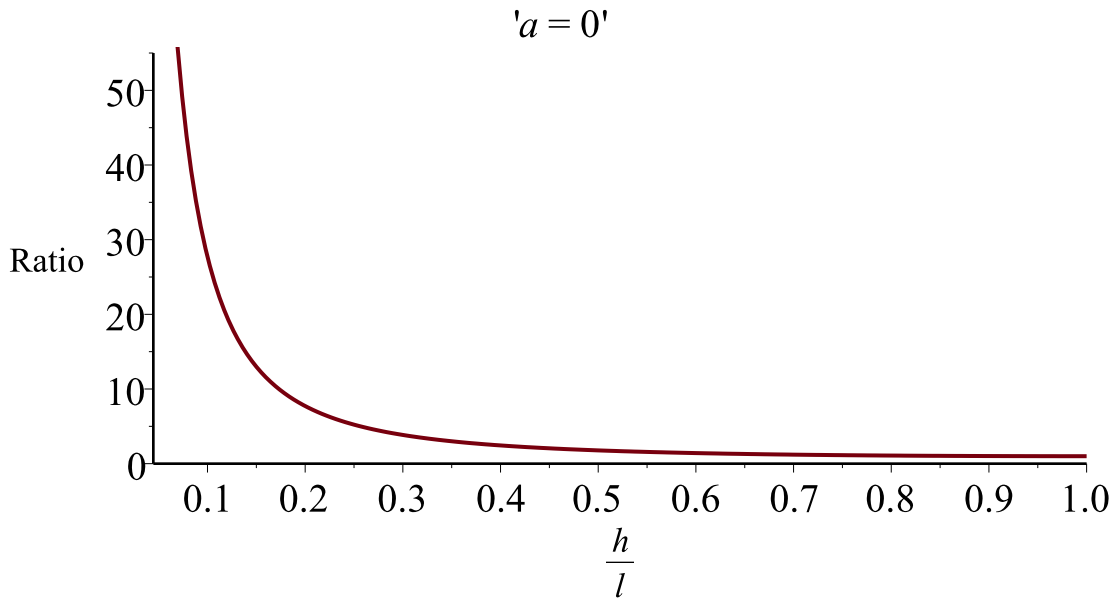
> $h := \frac{l}{20} : plot(subs(\{a = b \cdot l\}, Ratio), b = 0..1 - \frac{h}{l}, labels = [\frac{a}{l}, "Ratio"], title = "h = \frac{l}{20}");$

h = $\frac{l}{20}$

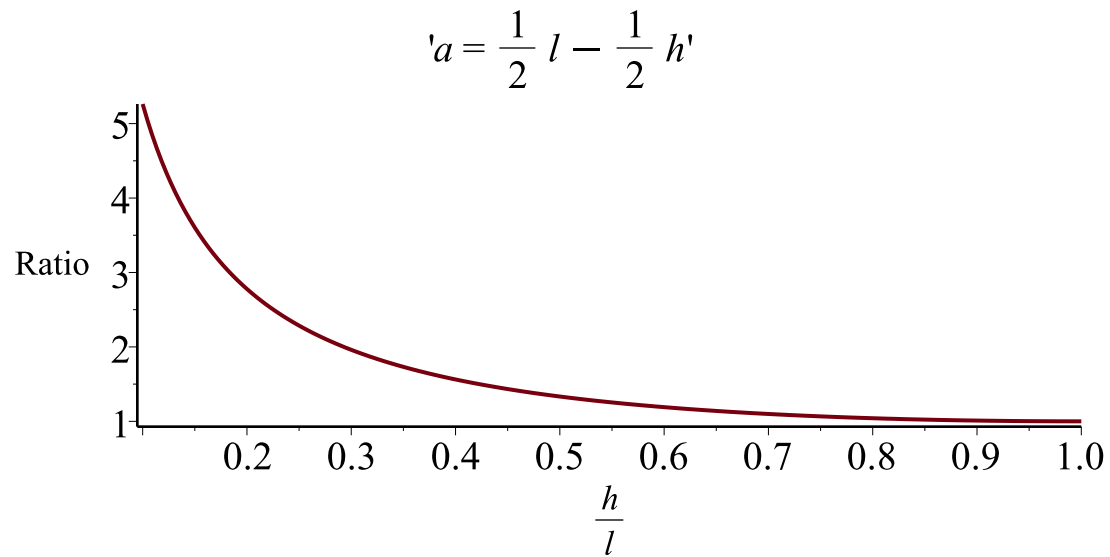
$$h = \frac{1}{20} l$$



```
> h := 'h': plot( subs( {a = 0, h = h·l}, Ratio), h = 1/20 .. 1, labels = [ h/l, "Ratio"], title = "a = 0");
# a = 0
```



```
> h := 'h': plot( subs( h = h·l, - l^2 / ((h - 2 l) h), h = 1/10 .. 1, labels = [ h/l, "Ratio"], title = "a = 1/2 (l - h)"); # ` `
```





Appendix D: FEM model

Structure

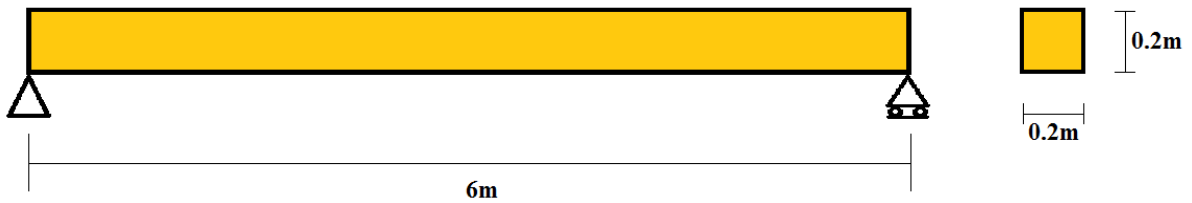


Figure 1.1: Beam geometry

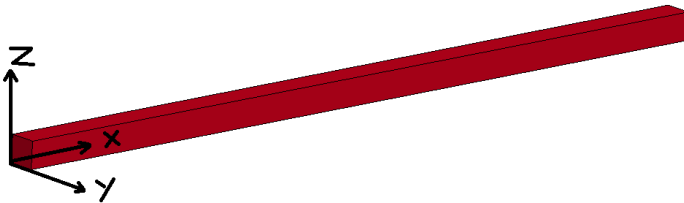


Figure 1.2: Coordinate system

Material

To describe the elastic-plastic deformation material card 003, *MAT_PLASTIC_KINEMATIC, in LS-Dyna has been chosen. The following parameters have been used:

Young's modulus	2.1E11 Pa
Tangent modulus	0
Poisson's ratio	0.0
Beta (0-1)	0 (=kinematic hardening)
Mass density	7850 kg/m ³
Yield strength	different values
Natural period	76.7 ms

Table 1.1: material properties

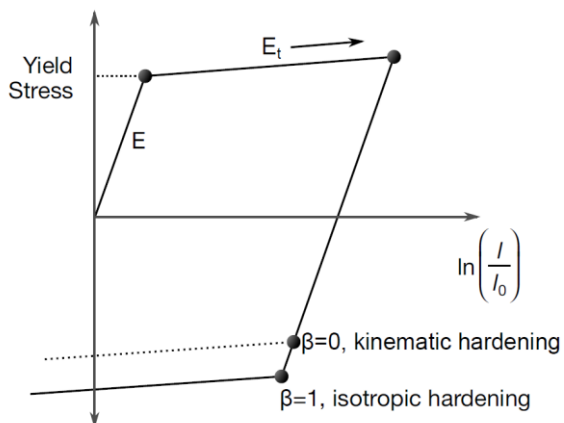


Figure 1.3: bilinear material deformation in LS-Dyna

Mesh

- 1280 elements in x direction and 1 element in y direction makes a total of 1280 elements.

Element properties

Fully integrated shell elements:

- Based on Reissner-Mindlin kinematic assumption
- 5 DOF in local coordinate system
- 2x2 integration in the shell plane
- 5 integration points through shell thickness

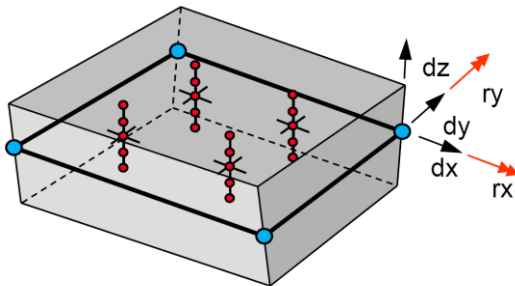


Figure 1.4: Fully integrated shell element

Boundary conditions

- $x=0$: $w_x=w_y=0$
- $x=l$: $w_y=0$

Loading

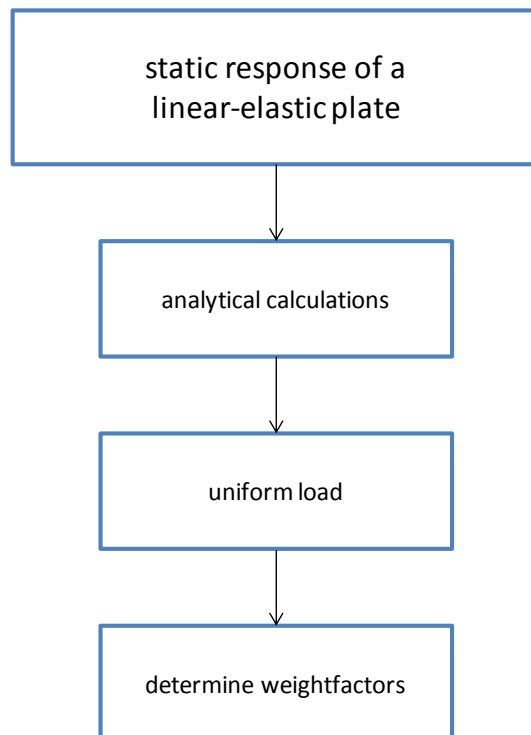
The pressure load has been applied in two different ways:

1. Blast load: by defining mass in TNT equivalent and of the explosion (x;y;z):
2. Segment load: the equivalent uniform load applied as function of time

Appendix E1

Analytical Calculation of the Weightfactors of a Plate

In this chapter the weightfactors have been determined for a simply supported linear-elastic plate. Using the weightfactors makes it possible to translate a non-uniform static load to an equivalent uniform static load and approximate the deflection at the centre of the plate. Linear-elastic deformation is assumed and all calculations are done analytically.



1.1 Weightfactors

To calculate the deflection of a partially loaded simply supported plate the Navier solution can be used [10]. This is a rapidly converging series. To ensure that almost no errors are made in the analytical calculations 10 (uneven) terms of the solution have been used to determine the deflection at the middle of the plate. When the deflection due to a partially loaded plate is divided by the deflection due to an entirely uniform loaded plate, the weightfactor for the loaded part is obtained.

Navier solution to calculate the deflection of the plate:

$$a_{mn} = \frac{16 \cdot q}{\pi^2 \cdot m \cdot n} \cdot \sin\left(\frac{m \cdot \pi \cdot \zeta}{a}\right) \cdot \sin\left(\frac{n \cdot \pi \cdot \eta}{b}\right) \cdot \sin\left(\frac{m \cdot \pi \cdot u}{2 \cdot a}\right) \cdot \sin\left(\frac{n \cdot \pi \cdot v}{2 \cdot b}\right)$$

$$w = (x, y) \rightarrow \frac{1}{\pi^4 \cdot D} \sum_{m=1, 3, 5 \dots}^{\infty} \sum_{n=1, 3, 5 \dots}^{\infty} \frac{a_{mn}}{\left(\frac{m^2}{a^2} + \frac{n^2}{b^2}\right)^2} \cdot \sin\left(\frac{m \cdot \pi \cdot x}{a}\right) \cdot \sin\left(\frac{n \cdot \pi \cdot y}{b}\right)$$

Where:

- q = value of the uniform distributed load [N/m²]
- ζ = distance of the centre of the load to the upper left corner in x-direction [m]
- η = distance of the centre of the load to the upper left corner in y-direction [m]
- u = width in x-direction of the loaded part [m]
- v = width in y-direction of the loaded part [m]
- a = width of the plate in x-direction [m]
- b = width of the plate in y-direction [m]
- D = flexural rigidity $Et^3 \cdot [12 \cdot (1 - \nu^2)]^{-1}$ [N/m²] (where ν is the poisson ratio)
- t = thickness of the plate [m]

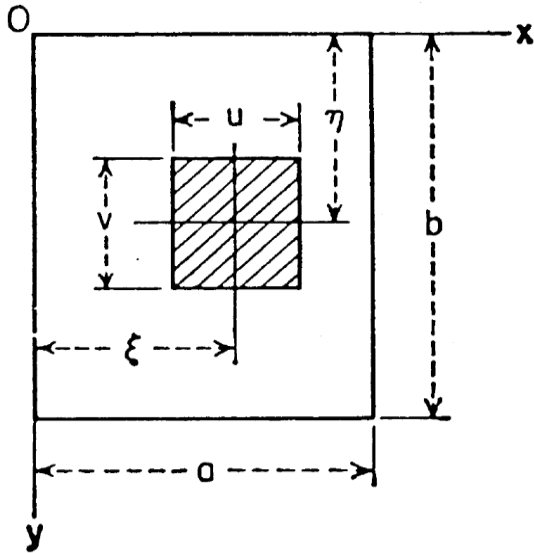


Figure 1.1: Rectangle plate

1.2 Conclusion

The weightfactors are independent of the material properties, but are dependent on the ratio between the length and width of the plate. In figure 6.2 the weightfactors are given for a square plate which is divided into 10x10 parts.

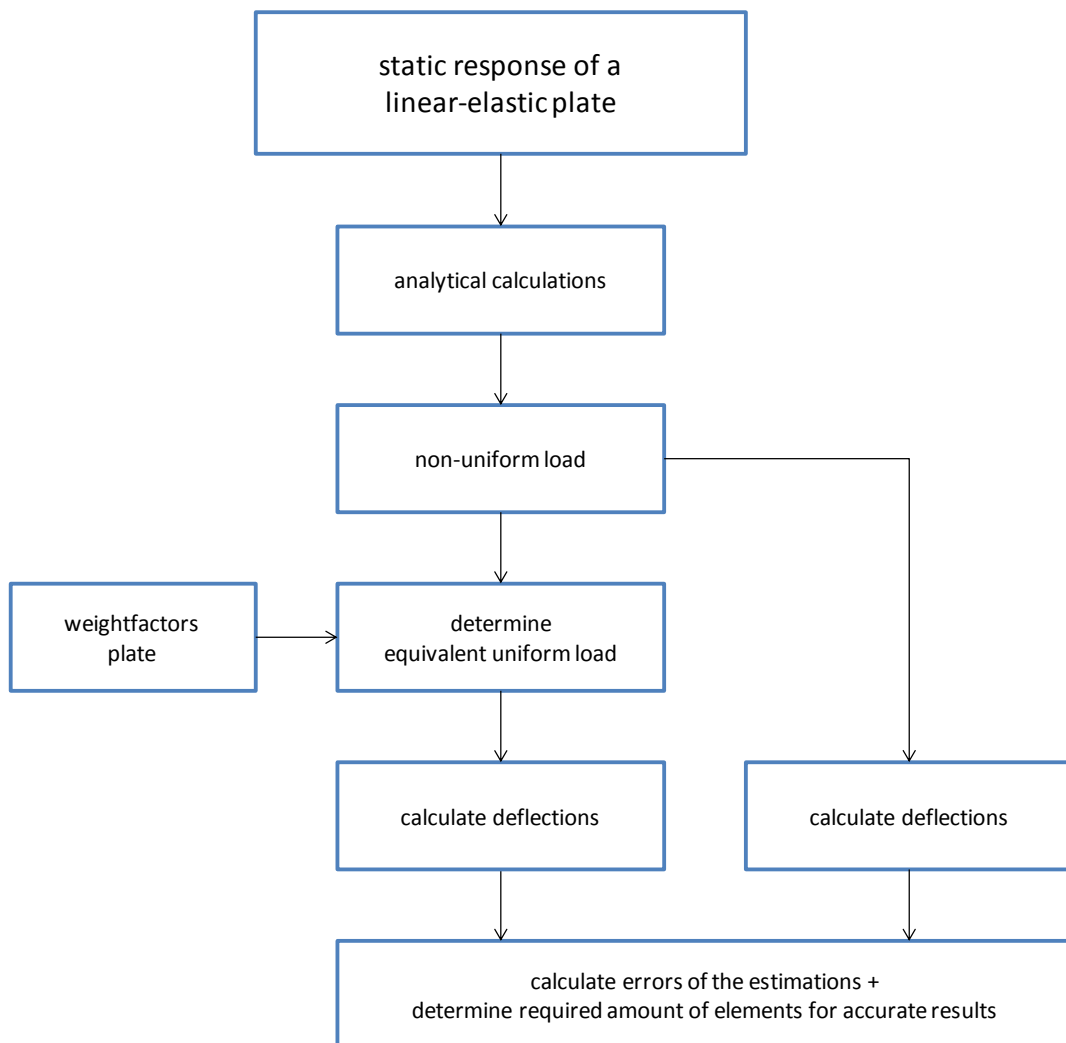
0.000530269	0.00155633	0.00247018	0.00317451	0.00356371	0.00356371	0.00317451	0.00247018	0.00155633	0.000530269
0.00155633	0.00457509	0.00728335	0.00939461	0.0105749	0.0105749	0.00939461	0.00728335	0.00457509	0.00155633
0.00247018	0.00728335	0.0116644	0.0151660	0.0171810	0.0171810	0.0151660	0.0116644	0.00728335	0.00247018
0.00317451	0.00939461	0.0151660	0.0199649	0.0228963	0.0228963	0.0199649	0.0151660	0.00939461	0.00317451
0.00356371	0.0105749	0.0171810	0.0228963	0.0267433	0.0267433	0.0228963	0.0171810	0.0105749	0.00356371
0.00356371	0.0105749	0.0171810	0.0228963	0.0267433	0.0267433	0.0228963	0.0171810	0.0105749	0.00356371
0.00317451	0.00939461	0.0151660	0.0199649	0.0228963	0.0228963	0.0199649	0.0151660	0.00939461	0.00317451
0.00247018	0.00728335	0.0116644	0.0151660	0.0171810	0.0171810	0.0151660	0.0116644	0.00728335	0.00247018
0.00155633	0.00457509	0.00728335	0.00939461	0.0105749	0.0105749	0.00939461	0.00728335	0.00457509	0.00155633
0.000530269	0.00155633	0.00247018	0.00317451	0.00356371	0.00356371	0.00317451	0.00247018	0.00155633	0.000530269

Figure 1.2: Weightfactors for a square plate which is divided into 10x10 parts

Appendix E2

Accuracy of the Static Response of a Linear-Elastic Plate

When a non-uniform load is translated to a uniform load an approximation is made. The accuracy of the obtained deflection depends on in how many parts the plate has been split to determine the equivalent uniform load. In this chapter it has been investigated how accurate the weightfactors can estimate the deflection due to different fictive non-uniform static load distributions and in how many parts the plate needs to be split to obtain accurate results.



2.1 Equivalent uniform load

The load has been simplified the same way as for a beam. See figure 8.1.

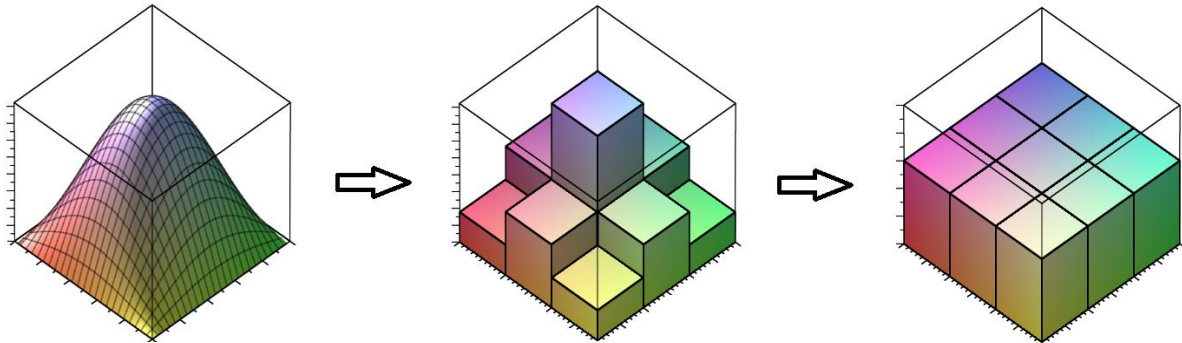


Figure 2.1: Simplification of a non-uniformly distributed load

2.2 Accuracy of the deflection of different load types

For different load distributions in the form of a fraction of a sine period the deflection at the centre has been approximated. For each load distribution the approximated value is compared to the exact deflection. The following loads have been investigated:

Load in the form of a half of a sine period:

$$q(x, y) = W \cdot \sin\left(\frac{\pi \cdot x}{x_l}\right) \cdot \sin\left(\frac{\pi \cdot y}{y_l}\right) \cdot (\text{Heaviside}(x) - \text{Heaviside}(x - x_l)) \cdot (\text{Heaviside}(y) - \text{Heaviside}(y - y_l))$$

Load in the form of a fourth of a sine period:

$$q(x, y) = W \cdot \sin\left(\frac{\pi \cdot (x + x_l)}{2x_l}\right) \cdot \sin\left(\frac{\pi \cdot (y + y_l)}{2y_l}\right) \cdot (\text{Heaviside}(x) - \text{Heaviside}(x - x_l)) \cdot (\text{Heaviside}(y) - \text{Heaviside}(y - y_l))$$

Load in the form of a sixth of a sine period:

$$q(x, y) = W \cdot \sin\left(\frac{3}{7} \frac{\pi \left(x + \frac{4}{3} x_l\right)}{x_l}\right) \cdot \sin\left(\frac{3}{7} \frac{\pi \left(y + \frac{4}{3} y_l\right)}{y_l}\right) \cdot (\text{Heaviside}(x) - \text{Heaviside}(x - x_l)) \cdot (\text{Heaviside}(y) - \text{Heaviside}(y - y_l))$$

Load in the form of a twelfth of a sine period:

$$q(x, y) = W \cdot \sin\left(\frac{3}{8} \frac{\pi \left(x + \frac{5}{3} x_l\right)}{x_l}\right) \cdot \sin\left(\frac{3}{8} \frac{\pi \left(y + \frac{5}{3} y_l\right)}{y_l}\right) \cdot (\text{Heaviside}(x) - \text{Heaviside}(x - x_l)) \cdot (\text{Heaviside}(y) - \text{Heaviside}(y - y_l))$$

A triangular load distribution:

$$q(x, y) = W \cdot \left(1 - \frac{x}{x_l}\right) \cdot \left(1 - \frac{y}{y_l}\right) \cdot (\text{Heaviside}(x) - \text{Heaviside}(x - x_l)) \cdot (\text{Heaviside}(y) - \text{Heaviside}(y - y_l))$$

The load is spread over a square part of the plate between (0,0) and (x₁,y₁).

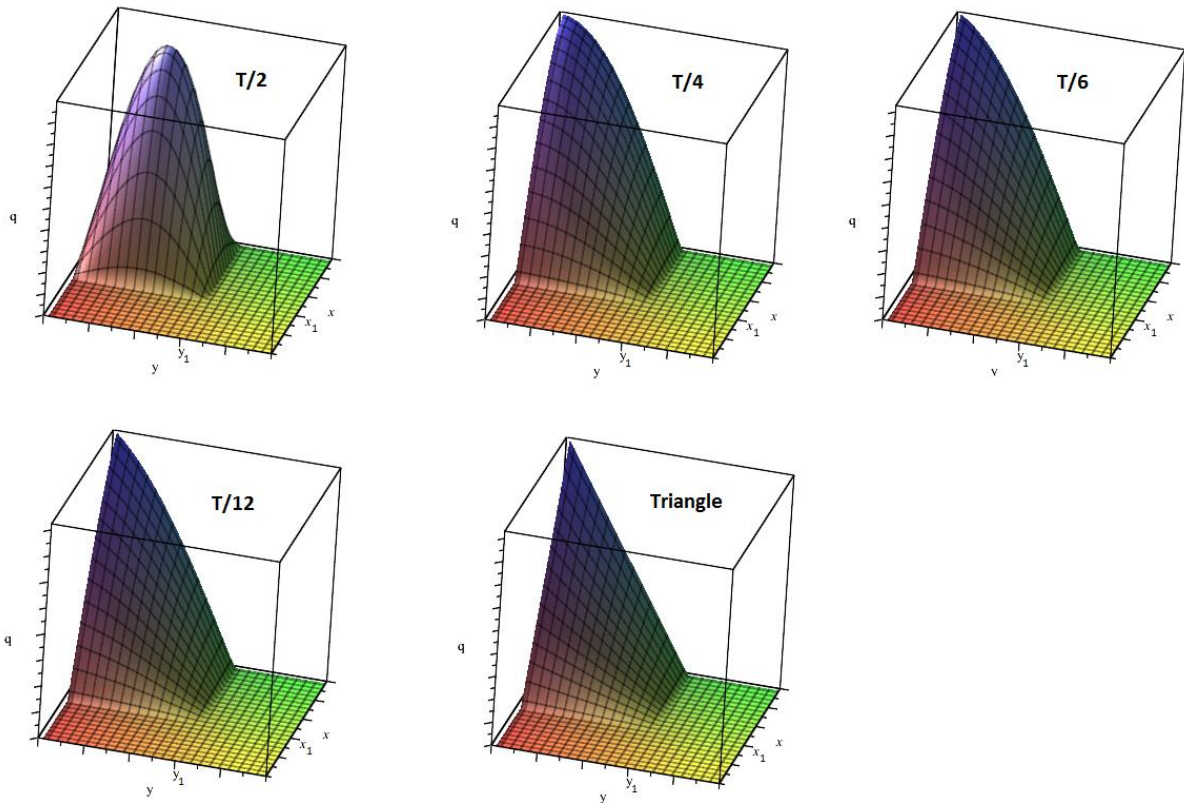


Figure 2.2: Different load scenarios

In table 7.1 an overview of the relative error is given for different ways of spreading the load. The size of x_1 is equal to y_1 . The plate is divided into 4 parts. The colour of each cell indicates the accuracy respectively to the other estimations of the corresponding row. Red being less accurate and green the most accurate. No useful conclusions can be made from these results. It can't be said that one load is approximated more accurate than the other, since no colour pattern can be found

$x_1 \cdot l$ (= $y_1 \cdot l$)	Rel. error [%] for sine T/2	Rel. error [%] for sine T/4	Rel. error [%] for sine T/6	Rel. error [%] for sine T/12	Rel. error [%] for triangle
1	-5.059	-1.227	-0.899	-0.687	0.000
0.9	-6.961	-1.950	-1.528	-1.256	-0.377
0.8	-2.758	1.420	1.807	2.059	2.884
0.7	-3.766	1.954	2.466	2.798	3.880
0.6	-12.813	-2.432	-1.566	-1.009	0.780
0.5	14.982	18.775	19.217	19.509	20.483
0.4	-28.564	-4.474	-2.610	-1.427	2.290
0.3	12.002	41.109	42.712	43.675	46.405
0.2	397.153	238.324	226.714	219.376	196.455
0.1	-100.000	-100.000	-100.000	-100.000	-100.000

Table 2.1: Relative error obtained by splitting a simply supported plate into 4x4 parts

To obtain a clearer overview of the accuracies of the different load types, instead of dividing the plate into 4 parts, the load has been divided into a certain amount of parts. In tables 8.2, 8.3 and 8.4 the accuracy of the deflection at the centre of the plates is gives for dividing the load into 2x2, 3x3 and 4x4 parts. It can be seen that if the load is divided in 4x4 parts it becomes clear which load distributions are more accurate.

x1*I	Rel. error [%] for sine T/2	Rel. error [%] for sine T/4	Rel. error [%] for sine T/6	Rel. error [%] for sine T/12	Rel. error [%] for triangle
1	-20.852	-4.481	-3.246	-2.462	0.000
0.9	-11.422	-2.977	-2.276	-1.825	-0.377
0.8	-11.036	-1.633	-0.836	-0.323	1.328
0.7	2.237	8.902	9.539	9.953	11.306
0.6	-12.813	-2.432	-1.566	-1.009	0.780
0.5	14.982	18.775	19.217	19.509	20.483
0.4	18.456	21.468	21.852	22.107	22.966
0.3	14.489	18.345	18.776	19.059	20.006
0.2	22.226	24.447	24.772	24.989	25.733
0.1	23.080	25.112	25.423	25.632	26.349

Table 2.2: Relative error obtained by splitting a simply supported plate such that the load is covered by 2x2 parts

x1*I	Rel. error [%] for sine T/2	Rel. error [%] for sine T/4	Rel. error [%] for sine T/6	Rel. error [%] for sine T/12	Rel. error [%] for triangle
1	-8.629	-2.057	-1.505	-1.149	0.000
0.9	-6.961	-1.950	-1.528	-1.256	-0.377
0.8	-2.758	1.420	1.807	2.059	2.884
0.7	-9.861	-3.795	-3.291	-2.966	-1.920
0.6	3.287	6.008	6.305	6.502	7.161
0.5	5.878	7.814	8.056	8.218	8.771
0.4	2.435	5.179	5.464	5.651	6.278
0.3	8.503	9.808	10.003	10.134	10.590
0.2	9.160	10.319	10.502	10.626	11.059
0.1	9.532	10.607	10.783	10.903	11.323

Table 2.3: Relative error obtained by splitting a simply supported plate such that the load is covered by 3x3 parts

x1*I	Rel. error [%] for sine T/2	Rel. error [%] for sine T/4	Rel. error [%] for sine T/6	Rel. error [%] for sine T/12	Rel. error [%] for triangle
1	-5.059	-1.227	-0.899	-0.687	0.000
0.9	-4.683	-1.415	-1.137	-0.958	-0.377
0.8	-1.601	0.988	1.235	1.397	1.931
0.7	-0.745	1.416	1.627	1.765	2.224
0.6	0.253	2.110	2.300	2.425	2.841
0.5	3.173	4.296	4.440	4.536	4.867
0.4	4.071	4.965	5.092	5.177	5.473
0.3	1.742	3.238	3.400	3.507	3.868
0.2	5.020	5.698	5.807	5.882	6.143
0.1	5.227	5.858	5.964	6.036	6.290

Table 2.4: Relative error obtained by splitting a simply supported plate such that the load is covered by 4x4 parts

2.2.1 Conclusion

When the load is divided into more parts it becomes clear how the course from less accurate to more accurate is divided over the load types. It can be seen that if the load is distributed over 70% of the plate or less the, deflection due to a half period of a sinusoidal load is more accurate than the deflection due to a triangle load (with a transition for the load distributions in between). However, when the load is distributed over a larger part, it is the contrary.

2.3 Summary

In this chapter it has been determined how accurate the weightfactors are for different fictive non-uniform static loads and in how many parts the plate needs to be split to obtain an accurate result.

Calculations have been done for different types of load distributions. When the loading is distributed over a small part of the plate it is hard to catch the load correctly. The plate needs to be divided into a large enough amount of parts to obtain an accurate estimation of the deflection at the centre. For the investigated load cases it holds that when the plate is divided in an amount of parts such that the load is covered by 4x4 parts, a maximum relative error of the estimation of the deflection at the centre of the plate of 6.3% is obtained.

If the relative errors for a plate are compared to the relative errors for a simply supported beam it is notable that the relative errors obtained for a four sided simply supported plate are approximate twice as large as that for a beam.